FROM METABOLITE PROFILING TO BIOMOLECULE QUANTIFICATION: MODERN MASS SPECTROMETRY TECHNIQUES APPLIED TO BIOLOGICAL RESEARCH

LEONARDO PARASECOLO

A DISSERTATION SUBMITTED TO

THE FACULTY OF GRADUATE STUDIES

IN PARTIAL FULFILLMENT OF THE REQUIREMENTS

FOR THE DEGREE OF DOCTOR OF PHILOSOPHY

GRADUATE PROGRAM IN CHEMISTRY

YORK UNIVERSITY

TORONTO, ONTARIO

May 2025

Abstract

Mass spectrometry (MS) is a versatile and powerful analytical technique that has revolutionized our ability to analyze complex biological systems. In this dissertation, we explore novel applications of various MS methodologies, including paper spray ionization (PSI), sandpaper spray ionization (SSI), matrix-assisted laser desorption/ionization (MALDI), and liquid chromatography-tandem mass spectrometry (LC-MS/MS). These techniques were applied to profile, detect, and quantify a wide range of metabolites and biomolecules across different biological contexts.

At York University, we employed sandpaper spray ionization mass spectrometry for the rapid and comprehensive analysis of maple leaves infected with distinct fungal species. This approach demonstrated the capability of this high-throughput and solvent-efficient screening technique to differentiate fungal infections by analyzing directly from the leaf surface without requiring sample preparation. The study highlighted SSI-MS as a powerful tool for in situ metabolomic analysis of plant-pathogen interactions, enabling the detection of key metabolic changes associated with different fungal infections.

Additionally, we developed a MALDI-high resolution MS method for the absolute quantification of the phytoalexins camalexin and scopoletin in *Arabidopsis thaliana*, providing novel insights into the plant's biochemical responses to environmental stressors. Furthermore, a semi-quantitative version of this method was employed to perform relative quantification of a broader set of phytoalexins in wild-type and mutant *Arabidopsis thaliana* plants lacking key transcription factors involved in their production.

In collaboration with Nucro-Technics Laboratories, we developed an ultra-sensitive immunoprecipitation-LC-MS/MS method for the quantification of low-abundance proteins in rat serum. This approach significantly enhances detection precision and sensitivity, allowing for the accurate quantification of trace-level proteins ($\geq$ 1 ng/mL) in plasma while requiring small sample volumes ($\leq$ 50 µL). This method meets the increasing demand for highly sensitive and reliable biomolecular assays in clinical and pharmaceutical research.

These applications underscore the adaptability and efficacy of modern mass spectrometry in tackling diverse biological questions, ranging from plant-pathogen interactions to clinical biomolecule analysis. The methodologies developed and optimized in this dissertation provide valuable tools for MS-based metabolite profiling, biomolecule quantification, and the exploration of complex biological matrices.

This research lays the foundation for future advancements in high-throughput screening, precision medicine, and plant metabolic studies.

Acknowledgements

I would like to express my sincere gratitude to Professor Demian Ifa, my supervisor, for giving me the incredible opportunity to join his research group. I am deeply thankful for his mentorship, which not only made of me a better mass spectrometry scientist but also enabled me to explore diverse projects and research avenues throughout my PhD. These years of PhD have been invaluable, transforming me into a more rounded, calm, and mature individual.

I would also like to extend my appreciation to Professors Philip Johnson and Derek Wilson, who served on my supervisory committee. Their suggestions and feedback during the annual Research Evaluation significantly improved the quality and impact of my research. Additionally, my heartfelt thanks go to Professors Katalin Hudak and Arash Zarrine-Afsar for graciously accepting the invitation to join my examination committee. I am grateful for their willingness to share their expertise during this pivotal milestone in my academic journey.

I am profoundly thankful to the entire team at Nucro-Technics, especially my supervisor Rick Bagshaw, whose guidance on ambitious and exciting projects has been transformative. Every day, I am grateful to have such a fantastic boss. My appreciation also goes to Albert, Bedrich, and John for allowing me to join the company, where I have grown and thrived both as a scientist and as a human being.

A special mention goes to the colleagues at Nucro's Toxicology department and students in Demian's lab with whom I had the pleasure of working. Whether it was advice on how to operate an instrument, shared moments of laughter during breaks, a night out drinking a beer (or more), or a simple smile and "good morning", your presence has been more important than what you could imagine and cherished part of my life. You will not be forgotten: Aby, Ann, Mandeep, Marco, Maryam, Ping, Rachel, Raymond, Rodinei, Sarah, Sebastian, Talita, Yvonne.

Above all, I want to acknowledge Laurentiu and Karl from York University and Consy and Majura from Nucro-Technics. Some people leave an indelible mark, and with them, there's a sense of deep affinity. For me, certain chapters of my life are intrinsically linked to these individuals and the relationships I built with them: you are the ones of my PhD time and have been the best people I could ever meet in my journey at York and Nucro. I am grateful that destiny made us come across and you will never be forgotten.

Even though our lives led us down separate paths, I would like to thank Eliana, who supported me during the first, extremely difficult year of my PhD in a new continent. Her presence, guidance, and encouragement during that time helped me navigate personal challenges and inspired me to become a better and more mature person.

Above all, I want to thank my family. We have never been the picture-perfect family where everything appears effortless and harmonious, and perhaps we never will be. Yet, through all our differences, one thing has remained unwavering: our love and presence for one another, especially in the moments that mattered most. This past winter, we faced a loss that left a permanent mark on us, yet we stood together, as we always have in times of hardship. If I am here today—content, proud of who I have become, and grateful for the life I live—it is because of you and the unwavering support you have given me, unconditionally and without fail.

Alla nonna, grazie di esserci stata sempre.

List of Tables

List of Figures

List of Abbreviations

AA – Amino Acid

ACN – Acetonitrile

ANOVA – Analysis of Variance

CID – Collision-Induced Dissociation

CS – Calibration Standard

CV – Coefficient of Variation

DHB – 2,5-Dihydroxybenzoic Acid

DMSO – Dimethyl Sulfoxide

EIC – Extracted Ion Chromatogram

ESI – Electrospray Ionization

EPO – Erythropoietin

FA – Formic Acid

HESI – Heated Electrospray Ionization

HPLC – High-Performance Liquid Chromatography

HRMS – High-Resolution Mass Spectrometry

ILM – Ionic Liquid Matrix

IP – Immunoprecipitation

IP-LC-MS/MS – Immunoprecipitation-Liquid Chromatography-Tandem Mass Spectrometry

IS – Internal Standard

LC-MS/MS – Liquid Chromatography-Tandem Mass Spectrometry

LOD – Limit of Detection

LOQ – Limit of Quantification

MALDI – Matrix-Assisted Laser Desorption/Ionization

MRM – Multiple Reaction Monitoring

MS – Mass Spectrometry

m/z – Mass-to-Charge Ratio

PBS – Phosphate-Buffered Saline

QC – Quality Control

QCM – Quartz Crystal Microbalance

QTOF – Quadrupole Time-of-Flight

RF – Radio Frequency

RP-HPLC – Reversed-Phase High-Performance Liquid Chromatography

RT – Retention Time

S/N – Signal-to-Noise Ratio

SPE – Solid-Phase Extraction

SSI – Sandpaper Spray Ionization

TOF – Time of Flight

UHPLC – Ultra-High-Performance Liquid Chromatography

UPLC-MRM – Ultra-Performance Liquid Chromatography-Multiple Reaction Monitoring

Chapter One: General Introduction

1.1) History and Fundamental Principles of Mass Spectrometry

The continuous development of mass spectrometers can be traced back to the pioneering discoveries of Wilhelm Wien and J.J. Thomson in the late 19th century [1]. In 1897, J.J. Thomson conducted experiments on the deflection of cathode rays in an electric field, allowing him to determine the mass-to-charge ratio (m/z) of the electron. This crucial discovery led to the identification of the electron as a subatomic particle [1, 2]. Thomson's experiments, using what would later be known as the "Crookes tube," showed that cathode rays were composed of negatively charged particles much lighter than atoms [2].

In 1898, Wilhelm Wien's analysis of positive anode rays (also known as canal rays) enabled him to determine the mass of the hydrogen atom, leading to the discovery of the proton [1, 3]. Wien's work involved deflecting positive ions in electric and magnetic fields, and he established that these ions had specific mass-to-charge ratios depending on their composition [3]. His findings laid the foundation for the development of mass spectrometry by demonstrating that ions could be separated based on their mass-to-charge ratios.

The inception of mass spectrometry as a distinct field began in 1907, when J.J. Thomson hypothesized that channel rays consist of charged particles, noting that lighter particles are deflected more than heavier ones in electric and magnetic fields. This principle became the foundation of mass spectrometry [1]. Thomson's work led to the development of the first mass spectrograph, which could separate and measure ions based on their m/z ratios. These discoveries set the stage for the development of modern mass spectrometers, which have profoundly impacted scientific research across various fields.

MS is a powerful analytical technique that is now integral to many scientific disciplines, including chemistry, biochemistry, food science, environmental science, biology, and medicine. MS has revolutionized the analysis of complex mixtures, with applications ranging from drug discovery and forensic science to environmental analysis [4-20]. MS is used to determine the molecular composition and quantity of sample components. In a typical process, molecules of interest are introduced into the mass spectrometer's ionization source, where they are ionized to produce positive or negative gas-phase ions [21].

These ions are then sorted based on their mass-to-charge ratio (*m/z*) as they pass through the mass analyzer and subsequently reach the detector [21]. The recorded signals are displayed as a mass spectrum, showing the relative abundance of ions as a function of their *m/z* ratio [21].

Coupling MS with complementary techniques, such as chromatography, often yields more reliable and comprehensive results, especially in terms of matrix effect reduction [22-23]. Additionally, MS is widely applied in proteomics and metabolomics to investigate the roles of proteins and metabolites within biological systems. This has significantly enhanced our understanding of molecular mechanisms underlying various diseases, facilitating the development of new drugs and therapies [24-26]. Regardless of the specific application, all mass spectrometers share four essential components: a sample input system, an ionization source, a mass analyzer, and a detector [21].

1.2) Electrospray Ionization Mass Spectrometry

Efforts to develop mass spectrometry techniques for studying large biomolecules faced significant challenges due to the difficulty of converting these molecules into gas-phase ions [27]. Traditional ionization methods relying on vaporization caused extensive decomposition, making them unsuitable for large biomolecules like proteins [28].

In 1989, John Fenn introduced electrospray ionization (ESI) as a soft ionization technique that overcame these challenges by allowing intact macromolecules to be ionized via multiple charging [29]. ESI uses strong electric fields to desorb ions from a solution into the gas phase, imparting very little residual energy to the analyte, thus preventing fragmentation [30]. The multiple charging mechanism produces ions with lower *m/z* values, making them compatible with common mass analyzers. Before ESI, existing ionization techniques could not accurately measure biologically important macromolecules such as proteins [31].

1.2.1) Mechanism of Electrospray Ionization

ESI employs electrical energy to transfer ions from a solution into the gas phase for mass spectrometric analysis [30]. The process begins with the formation of a mist of charged droplets, carrying the same polarity as the capillary voltage. Driven by a combination of pressure and

potential gradients, these charged droplets move toward the analyzer region of the mass spectrometer [30].

As the droplets travel, solvent evaporation causes a continuous reduction in droplet size, increasing the surface charge density [30]. Eventually, the droplet reaches the Rayleigh limit, where the Coulomb force of repulsion between the charges exceeds the surface tension, causing the droplet to break up into smaller droplets [28, 30]. This cycle of evaporation and disintegration continues until the droplets reach nanoscale radii, ultimately producing gas-phase analyte ions that are detected by the mass spectrometer [30].

Figure 1.1) (Adapted from Kebarle et al.) illustrates the electrospray ionization process [30].

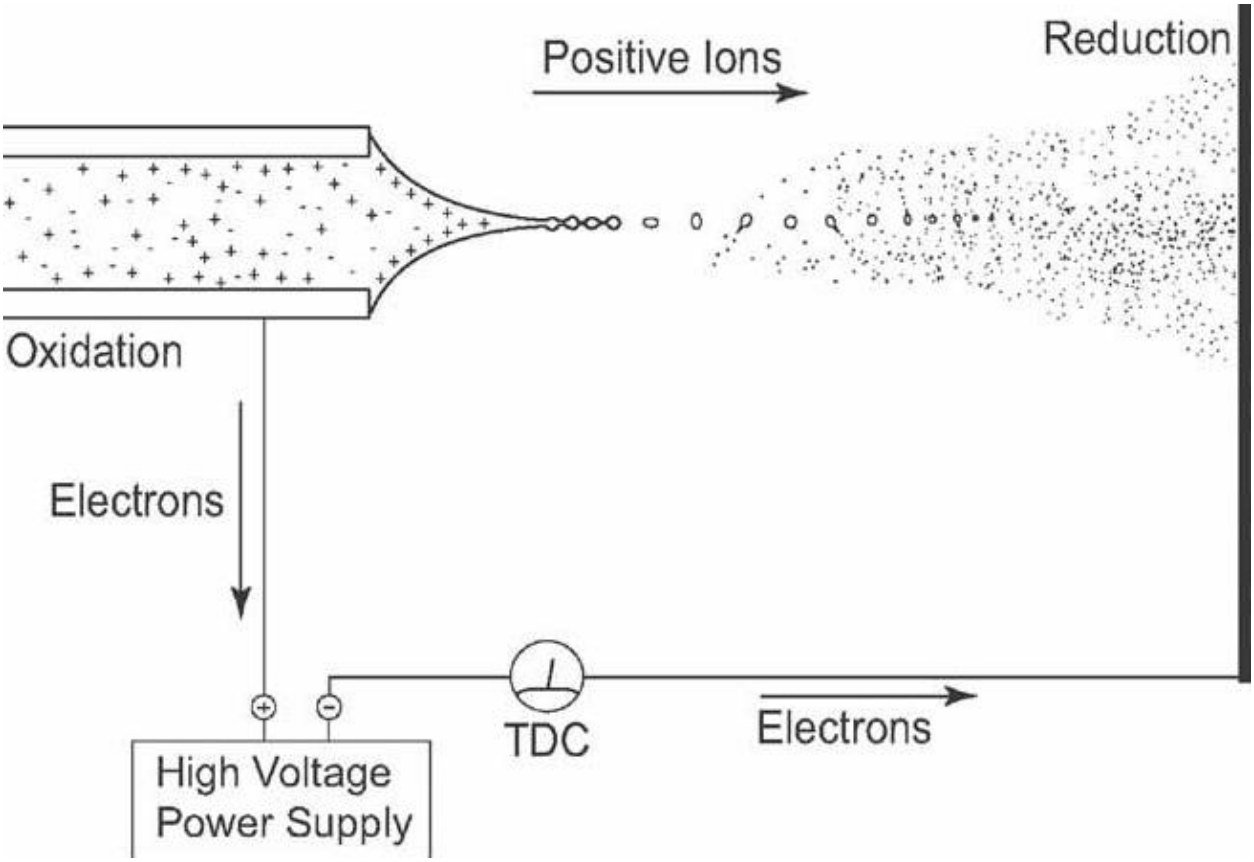

1.2.2) Mechanisms of Ion Formation

There are three primary mechanisms by which charged gaseous species are formed in ESI (Figure 1.2) [28-31]:

Ion Evaporation Model (IEM): Small, low molecular weight species are transferred into the gas phase by ejection of ions from charged nanodroplets [28, 30].

Charged Residue Model (CRM): Larger, globular species, such as native proteins, are released into the gas phase as the solvent evaporates [28, 30].

Chain Ejection Model (CEM): Partially hydrophobic, disordered polymer chains are ejected into the gas phase as the droplet evaporates [28, 30].

Figure 1.2 (Adapted from Konermann et al.) summarizes these mechanisms: (a) IEM, (b) CRM, and (c) CEM [28].

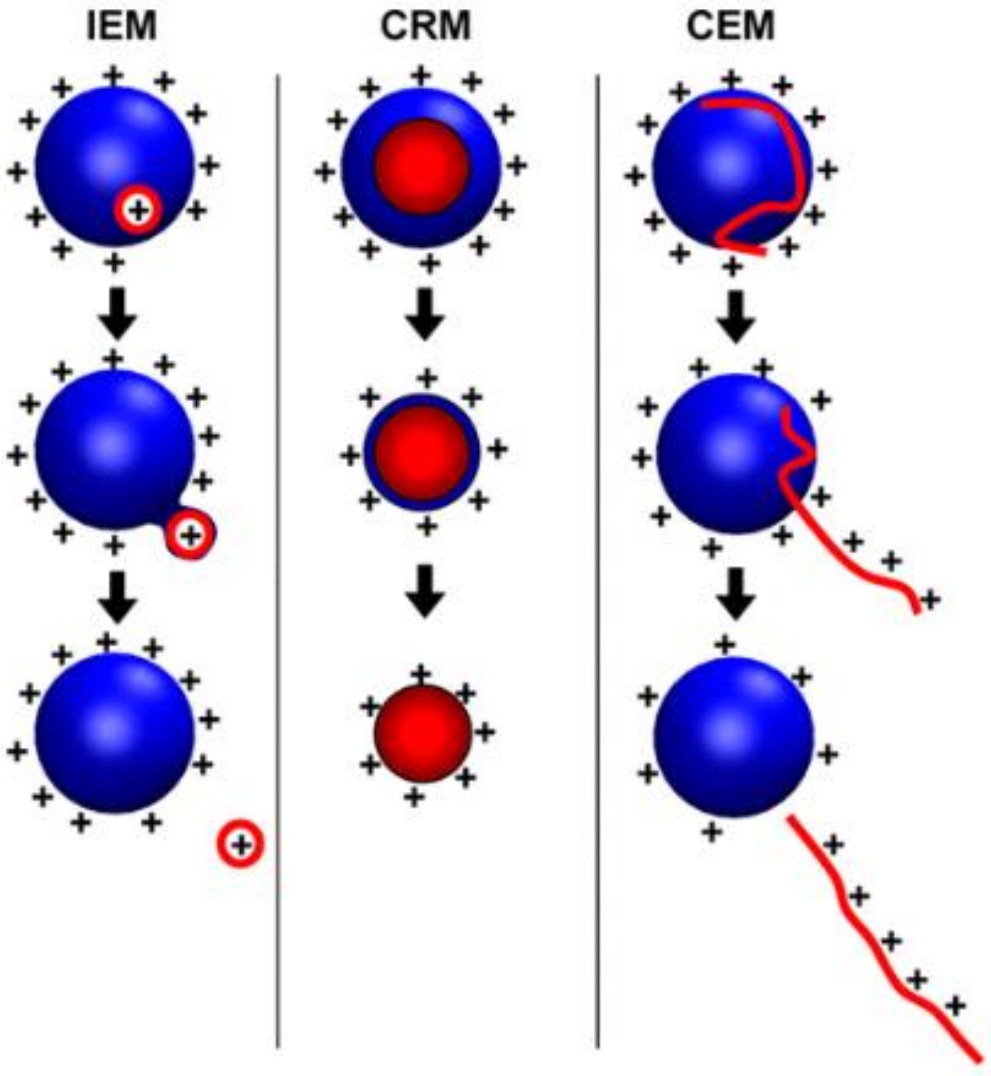

ESI-MS is a crucial technique for producing gas-phase ions from large macromolecules [28].

ESI enables structural characterization, accurate identification, and quantitative analysis of metabolites in complex biological samples by offering high sensitivity, compatibility with a wide range of analytes, and the ability to preserve molecular integrity during ionization, making it particularly valuable for non-volatile and thermally labile compounds [32]. ESI-MS is highly sensitive, reliable, and robust, enabling the analysis of non-volatile and thermally labile biomolecules from minimal sample volumes with exceptional precision. Its soft ionization process preserves molecular integrity, making it ideal for detecting and quantifying a broad spectrum of analytes in complex biological matrices [33].

1.2.3) Variants of Electrospray Ionization (ESI)

Electrospray Ionization (ESI) has evolved into several innovative variants that enhance its versatility and simplify sample preparation for mass spectrometric analyses. Paper Spray Ionization (PSI) utilizes a small triangular piece of paper onto which the sample is deposited. Applying a high voltage to the moistened paper tip generates a spray of ions, facilitating rapid analysis of complex mixtures such as biological fluids and environmental samples without extensive pretreatment [34].

Similarly, Leaf Spray Ionization employs plant leaves as the substrate for direct analysis of natural compounds. By applying a solvent and high voltage to the leaf tip, metabolites can be ionized and analyzed, making this method valuable for phytochemical studies [35].

An emerging technique, Sandpaper Spray Ionization (SPS-MS), utilizes sandpaper coated with the sample as a substrate for direct ionization. The textured surface of the sandpaper provides a large contact area, which enhances the extraction of analytes. When a solvent is deposited onto the sandpaper and a high voltage is applied, ions are generated directly from the sample, facilitating efficient and robust analysis of solid and semi-solid materials [36–38]. This method eliminates the need for extensive sample preparation, making it highly practical for applications involving complex matrices.

SPS-MS represents a significant advancement among ESI variants, offering several unique advantages. The sandpaper substrate is inexpensive, widely available, and adaptable to a wide

range of sample types, from biological tissues to environmental materials. By allowing rapid analysis with minimal manipulation, SPS-MS reduces both the cost and time associated with traditional sample preparation and chromatographic techniques. These attributes make SPS-MS a powerful tool for researchers seeking a fast, reliable, and cost-effective method for analyzing complex biological and non-biological samples.

1.3) Matrix-Assisted Laser Desorption/Ionization Mass Spectrometry (MALDI-MS)

Matrix-assisted laser Desorption/Ionization (MALDI) is a laser-based mass spectrometry technique specifically designed to ionize large biomolecules, including peptides, proteins, nucleic acids, and synthetic polymers, while minimizing fragmentation during the ionization process [39, 40]. The method works by embedding the analyte within a matrix that absorbs laser energy, facilitating the desorption and ionization of the molecules with minimal disruption to their structural integrity. This soft ionization process ensures that the molecular structure of large and complex biomolecules remains intact, making MALDI ideal for high-accuracy mass analysis. MALDI has found extensive applicability in a wide range of fields due to its versatility and ability to analyze complex mixtures. In proteomics, it plays a crucial role in identifying and characterizing proteins, including post-translational modifications, and in constructing protein interaction networks. It is also widely used in drug metabolism studies, where it enables the analysis of small molecule metabolites and their interactions with proteins. Additionally, MALDI is a powerful tool for analyzing synthetic polymers, offering insights into their composition and molecular weight distributions. Furthermore, in disease pathology, MALDI has been employed to identify biomarkers and map spatial distributions of biomolecules in tissues, providing valuable insights into the molecular basis of diseases [40, 41].

This combination of precision, versatility, and the ability to handle complex samples makes MALDI an indispensable technique across multiple disciplines, from basic biological research to applied fields such as biotechnology and clinical diagnostics.

1.3.1) Historical Development of MALDI

The use of lasers for ionizing organic molecules dates back to the early 1970s, marking a significant advancement in mass spectrometry [41]. During this period, researchers experimented with a variety of lasers that differed in wavelengths and pulse durations, combining them with

different types of mass spectrometers to evaluate their efficacy. These early efforts were foundational in developing laser-based ionization techniques, as they provided crucial insights into the mechanisms of energy transfer during ionization.

Through systematic experimentation, two fundamental principles for effective laser desorption emerged. First, efficient absorption of the laser wavelength by the analyte or the matrix is essential to ensure controlled and uniform energy transfer. The laser energy must be effectively absorbed to convert the molecules into gas-phase ions without causing unnecessary damage. Second, the energy transfer must occur within an extremely short time frame, typically in the range of nanoseconds, to prevent the thermal decomposition of thermally labile molecules and maintain their structural integrity [41, 42].

These principles have since guided the development of advanced techniques like MALDI, which uses a laser-absorbing matrix to protect and facilitate the desorption and ionization of large and delicate biomolecules. The lessons learned from these early experiments continue to influence the optimization of laser-based ionization systems in mass spectrometry today.

1.3.2) MALDI Methodology

MALDI is a powerful mass spectrometry technique that relies on embedding the analyte within a matrix compound to facilitate the ionization process. The matrix, typically a small organic molecule, plays a dual role by absorbing laser energy and protecting the analyte from direct exposure to intense energy, which could otherwise cause decomposition. For liquid samples, a small volume of analyte solution is mixed with the matrix solution and co-spotted onto a metal target plate. As the solution dries, matrix-analyte co-crystals form, ensuring close molecular interaction and effective energy transfer during ionization [42]. For solid samples, such as tissue sections, a thin and uniform layer of matrix is applied over the sample, allowing for efficient and consistent desorption and ionization across the sample's surface [39-42].

Once the sample is prepared, it is subjected to laser pulses, typically from a Neodymium-doped Yttrium Aluminum Garnet (Nd:YAG) laser. This laser is favored for its short pulse width, typically in the nanosecond range, and its ability to focus the laser beam onto small spot sizes. This precision

ensures that the matrix absorbs the laser energy efficiently and transfers it to the analyte in a highly controlled manner. The energy transfer facilitates the desorption and ionization of the analyte molecules while minimizing fragmentation, a key feature that distinguishes MALDI as a soft ionization technique [41, 42]. The ionization process in MALDI is particularly advantageous because it preserves the structural integrity of large, fragile biomolecules such as proteins, peptides, nucleic acids, and synthetic polymers. This makes MALDI ideal for analyzing complex mixtures and provides high-resolution data with minimal preprocessing requirements. The generated ions are subsequently detected and analyzed by the mass spectrometer, producing a mass spectrum that reveals critical information about the molecular composition of the sample, such as molecular weights and structural features [40-42].

Figure 1.3) (Adapted from Knochenmuss 2006) illustrates key processes in cluster-based MALDI ionization. Clusters formed during ablation contain preformed ions, with some carrying a net positive charge and others negative (not shown). Charged analytes (A), protonated in solution, may be released during cluster evaporation, or charge may transfer from the matrix (m) to the analyte via secondary reactions. For multiply charged analytes, hard and soft desolvation can yield distinct ion types. Partial neutralization by electrons or counterions occurs but remains incomplete [41].

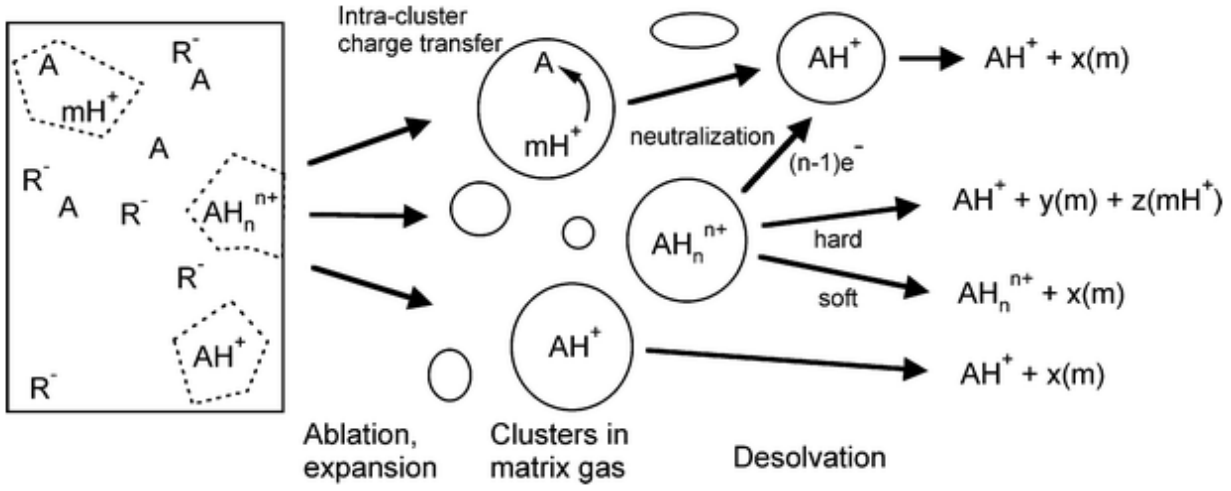

Overall, MALDI combines speed, sensitivity, and ease of use, making it an indispensable technique in modern biological and chemical research. By offering robust capabilities for

analyzing a wide range of samples, it continues to drive innovation in biotechnology, pharmaceuticals, and clinical diagnostics.

1.3.3) Applications of MALDI-MS

In addition to its precision and minimal sample preparation requirements, MALDI offers exceptional versatility. It has been widely applied in fields such as proteomics, where it enables the identification and characterization of proteins and their post-translational modifications, as well as in drug metabolism studies, where it facilitates the analysis of metabolites and their interactions. MALDI has found significant applications in the study of synthetic polymers, providing insights into their molecular weights and distributions. Its ability to analyze biomolecular distributions within tissues has also made it a powerful tool in disease pathology, where it aids in the identification of molecular biomarkers and the mapping of biomolecules within tissue sections [39–42].

MALDI-MS has become a cornerstone in proteomics, enabling the identification and characterization of proteins, peptides, and their post-translational modifications. Its ability to analyze complex protein mixtures with high sensitivity and minimal fragmentation makes it indispensable for mapping protein networks and studying cellular processes [40]. MALDI-MS is widely used in the characterization of synthetic polymers, offering detailed insights into their molecular weight distributions, composition, and structural variations. This application is critical for materials science, where understanding polymer properties is essential for developing advanced materials [43]. In the pharmaceutical industry, MALDI-MS is employed for drug metabolism studies, facilitating the identification and quantification of drug metabolites. It is also utilized for quality control to ensure the consistency and purity of pharmaceutical products throughout production [43-45]. Disease Pathology: MALDI-MS plays a vital role in disease pathology, particularly in identifying and detecting biomarkers associated with various diseases. Its ability to map biomolecular distributions within tissue sections has provided valuable insights into disease mechanisms, aiding in diagnostics and the development of targeted therapies [40, 46].

In summary, MALDI-MS is a highly versatile and sensitive tool that enables the analysis of large and complex molecules with minimal fragmentation. Its applications span multiple scientific

disciplines, including biochemistry, pharmaceuticals, materials science, and clinical research, and it continues to drive advancements in research and diagnostics [40-46].

1.3.4) MALDI-MS for Small Molecule Analysis

Recent advancements have significantly broadened the application scope of MALDI-MS, extending its utility to the analysis of small molecules, which traditionally fell outside its primary focus. This expansion has established MALDI-MS as an indispensable tool in fields such as metabolomics, where it enables the detailed profiling of metabolites across complex biological systems, and pharmaceutical research, where it is used to study drug compounds, their interactions, and their metabolites [43. 44].

Although MALDI-MS has been predominantly associated with the analysis of large biomolecules, such as proteins and peptides, recent developments have highlighted its exceptional capabilities in the detection and characterization of low molecular weight compounds, including metabolites, drugs, and small peptides. This ability to analyze smaller molecules is facilitated by advancements in matrix selection, optimization of laser parameters, and refined ionization techniques, which have collectively enhanced the sensitivity and accuracy of MALDI-MS for low-mass analytes.

Additionally, its speed, simplicity, and minimal sample preparation requirements make it particularly valuable for high-throughput applications, reducing the time and cost associated with traditional analytical methods. The technique offers unique advantages by preserving the structural integrity of small molecules during ionization, allowing for accurate molecular characterization and quantification. These qualities have significantly expanded the relevance of MALDI-MS in biological, clinical, and industrial research, making it a versatile platform for studying complex biochemical pathways, drug discovery, and disease mechanisms [45].

1.3.5) Challenges in Small Molecule Analysis

Analyzing small molecules using MALDI-MS has long been challenged by matrix-related background interference, particularly in the low-mass range, where peaks from traditional matrices often overlap with analyte signals. Organic matrices, such as α-cyano-4-hydroxycinnamic acid (CHCA) and 2,5-dihydroxybenzoic acid (DHB), while widely used, generate background ions that

complicate the interpretation of mass spectra. This issue is particularly problematic when analyzing low molecular weight compounds, where resolving analyte-specific signals becomes difficult [46, 47].

To address these challenges, researchers have explored alternative matrices that provide cleaner mass spectra and improved signal-to-noise ratios. For example, graphene oxide (GO) has emerged as a promising matrix material due to its high thermal conductivity, excellent energy absorption properties, and low background interference. Graphene-based matrices have been shown to enhance the detection of small molecules, offering both higher sensitivity and better reproducibility compared to conventional organic matrices [48]. Similarly, inorganic matrices and nanostructured substrates have gained attention as viable alternatives, as they offer improved desorption/ionization efficiency while reducing matrix-related interferences [49]. Additionally, significant advancements have been made in the development of conjugated polymers as novel MALDI matrices. These polymers function as dual-mode matrices capable of supporting both positive and negative ionization modes, making them highly versatile for small molecule analysis. Conjugated polymers also exhibit excellent stability and compatibility with a wide range of analytes, further broadening their applicability in mass spectrometry and imaging workflows [50].

While these alternative matrices, such as graphene oxide, inorganic substrates, and conjugated polymers, represent innovative approaches for overcoming the limitations of traditional matrices, they are not yet widely diffused or routinely adopted in laboratories. The optimization of existing organic matrices for small molecule analysis remains a highly valuable and more practical approach for most applications, providing a balanced trade-off between simplicity, cost-effectiveness, and analytical performance [45-50].

1.3.6) Advances in Matrices for Small Molecules

Although alternative matrices have been proposed, recent literature shows that traditional matrices, such as DHB, CHCA, DAN, and SA, remain widely used for small molecule analysis in MALDI-MS. Despite their initial design for larger biomolecules, advancements like sublimation have improved their performance by enhancing crystal uniformity and signal-to-noise ratios [46, 51, 52]. Additionally, strategies such as the incorporation of quaternary ammonium surfactants into CHCA matrices have further reduced background noise, making them more effective for low

molecular weight compound analysis [46].The versatility and compatibility of these traditional matrices are further enhanced by refined application methods, and supported matrices. These approaches allow for reduced background interference, better crystallization, and the detection of low-abundance analytes, ensuring that traditional matrices remain indispensable tools in MALDI-MS. While novel matrices and cutting-edge technologies continue to emerge, the combination of proper crystallization techniques and carefully selected traditional matrices provides a cost-effective and reliable solution for small molecule analysis in a variety of fields, including metabolomics and lipidomics [51- 53].

1.3.7) MALDI-MS-Based quantitative approaches

MALDI-MS has emerged as a promising tool for the quantification of small biomolecules, including steroid hormones, peptides, and other complex analytes, by offering high specificity, sensitivity, and rapid analysis. Quantitative MALDI-MS methodologies often overcome the challenges of poor ionization efficiency inherent to small molecules by employing derivatization strategies [54–56]. Additionally, the use of stable isotope-labeled internal standards and external calibration curves has enabled robust quantification with excellent precision and reproducibility.

Recent advancements have expanded the applicability of MALDI-MS quantification to diverse analytes. For instance, a MALDI-TOF MS method was developed for the quantification of guanidine-containing oligomers in consumer products, overcoming challenges related to their polydispersed molecular weight distribution by incorporating custom-synthesized ^{13}C-labeled internal standards and solid-phase extraction (SPE) with ionic liquid matrices to enhance reproducibility [57]. Similarly, a novel 2-nitrophloroglucinol (2-NPG) matrix was successfully employed for the quantification of the fungicide pyrimethanil in strawberries, demonstrating MALDI-MS's ability to achieve comparable performance to UPLC-MRM while providing rapid analysis and spatial distribution insights via MALDI imaging [58].

These approaches demonstrate the versatility of MALDI-MS in the direct analysis of complex matrices, offering shorter analysis times compared to traditional chromatographic techniques and making it a valuable alternative for clinical and research settings.

1.4) Liquid Chromatography-Tandem Mass Spectrometry (LC-MS/MS)

Liquid Chromatography-Tandem Mass Spectrometry (LC-MS/MS) is a versatile and powerful analytical tool with widespread applications in clinical, pharmaceutical, environmental, and metabolomic research. Its ability to combine robust chromatographic separation with highly sensitive and specific mass spectrometric detection has revolutionized the analysis of complex matrices, addressing challenges such as matrix effects and interference, which commonly affect other analytical techniques [59].

In clinical laboratories, LC-MS/MS is widely employed for therapeutic drug monitoring, toxicology, endocrinology, and newborn screening. For example, it is commonly used to monitor immunosuppressants, steroids, and vitamin D metabolites, offering multiplexing capabilities to analyze multiple analytes in a single run. This approach reduces sample volume requirements and improves analytical specificity compared to immunoassays, which are more susceptible to interferences [59, 60]. Furthermore, LC-MS/MS is advantageous for analyzing analytes in diverse matrices, including plasma, urine, saliva, and dried blood spots, making it invaluable for both clinical and forensic applications [60, 61].

The reduction of matrix effects—a critical issue in analytical chemistry—is one of the key strengths of LC-MS/MS. Robust chromatographic separation combined with ESI or atmospheric pressure chemical ionization APCI ensures efficient ionization while minimizing interference from co-eluting compounds. Internal standards, especially stable isotope-labeled compounds, further enhance accuracy and reproducibility by correcting for residual matrix effects [59, 60, 62].

In metabolomics, LC-MS/MS has proven invaluable for targeted and untargeted analyses. Targeted LC-MS/MS has been used to distinguish metabolic syndrome from obesity by quantifying metabolites associated with pathways such as purine metabolism and branched-chain amino acid degradation. These findings underscore its utility in characterizing disease-specific metabolic profiles and identifying potential biomarkers [63]. The method's versatility extends to environmental research, where it has been used to profile dissolved organic matter (DOM) in marine ecosystems [64]. Ultra-high-performance liquid chromatography coupled with high-resolution mass spectrometry enables comprehensive molecular characterization, and it is the gold standard method for quantifying a wide variety of small molecules [64, 65].

LC-MS/MS is a fundamental tool in pharmacological and toxicological analysis, providing high sensitivity and high throughput for drug detection and quantification. It is extensively used in pharmacokinetics and therapeutic drug monitoring, including the analysis of anticancer drugs [66], as well as in forensic toxicology for the screening of new psychoactive substances in biological samples with minimal matrix interference [67].

The adaptability of LC-MS/MS to diverse applications, its ability to address matrix effects, and its precision in quantitative and qualitative analyses make it a critical tool in modern analytical science. Its continuous development promises to expand its impact across a range of scientific and clinical disciplines [59–67].

1.4.1) LC-MS/MS-Based Proteomics

LC-MS/MS is particularly transformative in studying the pharmacokinetics of protein-based drugs, where precise measurement of these biomolecules in plasma or other tissues is essential. Protein drugs, such as monoclonal antibodies, hormones, and enzymes, exhibit complex pharmacokinetics due to their size, structural heterogeneity, and specific mechanisms of action. Traditional immunological techniques like enzyme-linked immunosorbent assay (ELISA), despite being more sensitive often lack the selectivity and multiplexing capabilities required for such intricate analyses [68]. LC-MS/MS proteomics, with its ability to differentiate closely related protein isoforms, post-translational modifications, and degradation products, addresses these challenges effectively.

One significant application of LC-MS/MS proteomics is the quantification of endogenous proteins and protein drugs in pharmacokinetic studies. The use of micro-LC/MS-MS methods, such as those developed by Suraj et al. (2018), illustrates the ability to simultaneously quantify multiple protein biomarkers with high precision and sensitivity. By monitoring selected peptides as surrogates for target proteins, LC-MS/MS facilitates accurate pharmacokinetic profiling, enabling insights into absorption, distribution, metabolism, and excretion (ADME) of protein-based therapeutics [69].

Moreover, the capability of LC-MS/MS proteomics to detect specific protein markers in processed biological samples has been demonstrated in food authentication and forensic sciences. Stachniuk et al. (2019) reported the use of heat-stable peptide markers derived from various animal species, enabling the identification of processed meat products. This highlights the method's robustness in

handling degraded or modified protein samples, a feature critical in pharmacokinetic studies of therapeutic proteins, which often undergo significant biochemical alterations in vivo. [70]. LC-MS/MS proteomics is not limited to quantification; it also offers qualitative insights into protein structure and function. For instance, TCUP, a computational method described by Boulund et al. (2017), integrates LC-MS/MS data with bioinformatics to characterize bacterial proteomes and antibiotic resistance markers. Such approaches underscore the potential of LC-MS/MS in therapeutic monitoring and resistance management, particularly in clinical settings. [71]. In the context of protein drugs, LC-MS/MS is pivotal in assessing immunogenicity and structural integrity. Prasad et al. (2019) discussed the criticality of bioanalytical quantification in protein therapeutic studies, emphasizing the method's reliability in delivering reproducible and accurate data. The application of quantitative LC-MS/MS ensures robust evaluation of therapeutic efficacy and safety by monitoring drug levels and related biomarkers [72]. The future of LC-MS/MS proteomics in pharmacokinetics lies in expanding its throughput and applicability. High-resolution mass analyzers and innovative quantification strategies, such as parallel reaction monitoring (PRM) and MRM, continue to enhance its precision and sensitivity. These advancements enable deeper insights into the pharmacokinetics of protein therapeutics, paving the way for personalized medicine and optimized therapeutic regimens. As protein-based drugs become more diverse and complex, LC-MS/MS proteomics will remain an indispensable tool for their comprehensive analysis, offering a bridge between molecular understanding and clinical application.

1.5) Immunoaffinity Purification

Immunoaffinity chromatography (IAC) is a cornerstone technique in proteomics, enabling the separation of specific proteins from complex mixtures through antibody-antigen interactions. Central to IAC is the immobilization of antibodies or other affinity reagents onto a solid matrix, facilitating the selective binding of target proteins. The process involves either immunodepletion, which removes high-abundance proteins (HAPs), or immunoenrichment, which isolates low-abundance proteins (LAPs), significantly reducing sample complexity and enhancing the detection of clinically significant biomarkers [73]. For instance, immunodepletion columns like the MARS Hu-14 and IgY14 systems, which target up to 14 of the most abundant plasma proteins, have demonstrated remarkable efficiency in reducing the dynamic range of protein concentrations,

enabling deeper proteome profiling of plasma, urine, and cerebrospinal fluid with enhanced coverage and reproducibility [73].

A key step in immunoaffinity purification is the preparation of high-quality antibodies, often produced in rabbits. Typically, polyclonal antibodies are generated by immunizing rabbits with the target antigen. To ensure high specificity and purity, the total IgG fraction is frequently isolated using Protein A chromatography, which exploits the high affinity of Protein A for the Fc region of IgG, prior to antigen-specific affinity purification. This approach is exemplified in the development of antibodies against mouse IgG2b and CD147, where Protein A purification was integral to obtaining high-purity antigen-specific antibodies, enabling sensitive applications like ELISA and sandwich assays [74, 75].

The flexibility of IAC extends beyond depletion and enrichment, with applications ranging from global proteome profiling to targeted quantification of proteins in biofluids. For example, the SISCAPA (Stable Isotope Standards and Capture by Anti-Peptide Antibodies) approach combines peptide-specific immunoenrichment with mass spectrometry for highly sensitive and precise quantification of low-abundance peptides and proteins [73]. While challenges such as non-specific protein loss and high antibody production costs remain, advancements in IAC technologies, including automation and the development of novel affinity reagents, continue to expand its potential in biomarker discovery and clinical proteomics [73].

1.5.1) Advantages of Immunoprecipitation in LC-MS/MS

The integration of immunopurification with LC-MS/MS represents a transformative approach in bioanalytical sciences, significantly reducing matrix effects and enhancing sensitivity in the quantification of low-abundance analytes. Immunoprecipitation (IP) allows for the selective isolation of target molecules, effectively removing interfering components from complex biological matrices. For example, Dubois et al. demonstrated the power of immunopurification in isolating the biologically active form of cetuximab (Erbitux) from human serum using soluble epidermal growth factor receptor (sEGFR) covalently linked to magnetic beads. This step drastically reduced nonspecific interactions and allowed for reliable quantification down to 20 ng/mL, with assay reproducibility below 20%, achieving sensitivity comparable to traditional ELISA methods [76]. Moreover, incorporating protein precipitation within hybrid IP-LC-MS

assays has proven particularly effective in addressing interference from abundant plasma proteins. Sun et al. reported this approach as a means of achieving ultrasensitive quantification of intact therapeutic insulin dimers in human plasma, illustrating the robustness of combining IP with selective precipitation techniques [77]. Beyond therapeutic proteins, Breitkopf et al. showcased the capability of IP-tandem MS to detect rare targets, such as a low-abundance BCR-ABL tyrosine kinase fusion protein in multiple myeloma cells. The precision of IP in isolating this fusion protein highlights its versatility in handling complex samples [78]. These advancements emphasize the critical role of immunopurification not only in reducing matrix effects but also in achieving unparalleled sensitivity and specificity, making it an indispensable tool in modern LC-MS/MS workflows for therapeutic protein quantification and biomarker discovery.

1.6) Instrumentation used

The following sections provide an overview of the mass spectrometers used in this research: the Thermo Finnigan™ LTQ™, Thermo Scientific™ QExactive™ Quadrupole-Orbitrap hybrid and the Thermo Scientific™ Orbitrap Exploris™ 120 mass spectrometers and the Thermo Scientific™ Vanquish™ UHPLC system.

1.6.1) Thermo Finnigan™ LTQ™ Mass Spectrometer

The Thermo Finnigan™ LTQ™ is a highly versatile and widely used mass spectrometer, designed to provide reliable and sensitive analysis of ions. It integrates an atmospheric pressure ionization (API) source, advanced ion optics, a linear ion trap mass analyzer, and a robust ion detection system. This configuration allows the LTQ™ to efficiently guide, trap, and analyze ions, making it an excellent tool for a wide range of analytical applications.

The ionization process begins in the atmospheric pressure ionization source, where ions are introduced into the instrument through the ion transfer capillary. This capillary facilitates additional desolvation of the ions as they enter the system. The ions are then focused by the tube lens and directed toward the skimmer. The skimmer acts as a critical barrier, separating the high-pressure ion source region from the lower-pressure region of the instrument, ensuring efficient ion transmission and minimizing contamination or ion loss.

Once past the skimmer, ions are funneled into the Q00 ion guide, a component responsible for stabilizing the ion beam. At this stage, the gate lens carefully regulates the injection of ions into the mass analyzer, ensuring a controlled and focused entry into the analytical region.

At the heart of the LTQ™ system lies its linear ion trap mass analyzer, a precision-engineered assembly designed to separate and analyze ions based on their mass-to-charge ratio (m/z). The analyzer comprises three key components: the front lens, the linear ion trap, and the back lens. The linear ion trap features hyperbolic rods arranged in a square configuration, with two central rods known as exit rods. These rods include slits through which ions are selectively ejected during analysis.

Inside the trap, ions are confined using a time-varying electric field, enabling precise isolation and fragmentation of target ions. Once analyzed, the selected ions are ejected and directed toward the ion detection system. This system detects the ions and generates signals that are subsequently amplified by sophisticated detection electronics, enabling accurate and sensitive data acquisition for downstream analysis [79].

Figure 1.4) Adapted from Thermo Electron Corporation LTQ hardware manual. [79] Construction details of the Thermo Finnigan™ LTQ™ mass spectrometer.

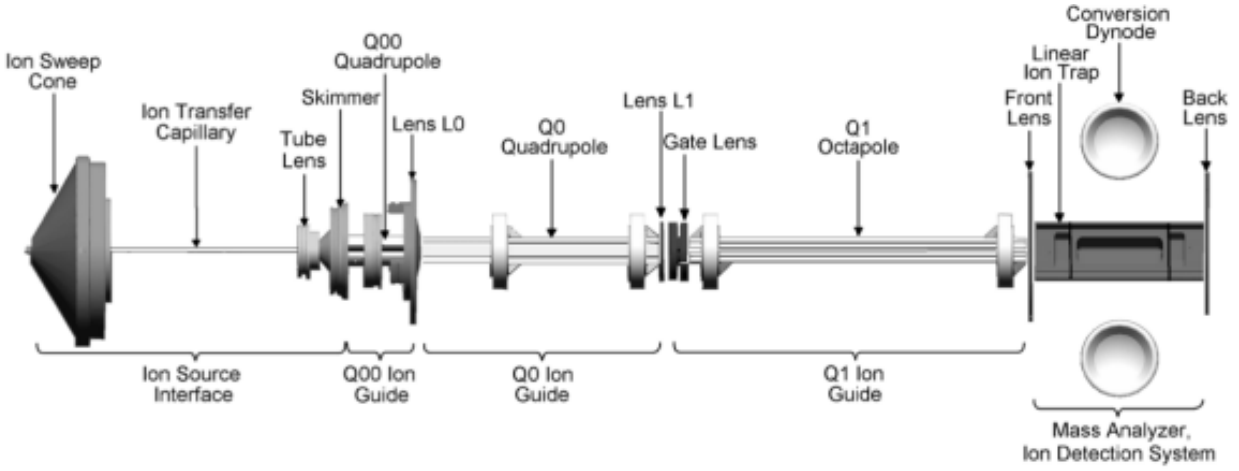

This combination of efficient ion handling and high-performance analysis makes the Finnigan LTQ™ a powerful tool for researchers, offering exceptional sensitivity and specificity in a variety of analytical workflows.

1.6.2) Thermo Scientific™ QExactive™ Hybrid Mass Spectrometer

The Thermo Scientific™ QExactive™ is an advanced hybrid mass spectrometer that integrates a quadrupole mass filter with an Orbitrap analyzer, making it a highly versatile and precise tool for complex analytical workflows. This instrument is specifically designed for high-resolution and high-sensitivity applications, catering to a wide range of experimental needs. It is widely used in proteomics, metabolomics, and small molecule analysis, offering seamless compatibility with liquid chromatography (LC) and nano-electrospray ionization (nano-ESI). Additionally, the QExactive can be coupled with a matrix-assisted laser desorption/ionization (MALDI) source for specialized applications, further enhancing its versatility and utility.

The QExactive system is built around five main components, each playing a crucial role in its operation.

The ion source generates ions from the analytes using atmospheric pressure ionization (API) techniques, such as electrospray ionization (ESI) or nano-ESI. These techniques are ideal for coupling with LC and ensure efficient ionization of a wide range of compounds. Acting as a selective mass filter, the quadrupole isolates ions based on their mass-to-charge ratio (m/z). This feature is critical for targeted analysis and ensures that only ions of interest proceed further in the system. The C-Trap serves as an ion accumulator and a focusing device. It temporarily stores ions, reduces their kinetic energy using nitrogen gas, and prepares them for high-resolution analysis in the Orbitrap analyzer. The collision cell facilitates Higher Energy Collisional Dissociation (HCD), a technique that fragments precursor ions into product ions. This step is essential for tandem mass spectrometry (MS/MS) experiments, allowing for detailed structural elucidation and sequence analysis of biomolecules. The Orbitrap analyzer is the heart of the QExactive system. It provides high-resolution and accurate mass measurements by trapping ions in a finely tuned electrostatic field. The analyzer is capable of resolving closely spaced mass peaks, making it ideal for applications requiring precise mass accuracy and high resolving power.

The pathway of ions through the QExactive system is meticulously designed for optimal performance and efficiency.

Ions generated by the source are directed through the injection flatapole, which focuses and transmits them to the quadrupole mass filter. This step ensures efficient ion transfer while

minimizing ion loss. The quadrupole separates ions based on their m/z ratio, allowing only the ions of interest to proceed to the next stage. This mass selection capability is essential for targeted analyses and complex sample workflows. After passing through the quadrupole, ions are accumulated in the C-Trap. Here, their kinetic energy is reduced using nitrogen gas, resulting in a focused and stable ion beam. This step ensures optimal conditions for subsequent analysis in the Orbitrap. The Z-lens focuses and transfers the ions from the C-Trap to the Orbitrap analyzer. In the Orbitrap, ions are subjected to a finely tuned electrostatic field, where they oscillate along a central spindle. The frequency of these oscillations is directly proportional to the ions' m/z ratio, allowing the Orbitrap to generate high-resolution mass spectra with exceptional mass accuracy.

Figure 1.5) Adapted from Thermo Fisher Scientific Exactive series operating manual. [80] Construction details of the Thermo Scientific™ QExactive™ mass spectrometer.

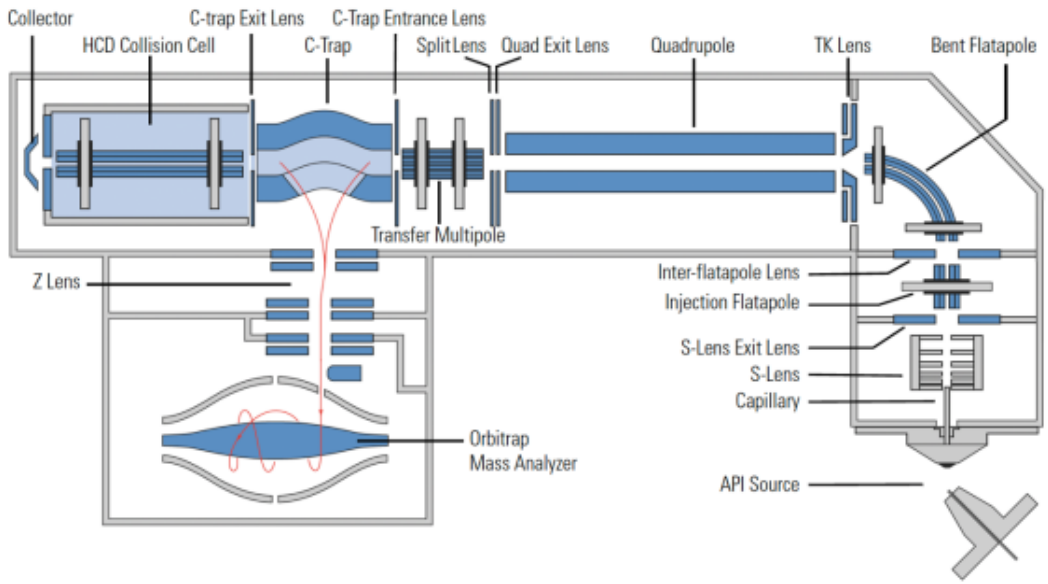

By combining the precision of the quadrupole mass filter with the resolving power of the Orbitrap analyzer, the QExactive system provides unparalleled performance for both qualitative and quantitative analyses. This hybrid approach makes it an indispensable tool for modern analytical laboratories, delivering high-resolution data and enabling in-depth characterization of complex samples [80].

1.6.3) Thermo Scientific™ Orbitrap Exploris™ 120

The Thermo Scientific™ Orbitrap Exploris™ 120 is a high-resolution mass spectrometer designed for precise and reliable qualitative and quantitative analysis across a wide range of applications, including proteomics, metabolomics, and pharmaceutical research. Utilizing Orbitrap-based high-resolution accurate mass (HRAM) technology, this instrument delivers superior mass accuracy, high dynamic range, and exceptional sensitivity, making it a powerful tool for complex sample analysis. The Exploris 120 is fully compatible with ultra-high-performance liquid chromatography (UHPLC) systems and supports multiple ionization techniques, ensuring seamless integration into various analytical workflows.

At the core of the instrument lies its ion transmission and detection system, which ensures optimal ion selection, fragmentation, and mass detection. Ions are generated in the OptaMax NG™ Atmospheric Pressure Ionization (API) Source, which supports electrospray ionization (ESI) and atmospheric pressure chemical ionization (APCI), offering flexibility for different analyte types. The ions then pass through the injection flatapole, which focuses and transmits them efficiently to the quadrupole mass filter. The quadrupole mass filter selectively isolates precursor ions based on their mass-to-charge (m/z) ratio, ensuring precise selection for further analysis. This is particularly crucial for targeted workflows, where accurate precursor isolation enhances sensitivity and specificity.

Following mass selection, ions are directed into the Ion-Routing Multipole (IRM), which facilitates Higher-Energy Collision Dissociation (HCD). This fragmentation process produces characteristic fragment ions necessary for detailed structural elucidation and sequence determination in tandem mass spectrometry (MS/MS) experiments. Fragmented ions are then accumulated in the C-Trap, where their kinetic energy is reduced before being injected into the high-field Orbitrap analyzer. Within the Orbitrap, ions oscillate along a central spindle in a finely tuned electrostatic field, and their oscillation frequencies are recorded to generate high-resolution mass spectra. The Exploris 120 offers a maximum resolving power of 120,000 at m/z 200, allowing for precise isotopic resolution and accurate mass assignments.

The system features a mass range of m/z 40–3000, making it highly versatile for both small-molecule and large-protein analysis. It provides mass accuracy of <3 ppm with external calibration and <1 ppm with internal lock mass correction, ensuring confidence in analyte identification and quantification. The instrument supports rapid polarity switching with full scan acquisition times

as short as 1.4 seconds at 60,000 resolution, making it well-suited for high-throughput workflows . With a dynamic range greater than 5000, the Exploris 120 enables accurate quantification across a broad concentration spectrum. Sensitivity tests confirm the ability to detect 200 fg of reserpine on-column with a signal-to-noise ratio of 100:1 in MS/MS mode, demonstrating its high analytical performance.

Figure 1.6) Adapted from Thermo Fisher Scientific Orbitrap Exploris Series operating manual. [81] Schematic of Orbitrap Exploris Series MSs with S-Lens.

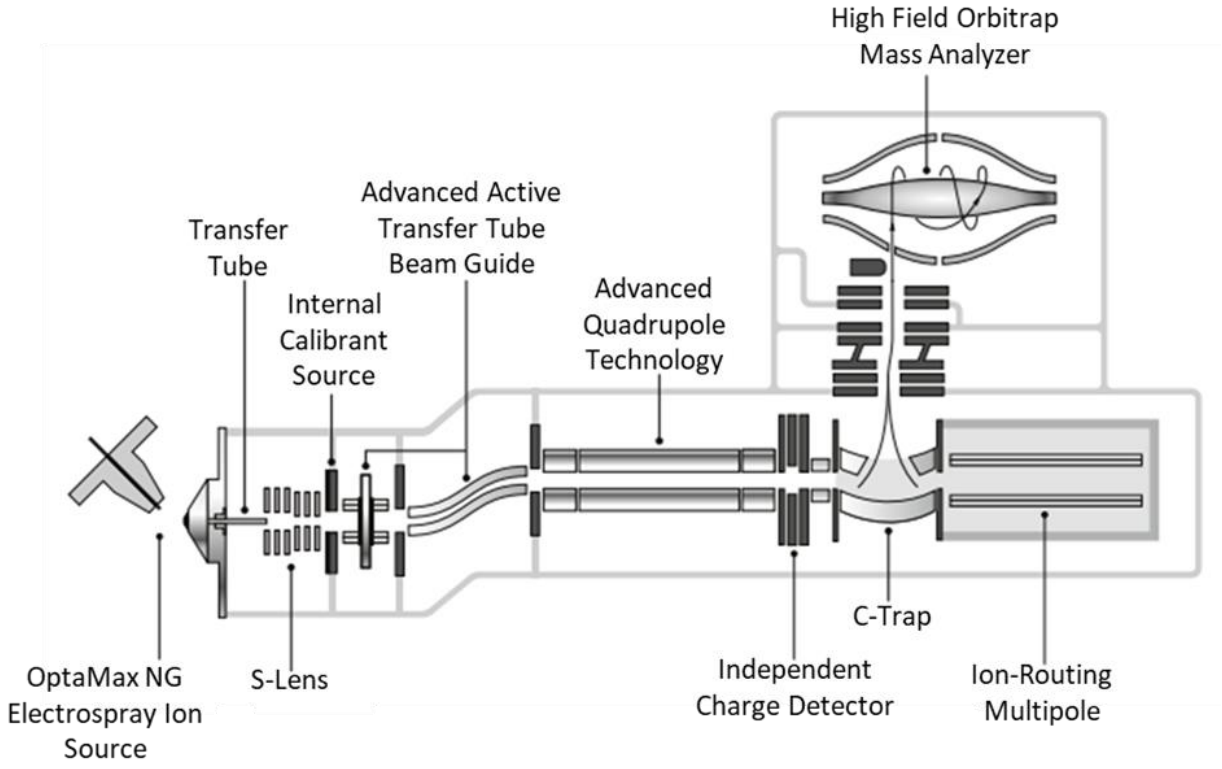

By integrating quadrupole precursor selection, HCD fragmentation, and high-resolution Orbitrap detection, the Orbitrap Exploris 120 combines speed, sensitivity, and mass accuracy to meet the demands of modern analytical laboratories. Its high-resolution capabilities make it an essential tool in proteomics for peptide mapping and biomarker discovery, metabolomics for metabolic profiling and lipidomics, and pharmaceutical research for therapeutic protein characterization and small-molecule quantification. The system's robust design, efficient ion transmission, and high dynamic range establish it as a powerful and indispensable mass spectrometry platform for both discovery-based and targeted analytical applications [81].

1.6.4) Thermo Scientific™ Vanquish™ UHPLC system

The Thermo Scientific™ Vanquish™ UHPLC system is a state-of-the-art liquid chromatography platform designed for high-performance and high-throughput analysis. It integrates cutting-edge technology to deliver superior resolution, sensitivity, and precision in chromatographic separations, making it a preferred choice for analytical laboratories in various fields, including pharmaceutical, biotechnological, and environmental sciences.

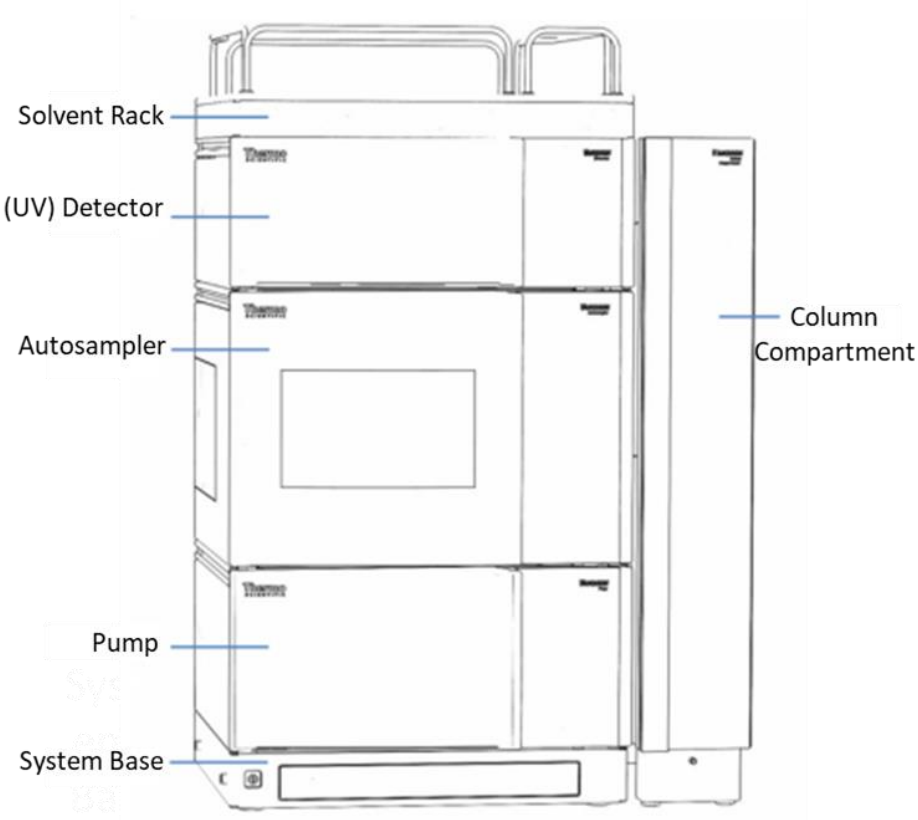

Figure 1.7) Adapted from Thermo Fisher Scientific Vanquish UHPLC and HPLC Systems Operating Manual [82] Schematic of Vanquish UHPLC and HPLC system.

The Vanquish UHPLC system is built with an innovative modular architecture, allowing seamless integration of its key components: the solvent rack, pump, autosampler, column compartment, and detector. This design ensures optimal performance and efficiency, enabling fast analysis times without compromising chromatographic quality. The system is engineered to operate at ultra-high pressures, allowing the use of sub-2 µm particle columns for enhanced separation efficiency and peak resolution.

At the core of the Vanquish system is its high-pressure binary or quaternary pump, which provides precise and consistent solvent delivery. The advanced autosampler ensures accurate sample

injection with minimal carryover, while the thermostatted column compartment maintains stable conditions to improve reproducibility.

The Vanquish system employs Thermo Scientific's proprietary SmartFlow™ technology, which minimizes pulsation and improves flow accuracy, crucial for maintaining chromatographic integrity. Additionally, its advanced gradient control ensures reproducible retention times across multiple injections. The system is controlled via the Chromeleon™ Chromatography Data System (CDS), which provides intuitive software capabilities for instrument operation, data acquisition, and processing.

With its robust design, high operational efficiency, and advanced control features, the Vanquish UHPLC system sets a new benchmark in chromatographic analysis, ensuring reliable and reproducible results in even the most demanding analytical applications [82].

1.7. Research Objectives

In this dissertation, the primary objective was to explore novel applications of MS techniques, including ESI, MS/MS, MALDI, SSI and IP-LC-MS/MS. The goal was to develop methods for the chemical profiling, detection, and quantification of a wide range of targeted and untargeted analytes in complex biological matrices. Below, I have outlined my contributions to each corresponding publication.

Chapter 2

Title: *Application of Sandpaper Spray Ionization Mass Spectrometry to Comprehensively Examine Maple Leaves Infected with Distinct Fungi*
DOI: https://doi.org/10.1002/jms.5000
Co-authors: Laurentiu G. Dabija, Rani Shouk, Dani Shouk, Rodinei Augusti, Demian R. Ifa

- Contributions:
    - Designed the experiments.

- Conducted sample preparation and sandpaper spray ionization (SSI) mass spectrometry analysis.
- Performed data interpretation and identified key metabolic differences between infected and healthy maple leaves.
- Prof. Demian Ifa and prof. Rodinei Augusti provided mentorship and guidance during data analysis and manuscript preparation.

Chapter 3

Title: *Development of a Matrix-Assisted Laser Desorption Ionization High Resolution Mass Spectrometry Method for the Quantification of Camalexin and Scopoletin in Arabidopsis thaliana*
DOI: https://www.researchgate.net/publication/383940229
Co-authors: Ivan Monsalvo, Nikola Kovinich, Demian R. Ifa

- Contributions:
    - Developed the MALDI-HRMS method for quantification of camalexin and scopoletin.
    - Conducted all sample preparation and mass spectrometry analysis.
    - Interpreted the results and wrote the manuscript.
    - Prof. Demian Ifa provided mentorship and feedback throughout the project.

Chapter 4

Title: *Development of an Immunoprecipitation-Liquid Chromatography-Tandem Mass Spectrometry (IP-LC-MS/MS) Strategy for the Detection of low-abundance proteins in Rat Serum*

- Contributions:
    - Designed and developed the IP-LC-MS/MS method for the detection and quantification of recombinant EPO in rat serum.

- Performed immunoprecipitation to selectively isolate EPO from complex serum matrices.
- Conducted all LC-MS/MS analyses and data interpretation.
- Rick Bagshaw provided mentorship and guidance throughout the method development and manuscript preparation process.

Chapter Two: *Application of sandpaper spray ionization mass spectrometry to comprehensively examine maple leaves infected with distinct fungi*

Chapter 2 is a version of the published manuscript: Parasecolo L, Dabija LG, Shouk R, Shouk D, Augusti R, Ifa DR. Application of sandpaper spray ionization mass spectrometry to comprehensively examine maple leaves infected with distinct fungi. J Mass Spectrom. 2024 Feb;59(2):e5000. doi: 10.1002/jms.5000. PMID: 38263874.

2.1) Abstract

This study describes a novel application for sandpaper spray ionization mass spectrometry (SPS-MS), to examine the surface of maple tree (*Acer* sp.) leaves.

By comparing mass spectrometry fingerprints, healthy leaves from those infected with powdery mildew and *Rhytisma acerinum* were distinguished.

Leaves were grated with sandpaper, cut into triangles, and placed before the mass spectrometer, with the addition of a methanol-formic acid solution.

Multivariate statistical analysis categorized the samples into three groups. Overall, SPS-MS effectively analyzed leaves with infectious microorganisms, potentially aiding in the creation of fungal identification databanks.

2.2) Introduction

Mass spectrometry (MS) has been commonly used as a method for obtaining small molecules and protein fingerprints of fungal species. However, traditional techniques like matrix-assisted laser desorption/ionization (MALDI) or MS coupled with chromatography separation systems often involve lengthy analysis times and complex sample preparation procedures that demand skilled personnel [83]. In contrast, sandpaper spray ionization MS (SPS-MS) offers an exceptionally rapid screening of solid sample components, with a straightforward sample extraction process that can be easily carried out outside the laboratory by less specialized personnel. SPS-MS represents a novel ambient ionization technique with several notable advantages. Santos et al. developed this technique to offer a textured surface with a significantly greater area than traditional paper, rendering it an excellent choice for directly analyzing solid materials. The authors demonstrated the ability of these techniques to analyze solid samples using raw green coffee beans as prototype samples. The beans were sanded using a triangular-shaped sandpaper, and the mass spectra were acquired via an identical procedure as that employed in the correlate paper spray ionization MS (PS-MS) technique [84].

SPS-MS presents several potential benefits, particularly in analyzing solid samples with adequate malleability, such as wood, plastic, and cultured grains. The advantages of SPS-MS are briefly summarized as follows: Enhanced Surface Coverage: Sandpaper's rough surface texture provides

superior surface coverage compared with traditional paper. This improved contact area allows for more efficient extraction and ionization of analytes from solid samples.

Direct Analysis of Solid Materials: SPS-MS enables the direct analysis of solid samples, eliminating extensive sample preparation. This feature is particularly advantageous when dealing with materials that are not easily dissolved or require complex extraction procedures.

Malleability and Versatility: Sandpaper can adapt to various solid materials, including wood, plastic, and cultured grains. This versatility makes SPS-MS a valuable tool for multiple applications, from food analysis to material characterization.

Minimal Sample Manipulation: Unlike other techniques that may require modification or pretreatment of samples, SPS-MS minimizes sample manipulation. This saves time and reduces the risk of introducing artifacts or contaminants.

Compatibility with Various Materials: The rough and conductive sandpaper surface efficiently ionizes a wide range of compounds, including polar and nonpolar analytes. This broad compatibility extends the applicability of SPS-MS across diverse sample types.

Cost-Effective Support: Sandpaper is a readily available and cost-effective material, making SPS-MS an economical choice for analytical laboratories.

In summary, SPS-MS presents a promising advancement in ambient ionization MS, particularly for analyzing solid materials. Its unique characteristics offer improved surface coverage, compatibility with several solid samples, and minimal (if any) sample preparation steps, thus positioning it as a valuable tool for researchers across multiple disciplines [84].

The Acer genus, belonging to the Aceraceae family and commonly recognized as maple trees, encompasses 129 distinct species and numerous subspecies. These plants are distributed across the northern hemisphere. They thrive notably in temperate regions, including East Asia, eastern North America, and Europe [85].

Powdery mildew is formed by several fungi species belonging to the Erysiphaceae family within the Ascomycota phylum. It is a plant disease characterized by its distinctive life cycle and parasitic relationship with host plants. These fungi were historically categorized under the genus Oidium

due to their production of hyphae with conidiophores that form chains of conidiospores. Powdery mildew exhibits an obligatory parasitic trophic relationship with host plants, primarily acting as ectoparasites by developing mycelium on the plant's surface. They penetrate the host's epidermis through specialized structures called haustoria, with some species capable of entering through stomata. The disease affects organs with high vegetative activity, including leaves, herbaceous shoots, and developing fruits. Initially, infected areas show discoloration, leading to tissue necrosis and, in fleshy organs like fruits, the development of splits [86, 87].

The tar spot, caused by *Rhytisma acerinum*, follows a distinctive life cycle and pattern of spread. Emerging leaves become vulnerable to infection in spring during cool and wet weather. This fungus primarily targets Norway Maple trees, forming large spots, an inch in diameter, on the leaves. As the maple leaves mature, they develop light to yellowish-green spots within the infected areas. In severe cases, infected leaves may drop prematurely [88, 89].

In addition to its impact on crops, tar spots can pose risks to some herbivore animals that may ingest infected vegetation and be adversely affected. Horses, in particular, are sensitive to certain fungi and may experience health issues upon consuming plants contaminated with fungal spores [90].

This work demonstrates the usefulness of SPS-MS to analyze maple leaves infected by powdery mildew or tar spots, taken as proof-of-concept samples. The MS profiles are compared to verify whether the healthy and infected leaves could be distinguished by their MS profiles. The reproducibility of SPS-MS is appraised by demonstrating whether analytical and biological replicates yield similar MS profiles.

Unsupervised statistical methods are applied to determine whether the samples can be allocated into distinct clusters. To our knowledge, the issue reported herein does not represent any severe threat to farming activities. However, the convenient attributes of maple leaves, mainly their easy access and convenient malleability, led us to select them as suitable samples to demonstrate the potential of SPS-MS in providing rapid, crucial, and helpful information for combating the harmful effects caused by fungal infestation of crops, a risky issue for farmers [91-94].

Moreover, the unique characteristics of SPS-MS allow for an efficient database construction for comprehensive fungal identification. This database, with the mass spectra profiles of various types

of fungi, could facilitate quick and accurate identification of fungi affecting plants, as previously described with bacteria [95]. Such a resource not only streamlines the diagnostic process but also empowers agricultural communities to make timely decisions and implement targeted interventions, bolstering the resilience of farming systems, thus benefiting crop protection and helping safeguard the well-being of livestock and other creatures within the agricultural ecosystem.

2.2) EXPERIMENTAL SECTION

2.2.1) Sampling

Three kinds of leaves were collected within the Keele campus of York University (North York, Toronto, ON, Canada). These were classified as healthy, infected by *Rhytisma acerinum* (tar spot), and powdery mildew (white mold; Figure 2.1). As previously explained, these samples were easily accessible and suitable for demonstrating the usefulness of the SPS-MS technique.

Biological triplicates of healthy and infected leaves were sampled on different days from diverse trees and analyzed on the same day of sampling. Each biological replicate (three of each group) was analyzed in three analytical replicates (n = 27).

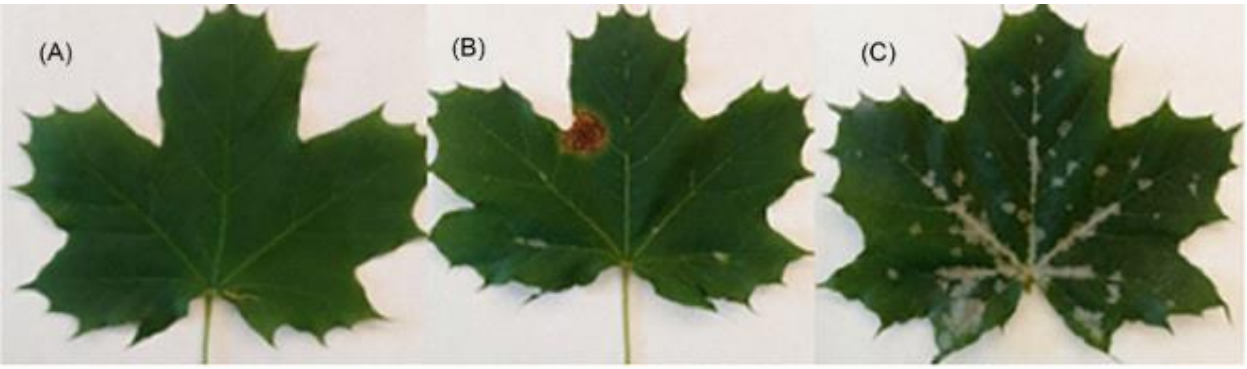

Figure 2.1) Optical images of maple leaves: (A) healthy; (B) infected by the mold *Rhystima actinium* (tar spot); (C) infected by the powdery mildew (white mold).

2.2.2) Sample Preparation

Richard 900 150-grit sandpaper was purchased from a local store. Various types of sandpaper, including 100 and 120 grits, were evaluated before the analysis. However, challenges arose during

the extraction process with finer grit sandpaper, as it tended to bend when rubbing the leaf, hindering the overall effectiveness of sample extraction.

For the experiments, each leaf was slightly rubbed against the sandpaper. The sandpaper, now bearing the rubbed material, was cut into an equilateral triangle shape with sides of 1.0 cm for each replicate. This careful process ensured the highest reproducibility between replicates. The triangle was placed 0.5 cm away from the MS inlet, aligned with the ion transfer path of the mass spectrometer, and held by an alligator clamp supplying the required high voltage. A workflow of this experimental procedure is provided in Figure 2.2.

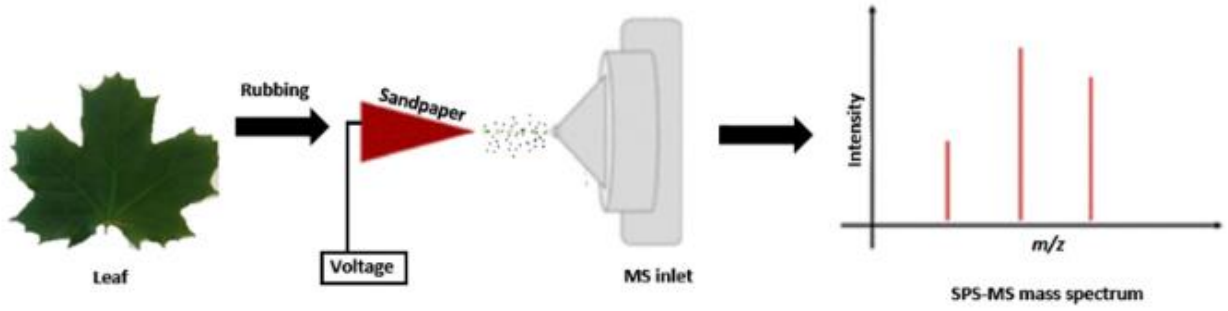

Figure 2.2) Schematic workflow of sandpaper spray ionization mass.

High-performance liquid chromatography (HPLC)-grade methanol (25 μL, Sigma Aldrich, St. Louis, MO, USA) with 0.1% formic acid (Sigma Aldrich, St. Louis, MO, USA) was deposited over the rubbed sample, and the acquisition started.

2.2.3) MS Parameters

The data were acquired using a linear ion trap mass spectrometer (LTQ, Thermo Fisher Scientific, San Jose, CA). The mass spectra were recorded under the following conditions:

- Automatic gain control and a maximum ion trap injection time of 200 ms with three micro scans.
- Spray voltage: ±4 kV.
- Capillary temperature: 300°C.

- Tube lens voltage: 102 V.
- Capillary voltage: 48 V.

The full-scan mass spectra were acquired in the positive and negative ion modes with an m/z range of 100–500. For MS/MS experiments, a precursor ion of interest was selected and dissociated using collision-induced dissociation (CID) with helium as the collision gas. Dissociation profiles were obtained using a normalized collision energy (NCE) between 20% and 40%.

2.2.4) Data Processing and Statistical Analysis

ProteoWizard's MSConvert software converted the RAW data into the mzXML format [96]. The top 10 ions with the highest abundance were selected from each sample. Deisotoping, feature alignment, and gap filling were performed using MZmine 2.53 [97].

A one-factor statistical analysis was conducted using MetaboAnalyst 5.0 [98]. The data underwent:

1. Normalization by sum.
2. Filtration based on the interquartile range (IQR).
3. Logarithmic transformation and mean centering.

Principal Component Analysis (PCA) and Hierarchical Cluster Analysis (HCA) were performed, employing Pearson's correlation as the distance measure and Ward's linkage as the clustering algorithm.

2.3) RESULTS AND DISCUSSION

Initially, leaf spray ionization was attempted by directly analyzing maple leaves cut into a triangle shape. However, the acquired mass spectra showed low-intensity and non-reproducible signals for each extraction solvent. This was likely caused by the waxy cuticle layer covering the leaves, which hinders the efficient extraction of analytes and their subsequent ionization [99, 100].

Therefore, Sandpaper Spray Ionization MS (SPS-MS) was tested as an alternative approach capable of providing a better response due to its superior ability to extract analytes from leaves.

With the selection of SPS-MS for its enhanced extraction capabilities, attention was then turned to optimizing the experimental variables. Conditions such as voltage, capillary temperature, solvent, and the distance and angle between the triangle tip and the mass spectrometer inlet were optimized based on signal intensity and stability. Three solvents were evaluated: methanol, acetonitrile, and chloroform. Chloroform did not provide significant signals; acetonitrile resulted in spectra with minimal noise but low intensity, whereas methanol yielded the best response and was selected as the carrier solvent for analysis.

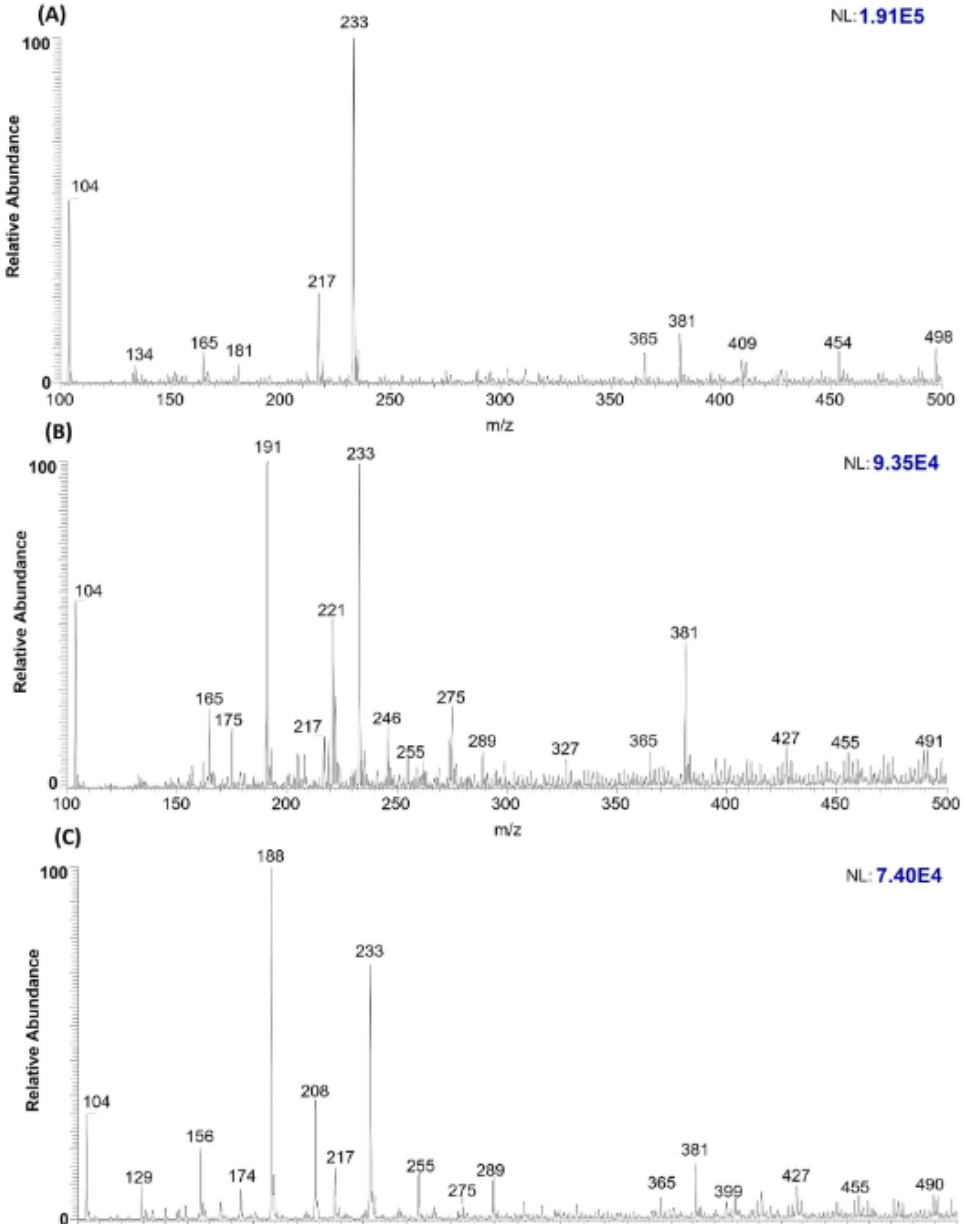

Figure 2.3) Sandpaper spray ionization mass spectrometry spectra of maple tree leaves in the positive ion mode: healthy (A), infected by *Rhytisma acerinum* (tar spot) (B), infected by powdery mildew (white mold) (C).

Additionally, traditional Paper Spray Ionization MS (PS-MS) was conducted for comparative analysis. While ions and their signal intensities were similar between PS-MS and SPS-MS, the stability of the sandpaper substrate in SPS-MS enhanced the analytical process. This increased stability facilitated the monitoring of diagnostic ions by yielding mass spectra with less noise and streamlining sample preparation. Furthermore, without the need for liquid–solvent extraction, the overall analysis time was significantly reduced. Thus, SPS-MS was deemed the optimal technique for this analysis.

Acquisitions were performed in triplicates in both the positive and negative ion modes, analyzing biological replicates for each leaf type (n = 9). The positive ion mode was chosen due to its superior response compared to the negative mode. The positive mode also allowed for straightforward data interpretation, with reference ions such as m/z 104, 365, and 381 (representing K^+ adducts of γ-aminobutyric acid and Na^+ and K^+ adducts of disaccharides) being well-documented as plant metabolites [101, 102].

In contrast, negative ion mode spectra primarily contained fatty acids in their deprotonated forms, which exhibited poor intra-day reproducibility. Additionally, blank spectra of the sandpaper substrate were collected at the start of each analysis, confirming no correspondence with the ions derived from the samples.

As shown in Figure 2.3, several ions associated with infected leaves were detected. Diagnostic ions included m/z 188/208 for white mold-infected leaves and m/z 191/221 for tar spot-infected leaves. These ions were consistently observed in all analytical and biological replicates of the infected leaves. MS/MS data for diagnostic ions m/z 188 (white mold) and m/z 191 (tar spot) were acquired (Table 2.1). Although putative identification was attempted, the lack of publications on MS-based data for specific fungi species and maple tree metabolites prevented a definitive match. Nevertheless, the MS/MS data identified sodium and potassium adducts of the same metabolite, such as m/z 365 and 381, ascribed to sucrose adducts in the healthy leaf spectrum (figure 2.3).

Precursor ion *m/z*	Optimal NCE	Product ions *m/z* (relative intensity)
188	25	129 (100), 187 (8), 169 (5), 146 (2)
191	20	173 (42), 159 (35), 163 (15), 161 (13), 145 (11)
217	35	157 (50), 113 (36), 173 (30), 199 (28), 119 (19)
233	25	215 (100), 84 (60), 173 (48), 171 (18)

Table 2.1) Precursor and Product Ions for Diagnostic Analysis of Maple Leaves Infected by Powdery and Tar Mold Fungi

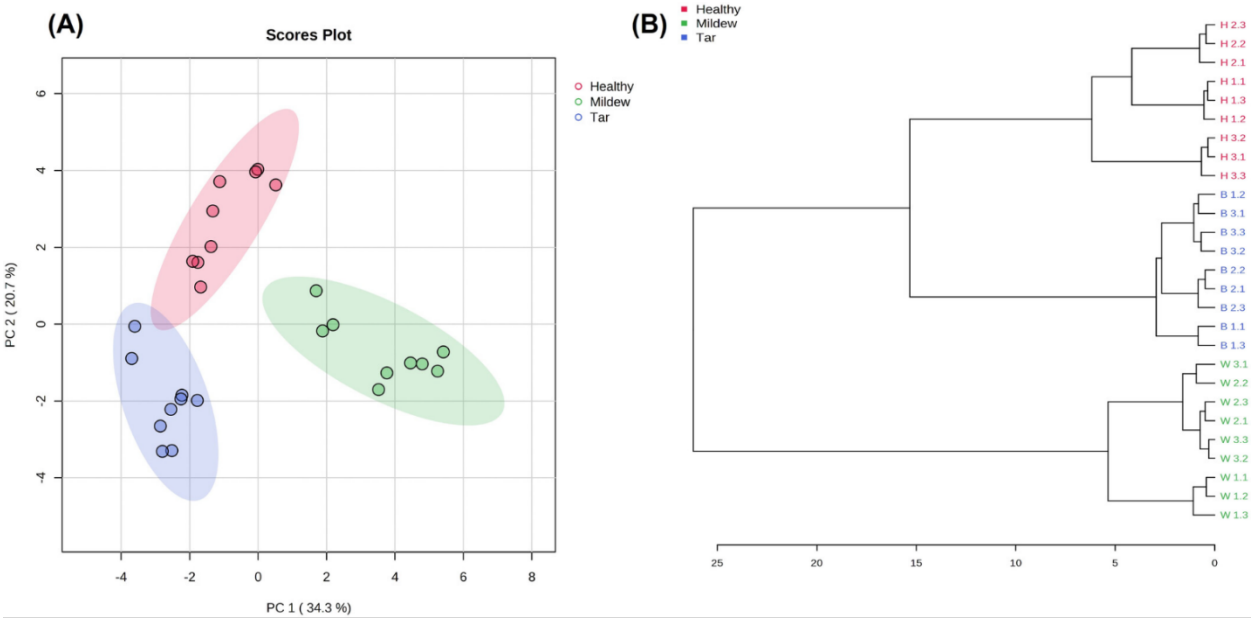

Figure 2.4) (A) Principal component analysis (PCA) score plot and **(B)** hierarchal clustering analysis (HCA) dendrogram displaying the split among the three types of maple tree leaves: healthy (red), infected with the white powdery mildew (green), and infected by the tar mold (blue) ($n = 9$ replicates per type of leaf).

Overall, identifying the most relevant ions was not the primary goal of this work. However, this approach could be applied to more thoroughly characterized biological samples using the same technique.

Principal Component Analysis (PCA) and Hierarchical Cluster Analysis (HCA) were used to distinguish leaf samples based on their unique chemical signatures. Despite being from the same species, variations in the chemical profiles were observed due to the presence of infection-specific ions at m/z 188, 208, 191, and 221 (Figure 2.4A, B). These ions had the highest scores in the loading plot, contributing to the correct clustering of samples.

Three distinct clusters representing healthy, white mildew-infected, and tar spot-infected leaves were evident in the PCA score plot (Figure 2.4A). HCA (Figure 2.4B) further visualized these clusters as branches in a dendrogram, confirming the reproducibility of the clustering pattern. The consistency between PCA and HCA results demonstrates the excellent analytical reproducibility achievable with SPS-MS for this prototype biological analysis. The overall variability was primarily determined by the sample type (healthy, mildew-infected, or tar spot-infected).

2.4) Conclusion

In conclusion, our proof-of-concept study demonstrated the successful application of SPS-MS as an innovative technique for direct and fast analysis of leaves infected with two distinct types of molds: white and tar. Through this approach, we achieved MS fingerprints, enabling prompt comparison of such different samples and the identification of diagnostic ions. The technique's efficacy and usefulness in this unprecedented application highlight its potential for rapid analysis of plant tissues and its promising role in environmental and biological research. One particularly intriguing future prospect is creating a comprehensive database, housing mass spectra profiles of various fungal strains. Such a resource would streamline the diagnostic process, enabling, for instance, agricultural communities to promptly detect and address fungal threats, thus bolstering the resilience of agriculture.

Chapter Three: Development of a Matrix-assisted laser desorption ionization high resolution mass spectrometry method for the quantification of Camalexin and Scopoletin in *Arabidopsis thaliana*

Chapter 3 is a version of the published manuscript: Parasecolo L, Leonardo Parasecolo, Ivan M. Monsalvo, Nikola Kovinich, Demian R. Ifa Development of a Matrix-assisted laser desorption ionization high resolution mass spectrometry method for the quantification of Camalexin and Scopoletin in Arabidospis thaliana. *Authorea.* September 10, 2024.

3.1) Abstract

Understanding plant defense mechanisms against pathogens is essential for enhancing agricultural productivity and crop protection. This study focuses on the quantification of camalexin and scopoletin, two critical phytoalexins in *Arabidopsis thaliana*, using mass spectrometry techniques. Precise measurement of these compounds provides insights into plant resistance and supports agricultural research.

Camalexin and scopoletin were quantified using matrix-assisted laser desorption ionization high-resolution mass spectrometry (MALDI-HRMS). The matrix and solvent conditions were optimized to maximize sensitivity and accuracy. MS/MS experiments confirmed compound identification with high mass accuracy (mass error < 5 ppm). The method was validated through comparative analysis of wild-type (WT) and mutant *Arabidopsis* lines, using internal standards and multiple replicates to ensure precision and reliability.

The method exhibited high linearity for scopoletin (R^2 = 0.9992) and camalexin (R^2 = 0.9987) across concentration ranges of 0.16–5 µM and 0.31–5 µM, respectively. Limits of detection (LOD) were 0.16 µM for camalexin and 0.04 µM for scopoletin, with limits of quantification (LOQ) at 0.2 µM and 0.08 µM, respectively. Samples analysis demonstrated reliable quantification in WT and mutant lines, with significant reductions in camalexin and scopoletin levels observed in the *atwrky33-2* and *atmyb15-1* mutants, respectively. Additionally, the method detected sub-physiological concentrations, confirming its sensitivity and robustness for low-level detection.

This study presents a validated, precise, and accurate MALDI-HRMS method for the quantification of camalexin and scopoletin in *Arabidopsis thaliana*. The approach not only enhances understanding of plant defense mechanisms but also offers potential applications for biotechnological and agricultural research, especially for investigating genetic variations and stress-induced phytoalexin production.

3.2) Introduction

Phytoalexins are specialized low-molecular-weight metabolites produced by plants in response to pathogen attacks. They vary in structure among plant species [74, 75] and are crucial for agricultural resistance to pathogens [104, 105]. For example, glyceollins confer resistance in

soybean to *Phytophthora sojae* and *Macrophomina phaseolina* [106, 107], while camalexin provides resistance in *Arabidopsis thaliana* to *Plasmodiophora brassicae* and *Alternaria brassicicola* [106, 107].

For the last three decades, *Arabidopsis thaliana* has served as a model organism to understand how phytoalexin production is regulated, as it can produce at least 12 different phytoalexins in response to biotic stressors [104]. The most well-studied phytoalexins are camalexin and scopoletin, for which all the enzymes involved in their biosynthesis have been characterized [104]. Camalexin, an indole alkaloid, provides resistance to pathogens such as *Botrytis cinerea*, *Piriformospora indica*, *Alternaria brassicicola*, and *Pseudomonas syringae* [108]. Similarly, scopoletin offers resistance to various pathogens, including bacteria, fungi, and protozoa [109]. Numerous studies highlight the genes involved in phytoalexin synthesis, underscoring their significance in plant biology [110-112]. Beyond agriculture, phytoalexins also show potential for treating human diseases [113-115].

Mass spectrometry (MS) is crucial for plant metabolomics, offering comprehensive insights into plant metabolomes, metabolism, and interactions with pathogens [116]. It has significantly advanced our understanding of plant adaptation to environmental and biotic stresses [117]. Despite challenges in identifying unknown metabolites and achieving accurate quantitative analysis, ongoing MS advancements show promise [118].

Analytical methods for the quantification of camalexin and scopoletin have been developed over the past decades [119-127]. While these methods demonstrate remarkable analytical performance, particularly in sensitivity, they often require extensive sample preparation and significant solvent use, leading to high costs and prolonged analysis times. These factors pose considerable drawbacks, especially when processing large sets of samples.

MALDI-MS stands out for biomolecule analysis due to its speed and ease of use. Initially used for qualitative analysis, it now supports quantitative analysis despite challenges with low-mass analytes [128]. Optimizing experimental parameters and sample preparation, particularly matrix selection and crystallization, minimizes variability. Careful design and optimization allow for meaningful quantitative comparisons, making MALDI-MS valuable in biological research [128, 129].

This study developed a MALDI-HRMS method for the absolute quantification of camalexin and scopoletin in *Arabidopsis* plants. The method's performance was evaluated for linearity, LOD, LOQ, accuracy, and precision to ensure reliability and reproducibility. This advancement provides a rapid, precise, and accurate tool for studying plant defense mechanisms and supports future research in plant biology, biotechnology, agriculture, and pharmaceuticals.

3.3) Experimental Methods

3.3.1) Reagents

All reagents used in this study were sourced from Sigma-Aldrich (Oakville, Canada), unless otherwise stated. These included Murashige and Skoog (MS) medium with vitamins, sucrose (≥99.5%), and Gelzan™ CM for seed plating and media preparation. Solvents for extraction included methanol (HPLC grade), water (LC-MS grade), acetic acid (≥99.7%), acetone (≥99.5%), and acetonitrile (HPLC-MS grade). MALDI matrices—9-aminoacridine (9-AA, ≥99.5%), 5-chloro-2-mercaptobenzothiazole (CMBT, ≥90%), and 1,5-diaminonaphthalene (DAN, ≥95%)—were used for ionization studies. Ethanol (≥99.5%) and methanol (HPLC grade) were employed to extract *Taraxacum officinale* powder. Standards included scopoletin (≥99%) and camalexin (≥98%), with indolepropionic acid (≥99%) and daidzein (≥98%) as internal standards. Liquid nitrogen was used for snap-freezing samples. The synthetic elicitor flg22 peptide was purchased from PhytoTech Lab. Pierce™ Negative Ion Calibration Solution for negative ionization mode was purchased from Thermo fisher (Thermo Fisher Scientific, San Jose, CA).

3.3.2) Plant metabolite extraction

For method optimization and target compound detection, *Arabidopsis* seeds were sterilized following Denoux et al. (2008) [130]. The sterilized seeds were plated on solid MS medium with vitamins, along with 1% sucrose and 2.5 g/L Gelzan to solidify the medium, at pH 5.8. Seeds were kept in darkness at 4°C for 3 days, exposed to cool white T5 fluorescent lights (100 $\mu Em^2/s$) for 5–6 hours, and returned to darkness at 22°C for 3 days. Seedlings were transfer into a 16 hour photoperiod using cool white T5 fluorescent lights (100 $\mu Em^2/s$). Five-day-old seedlings (15–20) were transferred to liquid MS medium in 12-well plates and grown for five more days. A day before treatment, the medium was replaced with fresh MS medium. On day 10, the seedlings were treated with 5 μM flg22 (a 22 aminoacids peptide fragment from bacterial flagellin that triggers

phytoalexin production; QRLSTGSRINSAKDDAAGLQIA) for 16 hours. They were then snap-frozen in liquid nitrogen, lyophilized, weighed, and homogenized using a ball mill [100]. For extraction, 1 mL of methanol was added to the homogenized sample, followed by 30 minutes of sonication and centrifugation at 13,200 g for 15 minutes. The supernatant was collected and dried under nitrogen gas (first extract). A second extraction was performed using 20 µL of MeOH:H2O:AcOH (80:19:1) per mg of dry sample. The supernatant from this step was used to dissolve the first extract for subsequent MS analysis.

3.3.3) MALDI-HRMS condition optimization

MALDI-HRMS experiments were conducted using a Q-Exactive mass spectrometer (Thermo Fisher Scientific) equipped with a Spectroglyph ESI/MALDI ion source (Spectroglyph LLC, Kennewick, WA). The acquisitions were performed with a resolving power of 70,000 at m/z 200, a maximum injection time of 200 ms, AGC target=1E6, and an m/z range of 100–1,000. The acquired ion intensities were extracted using Thermo Xcalibur Qual Browser. To optimize camalexin detection, various MALDI matrices known for ionizing small molecules [45, 131] were tested: 9-AA and CMBT in negative mode, and DAN in positive and negative modes. These matrices were solubilized until saturation and evaluated with different solvents (acetone, methanol, and acetonitrile). Plant extract and matrix solutions were mixed 1:1, and 4 µL of the mixture was applied to a Teflon-coated slide (Tekdon Incorporated, Myakka City, FL), dried, and analyzed. Laser currents were set to 2 A for CMBT, 1.8 A for DAN, and 2.5 A for 9-AA, with a repetition rate of 300 Hz. Each acquisition was performed by scanning the sample for 30 seconds.

The identification of target compounds, scopoletin (m/z 191.0350) and camalexin (m/z 199.0330), involved analyzing standard solutions and comparing them with treated samples. Only m/z values within 5 ppm of the exact target masses were considered. Fragmentation spectra from both standard solutions and flg22-treated samples were cross-referenced with the Human Metabolome Database (HMDB) for further confirmation [132]. MS/MS analysis used a normalized collision energy of 40.0 (z = 1) with a laser current of 1.8 A, a 300 Hz repetition rate, and an acquisition range of m/z 50–200. Target ions were monitored at m/z 191.0 ± 0.2 for scopoletin and 199.0 ± 0.2 for camalexin (Figure S3.1).

3.3.4) Preparation of Samples for Calibration and Analysis

A biological matrix resembling the *Arabidopsis* metabolome was created as follows: *Taraxacum officinale* samples were washed with ethanol, dried at 60°C, and ground into a powder. Metabolites were extracted using 80% methanol at 20 µL per mg of powder. The mixture was centrifuged (5 minutes at 14K RPM) to separate the supernatant, which was then divided into 40 µL aliquots. These aliquots were used to create calibration curves and quality controls at low, medium, and high concentrations.

3.3.5) Blank analysis

Before adding the target analytes and their internal standards to the biological matrix, one portion was combined with a matrix solution in a 1:1 ratio. This mixture was then analyzed using MALDI-HRMS to confirm the absence of target compounds, internal standards, or any other isobar substances derived from either the MALDI matrix or the biological matrix (Figure S2.2 and S2.3). The blank analysis was conducted in triplicate alongside the calibration curve and quality control analysis to strengthen the reliability of our findings.

3.3.6) Standard Addition, Internal Standard Selection and Calibration curve

After confirming the absence of interference, 40 µL aliquots were spiked with 5 µL of camalexin and scopoletin standards (0.39–50 µM), yielding final concentrations of 0.04–5 µM (0.16–20 µg/g for camalexin, 0.16–19.20 µg/g for scopoletin) after adding 5 µL of internal standards (IS). These concentrations align with literature values for elicited *Arabidopsis* [119-127]. Indolepropionic acid (1.25 µM) and daidzein (0.62 µM) were used as IS for camalexin and scopoletin (Figure 3.1), respectively, with IS concentrations set at the calibration curve midpoint. Each calibration curve point was acquired in duplicate (n=2), according to and exceeding FDA guidelines, which typically require only single replicates (n=1).

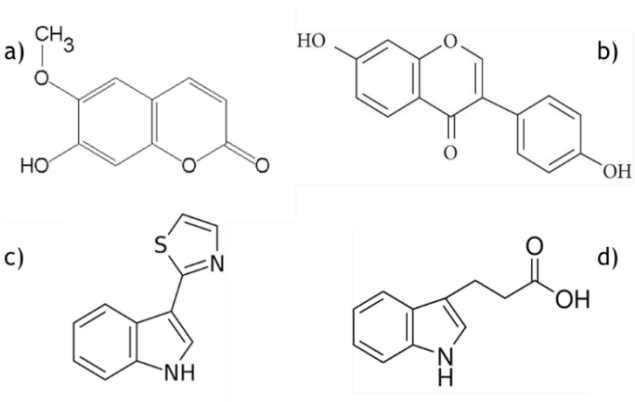

Figure 3.1) Target analytes and their internal standards: a) Scopoletin, b) Daidzein, c) Camalexin, d) 3-Indole-propionic acid

3.3.7) Evaluation of Accuracy, Precision, and sensitivity

The accuracy and precision of the method were assessed through triplicate analyses of quality control samples prepared at three different concentrations: 4 µM (QCH), 1 µM (for camalexin), and 0.9 µM (for scopoletin) (QCM), as well as 0.5 µM (for camalexin) and 0.45 µM (for scopoletin) (QCL). Additionally, the limits of detection (LOD) and quantification (LOQ) were determined by preparing batches at decreasing concentrations until a signal-to-noise ratio of at least 3 and 10, respectively, was achieved.

3.3.8) Arabidopsis thaliana samples analysis

The developed method was applied to the analysis of Arabidopsis thaliana extracts, prepared as described in Section 3.2. Quantitative comparisons were conducted between wild-type (WT) and mutant lines for each compound. For camalexin quantification, we compared the WT with the *atwrky33-2* mutant, which is expected to exhibit reduced camalexin levels [101]. Similarly, for scopoletin quantification, the WT was compared to the *atmyb15-1* mutant, anticipated to show diminished scopoletin production [133]. WT and both mutant lines were obtained from the Arabidopsis Biological Resource Center (ABRC).

Each line underwent two treatments: flg22 (an elicitor) and DMSO (negative control), resulting in six sample groups. Each group consisted of three biological replicates, and each biological replicate was analyzed in triplicate to ensure precision and minimize analytical variability.

For sample preparation, after metabolite extraction (Section 3.2), 10 µL of internal standard solution was added to 40 µL of the extracted metabolome. 10 µL of indolepropionic acid (6.25 µM) was added to both *atwrky33-2* mutant and WT samples for camalexin quantification, and 10 µL of daidzein (3.1 µM) was added to both *atmyb15-1* mutant and WT samples for scopoletin quantification. Then, 20 µL of each prepared sample was mixed with 20 µL of saturated DAN-acetone solution, and 4 µL of the mixture was aliquoted onto a Teflon slide, dried, and analyzed following the developed method. The final concentrations of indolepropionic acid (1.25 µM) and daidzein (0.62 µM) were consistent with the calibration curve and QC samples, ensuring accurate quantification of camalexin and scopoletin, respectively.

3.4) Results and discussion

The analytical performance of the method for absolute quantification of camalexin and scopoletin was comprehensively evaluated.

3.4.1) Matrix selection

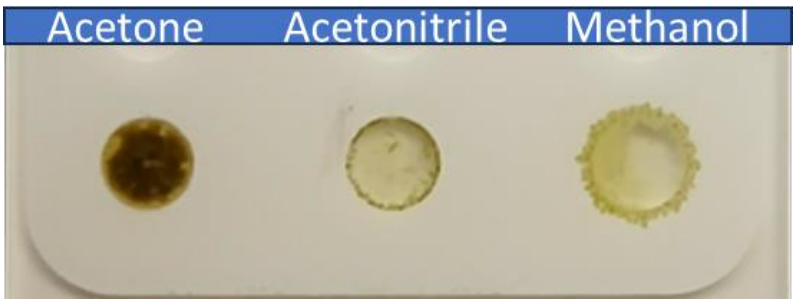

Figure 3.2) Acetone facilitated superior solubilization of DAN, resulting in greater deposition of the MALDI matrix on the slide. Its rapid evaporation promoted more uniform crystallization. These factors likely contributed to the enhanced signal intensity observed, making acetone the preferred solvent for method development.

Initial tests revealed low or no signals with 9-AA and CMBT in negative mode, and DAN in positive ion mode. In contrast, the saturated solutions of DAN in methanol or acetone, in negative mode, produced promising results. These combinations (DAN + acetone and DAN + methanol) were evaluated in triplicate and compared (Table 3.1). Acetone's rapid evaporation and superior

Scopoletin	**Replicate 1**	**Replicate 2**	**Replicate 3**	**Average**
Methanol+DAN	6.43E2	2.51E2	3.73E2	4.22E2
Acetone+DAN	1.31E3	2.18E3	1.88E3	1.79E3
Camalexin	**Replicate 1**	**Replicate 2**	**Replicate 3**	**Average**
Methanol+DAN	2.78E2	9.02E2	7.84E2	6.54E2
Acetone+DAN	2.28E3	9.44E3	2.47E3	4.73E3

Table 3.1) displays ion counts for the m/z values corresponding to scopoletin and camalexin, emphasizing DAN combined with acetone's superior performance. Variability is noted, stemming from the decision to omit normalization in this phase of the study, which may have been unnecessary.

solubilization of DAN promoted consistent crystallization, improving signal strength and reproducibility, establishing it as the optimal solvent for method development (Figure 3.2).

3.4.2) Calibration Curve and Linearity

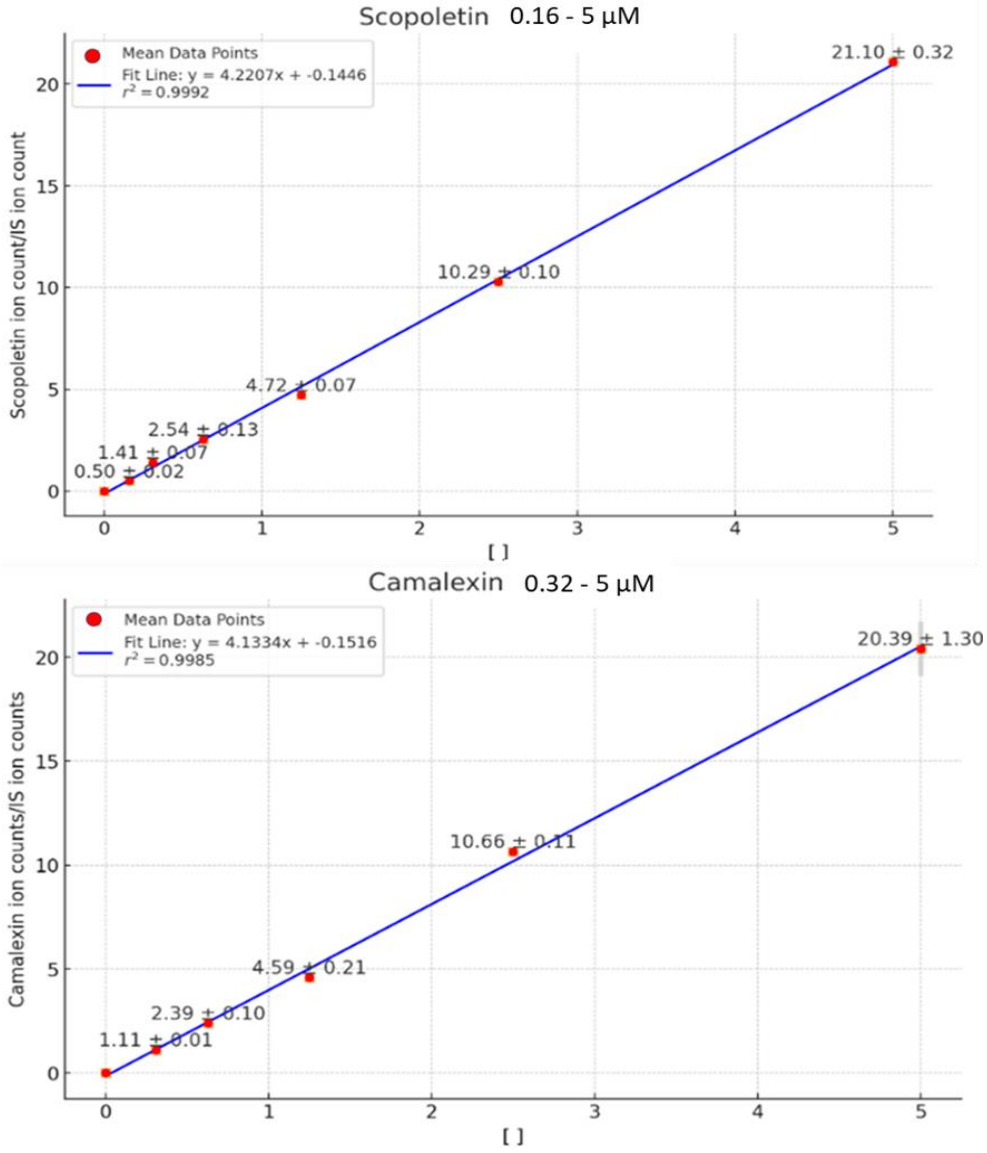

Figure 3.3) Calibration curve assessed for Scopoletin (top) and Camalexin (bottom). On the X axis is reported the range of spiked concentration, on the Y axis the signal of the target compound divided by the signal of its internal standard.

For camalexin and scopoletin, the concentration ranges for the calibration curves were determined based on achieving a signal-to-noise ratio (S/N) exceeding 10. Consequently, a concentration range of 0.16-5 µM (0.64-19.20 µg/g) was established for scopoletin, while a range of 0.31-5 µM (1.25-20 µg/g) was chosen for camalexin. The linearity of the method was verified by examining the obtained R^2 values, both exceeding 0.99. Each point was analyzed in duplicate and the reported results for each point are the average values obtained by the replicate analyses (Figure 3.3).

3.4.3) Sensitivity Assessment

The sensitivity of the method was evaluated by determining the LOD and LOQ for camalexin and scopoletin. Camalexin's LOD was established at a concentration of 0.16 µM, with an S/N of 4.68, while scopoletin's LOD was assessed at 0.04 µM, yielding a S/N ratio of 4.24. LOQ for camalexin was determined to be 0.2 µM, with an S/N of 10.95, and for scopoletin, it was 0.08 µM, with an S/N of 10.90 (Figure S 3.1).

3.4.4) Accuracy and Precision Assessment

Accuracy and precision were evaluated by analyzing quality control (QC) samples in triplicate. Satisfactory performance was observed across all concentration levels for both camalexin and scopoletin. Notably, optimal outcomes were achieved for QC samples at medium concentrations, indicative of typical sample compositions. Table 3.2 summarizes the accuracy, expressed as relative error, and variability, expressed as the coefficient of variability, for camalexin and scopoletin QC samples at different concentration levels. The method demonstrates sufficient sensitivity for detecting and quantifying camalexin across various samples, including WT and mutated varieties. Moreover, it exhibits exceptional sensitivity for scopoletin, enabling detection even at sub-physiological concentrations.

		RE	RSD
Camalexin	QC High 4 µM	6.03%	3.25%
	QC medium 1 µM	1.14%	0.15%
	QC low 0.5 µM	-4.55%	0.90%
Scopoletin	QC High 4 µM	0.57%	3.99%
	QC medium 0.9 µM	-1.96%	1.10%
	QC low 0.45 µM	-9.79%	2.30%

Table 3.2) Accuracy, expressed as relative error (RE), and Variability, expressed as relative standard deviation (RSD), are shown for camalexin and Scopoletin. For each compound, the values obtained for QC samples prepared at High (n=3), Medium (n=3), and Low (n=3) concentrations.

3.4.5) *Arabidopsis thaliana* samples analysis

The results of the sample analysis, presented in Figure 3.4, show that concentrations in WT samples align with values reported in previous studies using various analytical methods [119-127]. The method demonstrates high reliability, accurately detecting both physiological and sub-physiological concentrations, highlighting its sensitivity to genetic variation. Significant reductions in camalexin levels were observed in the *atwrky33-2* mutants [111], while *atmyb15-1* mutants exhibited reduced scopoletin levels [133].

It is worth noting that in one biological replicate of the *atwrky33-2* mutants, despite achieving a signal-to-noise ratio above 10, the calculated concentration (0.24 µM, Table S 3.2) fell below the lowest point of the calibration range. Nevertheless, camalexin was still detected, demonstrating that the method is sensitive enough to identify trace amounts, even when they fall outside the validated calibration range, ensuring reliable detection of low-level presence.

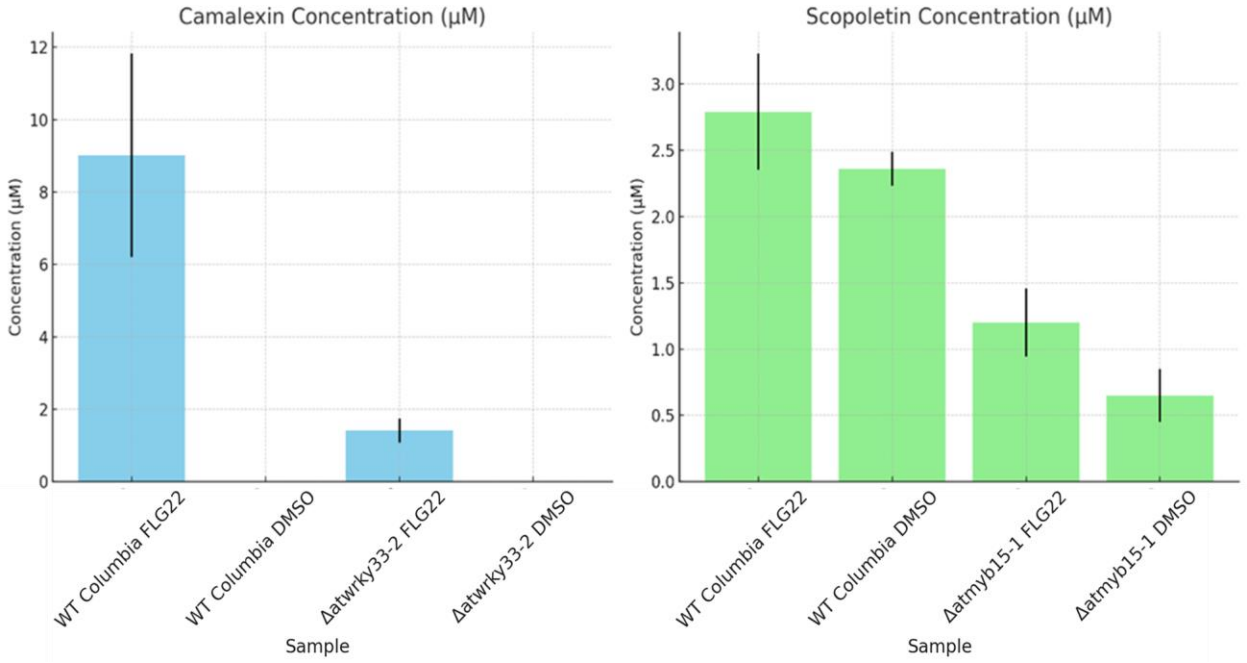

Figure 3.4) Left, concentrations of camalexin in WT FLG22, WT DMSO, Mutated atwrky33-2 FLG22, and Mutated atwrky33-2 DMSO. Right, concentartions of scopoletin inWT FLG22, WT DMSO, Mutated atmyb15-1 FLG22, and Mutated atmyb15-1 DMSO. Error bars are representative of biological variability.

The method's specificity is further confirmed by camalexin being below the LOD in non-elicited samples, consistent with its inducible response to biological stress [127, 130]. In contrast,

scopoletin was detected in both DMSO- and flg22-treated samples, supporting previous reports that it is present under normal physiological conditions as its glucosinolate form and hydrolysed upon abiotic stress [133-135].

In WT samples, scopoletin concentrations were predominantly found in the low-to-mid range of the calibration curve. However, the higher end of the calibration range may be useful for quantifying scopoletin under conditions of enhanced production, such as elicitation by abiotic stress [135] or in genetically modified organisms where its biosynthesis is upregulated. These findings validate the capability of the method for comparing WT and mutant varieties under both basal and stress-induced conditions.

3.5) Conclusion and future directions

We have developed a method for the absolute quantification of camalexin and scopoletin, two crucial phytoalexins in *Arabidopsis*, using MALDI-HRMS. Our optimization of matrix and solvent conditions, along with method validation, showed strong linearity, sensitivity, accuracy, and precision, even at low concentrations. The method was validated using *Arabidopsis* wild-type (WT) plants and mutant lines, specifically *atwrky33-2* and *atmyb15-1*, which exhibit reduced levels of camalexin and scopoletin, respectively. Quantitative comparisons between these genotypes confirmed the method's capacity to detect significant reductions in phytoalexin concentrations. Compared to conventional methods, our approach offers a significantly faster analysis with minimal sample consumption, requiring only 2 µL per run. Each analysis is completed in just 30 seconds, a stark contrast to the several minutes needed for liquid chromatography or the hours required by some gas chromatography methods. While our method is less sensitive than separation-based techniques, which have reported linear ranges for camalexin down to 0.1 µg/g [120, 121, 123], it is highly effective for analyzing elicited *Arabidopsis* samples. Specifically, our method reliably quantifies scopoletin when concentrations exceed 0.15 µg/g and camalexin above 1.25 µg/g, as demonstrated by the linear range of the calibration curve and by the analysis of the *Arabidopsis* sample.

Phytoalexins play crucial roles in plant-pathogen interactions, and understanding their regulation is essential for enhancing plant defense strategies. By providing a reliable and fast method for

quantifying these key metabolites, our work lays the groundwork for deeper insights into plant defense mechanisms against biotic and abiotic stresses.

This advancement supports future research in plant biology and biotechnology, contributing to agricultural and pharmaceutical developments. Our study highlights the significance of MALDI-HRMS in metabolomics research and its potential for elucidating complex biological processes in plants. By offering valuable analytical methods and integrating them with biological questions, we aim to advance our understanding of plant metabolism and physiology, ultimately contributing to increased agricultural productivity and crop yields.

Chapter four: Development of a High-Sensitivity IP-LC-MS/MS Method for Protein Quantification in the Low ng/mL Range: Application to Erythropoietin

Chapter 4 presents a partial draft of a standard operating procedure (SOP) currently in development at Nucro-Technics for IP-LC-MS/MS analysis of low-abundance proteins in rat serum or plasma. This chapter summarizes the research I have conducted over the past months within the industrial setting of Nucro-Technics Inc. (Scarborough, ON), under the guidance of Dr. Rick Bagshaw, research supervisor of the company's toxicology department. Dr. Bagshaw brings extensive expertise to this work, holding a PhD, postdoctoral training, and over a decade of experience in the pharmaceutical industry.

4.1) Abstract

The quantification of proteins at low ng/mL concentrations in biological matrices presents a significant analytical challenge, particularly in preclinical studies where sample volumes are limited. To address this limitation, we developed a highly sensitive method for protein quantification, using recombinant human erythropoietin (rhEPO) as a test case.

Recombinant rhEPO, provided by the Center for Molecular Immunology (CIM), was used to evaluate the method's applicability to therapeutic protein analysis. Selective enrichment of rhEPO from rat serum was achieved through immunoprecipitation, utilizing polyclonal IgG antibodies generated in New Zealand rabbits. These antibodies were purified via Protein A Sepharose chromatography and further isolated using an EPO-conjugated Sepharose gel column. The purified antibodies were biotinylated and conjugated to avidin M80 magnetic beads, ensuring highly specific extraction of rhEPO from complex biological matrices.

Following immunoprecipitation, protein digestion was performed to generate target peptides for quantification. Peptide mapping with Skyline software identified SLTTLLR as the optimal target peptide, and a stable isotope-labeled internal standard (+10 Da) was synthesized to enhance accuracy. The final analysis was conducted using UHPLC-MS/MS, with ongoing optimization to maximize sensitivity.

Preliminary results confirmed the successful enrichment and detection of rhEPO at low ng/mL concentrations in rat serum, demonstrating the method's potential for ultra-sensitive protein quantification. Once fully optimized, this workflow will provide a robust tool for pharmacokinetic and pharmacodynamic assessments of therapeutic proteins, extending beyond EPO to other biologics requiring high-sensitivity detection.

4.2) Introduction

The quantification of low-abundance proteins in biological matrices presents a significant analytical challenge, particularly in preclinical research where sample volumes are inherently limited. While mass spectrometry (MS)-based techniques have revolutionized protein analysis by offering high specificity and structural resolution, their application to low-concentration proteins in small-volume samples remains constrained by sensitivity limitations [136]. Many conventional workflows require large plasma or serum volumes to ensure adequate analyte recovery, rendering them impractical for studies involving small animal models, such as rats, where available sample volumes often do not exceed 100 µL per collection. Addressing this limitation is critical for advancing pharmacokinetic and pharmacodynamic studies of biotherapeutics, necessitating the development of highly sensitive and selective methodologies capable of detecting proteins in the low ng/mL range [136-138].

Erythropoietin (EPO), a glycoprotein hormone primarily synthesized in the kidneys, serves as an ideal test case for developing such a method. EPO plays a crucial role in erythropoiesis by stimulating the survival, proliferation, and differentiation of erythroid progenitor cells in response to hypoxia [137]. Its recombinant form (rHuEPO) has been widely used in the treatment of anemia associated with chronic kidney disease and chemotherapy-induced myelosuppression. However, the accurate quantification of EPO in biological samples is particularly challenging due to its low endogenous concentration, extensive glycosylation (~40% of its molecular weight), and structural heterogeneity [137, 139]. These factors complicate both immunoassay-based and MS-based analytical approaches.

Traditional enzyme-linked immunosorbent assays (ELISAs) are frequently employed for EPO detection due to their high sensitivity. However, these assays lack the specificity required to distinguish between endogenous and recombinant EPO, posing significant limitations in applications such as pharmacokinetics, anti-doping analysis, and biosimilar characterization [68]. In contrast, MS-based methods provide high-resolution characterization of intact proteoforms, glycosylation patterns, and sequence variations, making them indispensable for regulatory and research applications. Yet, despite their advantages, existing MS workflows often require large sample volumes or extensive sample preparation steps to achieve sufficient sensitivity [140, 141].

Previous studies have demonstrated the feasibility of LC-MS/MS-based quantification of EPO and its analogs, such as darbepoetin α, in equine and human plasma. Guan et al. successfully confirmed rHuEPO in equine plasma with a detection limit of 0.1 ng/mL using immunoaffinity separation coupled with LC-MS/MS [140]. However, this approach required ≥1 mL of plasma per sample, an impractical volume for rodent studies. Similarly, other MS-based strategies have provided valuable insights into EPO's glycosylation heterogeneity but have not been optimized for quantification in small-volume, low-concentration matrices such as rat serum [140, 142, 143]. This discrepancy underscores the need for a highly sensitive method capable of analyzing EPO in minimal sample volumes while maintaining precision and reproducibility.

The reliance on high sample volumes, as demonstrated in Guan et al.'s work, highlights a fundamental limitation for MS-based EPO quantification in small animal models. Immunoaffinity separation coupled with LC-MS/MS achieved robust sensitivity but required 1 mL of plasma to ensure sufficient analyte recovery [140]. Such volume demands are infeasible in rat models, where blood collection constraints limit the availability of plasma, making it difficult to apply traditional workflows [144, 145]. Developing new strategies to enhance MS sensitivity while minimizing sample volume requirements is therefore essential.

To bridge this gap, this study aims to develop a highly sensitive LC-MS/MS method for quantifying rhEPO in rat serum at low ng/mL concentrations. Unlike previous workflows designed for larger sample volumes, this approach integrates immunoprecipitation (IP) for selective enrichment of rhEPO prior to MS analysis, maximizing sensitivity while minimizing matrix effects. By leveraging affinity purification strategies and targeted peptide quantification, the proposed method seeks to provide a robust tool for preclinical pharmacokinetic studies, enabling accurate assessment of rhEPO exposure in small animal models. Ultimately, the successful development of this method will extend the applicability of MS-based protein quantification to low-abundance biotherapeutics, enhancing their characterization in both research and regulatory settings [140, 147, 148].

The extremely low concentration of rhEPO in rat serum presents significant analytical challenges, as these levels are often below the detection limits of many standard methodologies. Despite this, serum remains the preferred matrix due to its higher concentration of rhEPO compared to other biological fluids, such as urine. In light of these inherent difficulties, the aim of this study was to

develop a highly sensitive and reliable LC-MS/MS method capable of detecting and quantifying rhEPO at nanogram levels in rat serum. Unlike previously described approaches for equine plasma, which successfully confirmed rhEPO and DPO without requiring quantification [139], this method integrates immunoprecipitation (IP) for sample enrichment prior to LC-MS/MS analysis, ensuring sufficient sensitivity to overcome the low abundance of rhEPO in rat plasma. This advancement addresses the limitations of existing workflows and provides a robust tool for preclinical pharmacokinetic studies where small sample volumes and low analyte concentrations pose significant obstacles.

4.3) Material and Methods

4.3.1) Test Item Standard Solution

The test item was provided as a formulation for nasal administration, supplied in glass vials by the CIM at a concentration of 1 mg/mL. The formulation contains low sialic acid recombinant human erythropoietin (1 mg), along with sodium chloride, hydroxypropylmethylcellulose K4M, monobasic sodium phosphate, dibasic sodium phosphate, polysorbate 80, disodium ethylenediaminetetraacetic acid (EDTA), and water for injection.

4.3.2) Peptide Mapping

A 10 µL aliquot of the test item was mixed with 90 µL of digestion buffer composed of 100 mM ammonium bicarbonate (Sigma Aldrich) and 10 mM CaCl2 (Sigma Aldrich). The sample was incubated in a heated water bath at 60 °C for 30 minutes to promote protein unfolding. The temperature was then lowered to 47 °C, and 5 µL of a 1 mg/mL bovine trypsin solution (Sigma Aldrich) was added to initiate digestion. The reaction was allowed to proceed for 1 hour and was subsequently quenched with 2 µL of HPLC-grade formic acid (Sigma Aldrich).

The digested sample was analyzed using an HPLC-MS/MS system comprising a Q Exactive Orbitrap mass spectrometer (Thermo Scientific) coupled to a Thermo Scientific Dionex UltiMate 3000 Series UHPLC system. Chromatographic separation was performed using a Phenomenex Aeris Peptide XB-C18 Reversed Phase analytical column (3.6 µm, 4.6 mm × 100 mm). The mobile phase consisted of solvent A, 0.1% formic acid in USP-grade purified water, and solvent B, 0.1% formic acid in acetonitrile (Sigma Aldrich).

The gradient elution profile was as follows: Initial conditions: 99% solvent A and 1% solvent B at a flow rate of 400 µL/min. At 15 minutes: 90% solvent A and 40% solvent B. At 17 minutes: 90% solvent B. The gradient returned to initial conditions (99% solvent A and 1% solvent B) at 17.25 minutes and re-equilibrated by 20 minutes.

The mass spectrometer was operated in positive ionization mode using a heated electrospray ionization (HESI) source. Key parameters included a spray voltage of 3900 V, a capillary temperature of 320 °C, sheath gas flow of 45 (arbitrary units), and auxiliary gas flow of 15 (arbitrary units). The S-lens RF level was set at 70. Probe heater temperature was maintained at 300 °C. Calibration for mass accuracy was performed within a week from the time of the analysis, ensuring high-resolution and accurate data acquisition.

4.3.3) EPO Seppharose column binding

The rhEPO underwent an initial filtration process to remove contaminants such as EDTA and other residual solvents. This step was conducted using Spectrum™ Labs Spectra/Por™ 2 Standard RC Dry Dialysis Kits with a molecular weight cutoff (MWCO) of 12–14 kDa. Approximately 10 bulbs of rhEPO (equivalent to ~10 mg) were dialyzed against 2 liters of coupling buffer (0.1 M sodium bicarbonate, pH ~8) for 4 hours at room temperature under gentle stirring. This procedure ensured the removal of impurities while maintaining the integrity and bioactivity of rhEPO, preparing it for subsequent conjugation steps.

For the conjugation process, 1 gram of CNBr-activated Sepharose was washed thoroughly with 50 mL of 1 mM HCl for three cycles (centrifugation at 100 × g for 3 minutes each cycle). After the washing step, the 1 gram of activated beads was mixed with the 10 mg of rhEPO, previously filtered to deplete excipients, and the final volume was adjusted to 30 mL by adding additional coupling buffer. The mixture was incubated overnight at room temperature under gentle shaking to allow for efficient coupling.

The Sepharose beads coupled with rhEPO were then packed into an elution reservoir (Agilent). The column was washed sequentially with 75 mL of coupling buffer to remove unbound material, followed by three alternating cycles of acidic (0.1 M acetic acid/acetate with 0.5 M NaCl) and basic (0.1 M Tris-HCl, pH 8, with 0.5 M NaCl) washes. Each wash cycle was performed using three column volumes to ensure thorough removal of non-specifically bound impurities.

Finally, the column was equilibrated with 10 column volumes of PBS and stored at 4°C in PBS containing sodium azide to preserve the coupled rhEPO for subsequent use.

4.3.4) EPO specific antibodies isolation

New Zealand White rabbits were immunized with recombinant human erythropoietin (rhEPO) under the care of the animal facility technicians at Nucro Technics. At the terminal bleed, performed at the time of sacrifice, a total of 91 mL of serum was collected. This serum was subsequently processed to isolate and purify IgG antibodies specific to rhEPO.

From the collected sera, 40 mL was diluted 1:2 with phosphate-buffered saline (PBS) and filtered through 45-micron filters to remove particulates. Solid Phase Extraction (SPE) was then performed using a Sepharose™ CL-4B column conjugated with Protein A (Cytiva) to selectively bind the IgG fraction. The column was thoroughly washed with PBS to eliminate unbound proteins and residual impurities. To elute the IgG antibodies, the column was acidified using a 0.1 M glycine buffer at pH 3. To ensure antibody stability and prevent degradation, the eluates were immediately neutralized with Tris-HCl at pH 8, with pH adjustments monitored using a pH meter to confirm neutrality. Positive fractions, identified via Bradford Assay, were pooled together and filtered to remove any remaining buffer components. To ensure complete removal of low-molecular-weight contaminants and buffer residues, molecular weight filters with a cutoff of 14–16 kDa were applied.

The purified IgG antibodies underwent a second purification step on a Sepharose column conjugated with rhEPO. This step specifically enriched for antibodies targeting rhEPO. After PBS washes to remove non-specific IgG, antibodies bound to rhEPO were eluted with acidic glycine buffer (0.1 M, pH 3) and immediately neutralized with Tris-HCl. The fractions containing rhEPO-specific IgG were pooled and concentrated using Amicon® Ultra-2 mL Centrifugal Filters with a molecular weight cutoff of 100 kDa. This process yielded a final volume of 730 µL at a concentration of 5 mg/mL.

For biotinylation, 14 µL of Biotinamidohexanoic acid 3-sulfo-N-hydroxysuccinimide ester sodium salt (Sigma Millipore) (10 mg/mL in 6% DMSO) was added to the antibody solution. The reaction mixture was kept under gentle agitation at 200 rpm for 1 hour. Excess biotinylation reagent was removed via gel filtration chromatography. Protein-containing fractions were identified with a

Bradford Assay, yielding approximately 4.5 mL of purified biotinylated antibodies, which were stored at 4°C.

The protein concentration of the biotinylated antibodies was determined to be 0.5 mg/mL using spectrophotometry. The success of the biotinylation process was confirmed using an Avidin/HABA (4′-hydroxyazobenzene-2-carboxylic acid) pronase assay as recommended by vendor. These biotinylated antibodies were then utilized in downstream applications.

4.3.5) EPO-specific antibodies conjugation to magnetic beads

The biotinylated antibodies were conjugated to Dynabeads™ M-280 Streptavidin (Thermo Fisher Scientific) through a carefully controlled process to ensure efficient binding and functionality. A 1 mL slurry of Dynabeads™ M-280 Streptavidin (10 mg/mL) was initially washed three times with phosphate-buffered saline (PBS) using a magnetic separator to remove the storage buffer and prepare the beads for conjugation. Following this, 200 µL of the biotinylated antibody solution (0.5 mg/mL) was added to the washed beads. The volume was adjusted to 1 mL with PBS to create an optimal environment for the interaction between the streptavidin-coated beads and the biotinylated antibodies.

The mixture was incubated under gentle rotation for 30 minutes at room temperature, facilitating the binding of the antibodies to the beads. After the incubation period, the supernatant was removed using a magnetic separator to eliminate any unbound antibodies. To ensure the removal of residual contaminants and non-specifically bound proteins, the beads underwent five sequential washes, each performed with 1 mL of 0.1% BSA in PBS, with a washing time of 5 minutes per cycle.

Following the washing steps, the beads were resuspended in 1 mL of PBS. For downstream use, 100 µL aliquots of the bead suspension were transferred to 1.5 mL microcentrifuge tubes and diluted with 900 µL of PBS to achieve a final concentration of 1 mg/mL. The conjugated beads were then stored at 4°.

4.3.6) EPO Selective Extraction from plasma

The plastic wells used in the immunoprecipitation were kept at 4C overnight with aliquots of 700 µL of 1% bovine serum albumin to avoid aspecific binding of the proteins to the plastic.

Samples, calibration standards (CSs), and quality controls (QCs) were immunoprecipitated as follows: 100 µL of magnetic beads conjugated with biotinylated antibodies (concentration: 1 mg/mL) were added to 50 µL of serum sample, bringing the total volume to 500 µL with the addition of PBS.

The samples were incubated for 1 hour at room temperature (23°C) under gentle agitation (400 rpm) to allow the antibodies on the beads to interact selectively with rhEPO. Following incubation, the beads were separated magnetically, and the supernatant was removed. The beads were washed two times with PBS and two times with daily fresh USP purified H2O. Each wash lasted approximately 5 minutes using 500 µL, ensuring thorough removal of non-specific bindings. After the final wash, the beads were magnetically separated, and the supernatant was discarded.

To elute and digest the bound rhEPO, the beads were resuspended in 30 µL of digestion buffer (50 mM ammonium bicarbonate) containing the heavily labelled peptide functioning as IS. Subsequently, 5 µL of Smart digest trypsin solution (Thermo fisher) were added, and the mixture was incubated overnight at 70 °C for protein digestion for 3 hours, the reaction was quenched with 1 µL HPLC grade formic acid (Thermo fisher).

The beads were magnetically separated once more. The beads were discarded and the resulting tryptic digest was collected and analyzed using mass spectrometry to confirm the successful extraction and identification of rhEPO.

4.3.7) EPO quantification

The calibration curve was prepared by spiking rat serum with eight increasing concentrations of rhEPO, corresponding to 0.37, 0.75, 1, 4, 10, 50, 85, and 100 ng/mL (Calibration Standards, CS 1–8). QC at low, medium and high concentrations were prepared in the same way at 5, 25 and 75 ng/mL for accuracy estimation. Following the immunoprecipitation process, the internal standard (IS) peptide contained in the digestion buffer (50 mM AmBIC) was added at a final concentration of 1.25 ng/mL, which corresponds to 37 ng/mL of the intact protein. The spiked samples were extracted as described in 4.3.6. For the neat calibration curve, which was utilized for recovery estimation, the protein amount was adjusted based on the molecular weight ratio of the tryptic fragment to the full-length protein, applying a correction factor of 803/30,000. Consequently, the

final concentrations for the neat calibration standards (CS 1–8) were 10, 20, 27, 100, 207, 1330, 2270, and 2690 pg/mL.

4.3.8) Test samples

At the midpoint of the study (six months after the initiation of intranasal dosing), serum samples from rats administered biweekly with high (100 µg/rat), medium (46.5 µg/rat), and low (15.5 µg/rat) concentrations of rhEPO were collected for mass spectrometry analysis and method validation. Additionally, two positive control samples from rats dosed via intravenous (IV) administration were included to assess method performance. All samples, including calibration standards, underwent the same extraction and analytical workflow, ensuring consistency in sample processing and enabling a direct comparison of detected signal intensities across dosing regimens.

4.3.9) UHPLC-HRMS Conditions and Data Extraction

The analysis was conducted using a Thermo Exploris 120 mass spectrometer coupled to a Vanquish UHPLC system, ensuring high-resolution detection of the target analyte. Chromatographic separation was achieved on a Waters Peptide BEH C18 column (2.1 mm × 50 mm, 1.7 µm particle size), maintained at 40°C under still-air temperature control. The mobile phase consisted of 0.1% F.A. in water (solvent A) and 0.1% F.A. in acetonitrile (solvent B), with a flow rate of 0.400 mL/min. A gradient elution program was employed, starting at 5% solvent B, increasing to 27% at 8 minutes, followed by a sharp rise to 65% at 9 minutes, where it was maintained until 12.5 minutes before returning to the initial conditions at 13 minutes, with a total run time of 16 minutes. The mass spectrometer operated in positive ESI mode, with a spray voltage of +3400 V, complemented by sheath gas at 25, auxiliary gas at 5 arbitrary units. The ion transfer tube temperature was maintained at 320°C, while the vaporizer temperature was set to 75°C. Data acquisition was performed in full scan mode (m/z 170–900) with an Orbitrap resolution of 60,000. High-energy collision dissociation (HCD) was applied at 18, and the RF lens was set to 60. For quantification, the extracted ion chromatograms (XICs) were generated using the precursor ions m/z 402.2529 for the EPO peptide target and m/z 407.25 for its stable isotope-labeled internal standard, both with a charge state of +2. The expected LC peak width was set to 6 seconds to accommodate chromatographic peak broadening while maintaining sensitivity. Data processing and peak extraction were performed using Thermo Scientific FreeStyle and Skyline software, ensuring

robust peptide quantification and method reproducibility. The ions used for data extraction and peak area calculations were m/z 613.38787, 512.34026, 398.25008, 201.12299, and 173.12827 for the internal standard, and m/z 603.38180, 393.24620, 173.12828, and 502.33404 for the target peptide.

4.4) Results

4.4.1) Peptide mapping

Peptide mapping enabled the identification of most peptides composing rhEPO (Figure 4.1).

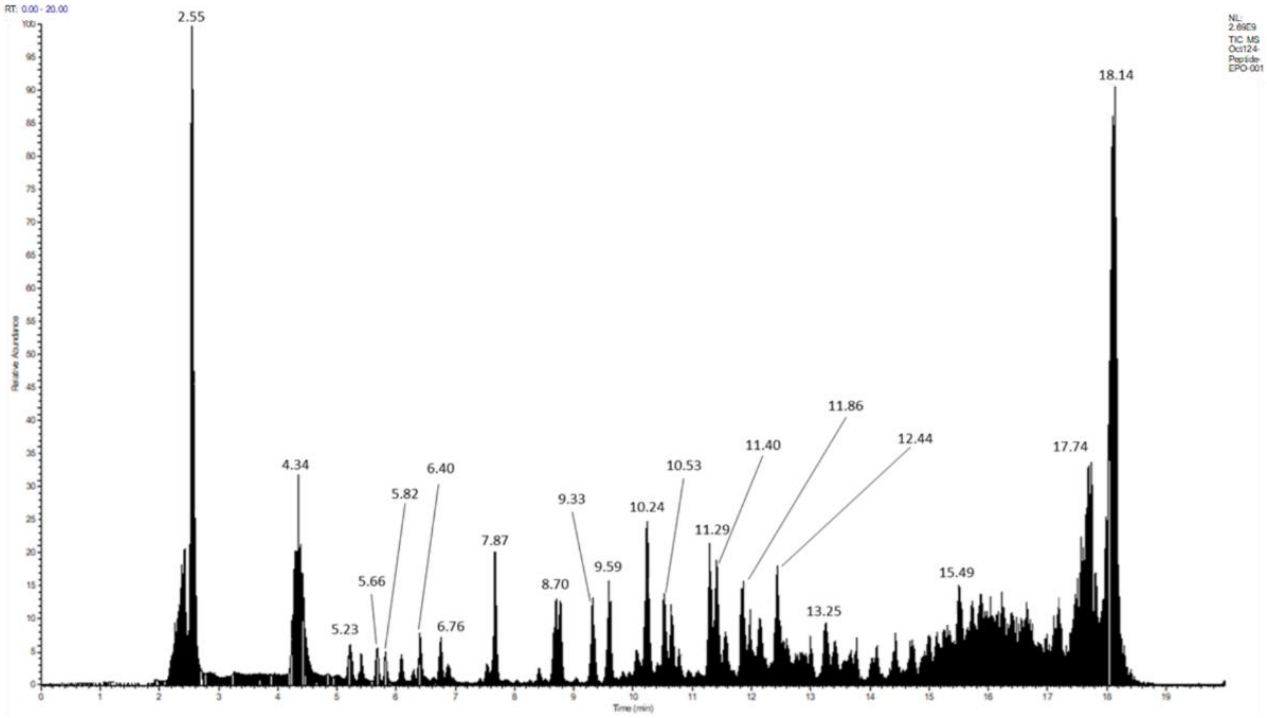

Figure 4.1. Total ion chromatogram from peptide mapping analysis. The chromatogram represents the total ion signal acquired during peptide mapping of rhEPO.

The peptides were identified using the De Novo Sequencing function in PEAKS Studio 12.5 [148], based on the human EPO sequence retrieved from the UniProt database [149].

The peptides with a match score higher than 90 are shown in Table 4.1.

Among the identified peptides, SLTTLLR was selected for further method development due to its strong instrumental response (peak height of 3.7×10^8) and its lack of homology with the endogenous rat EPO sequence, minimizing the risk of interference in quantitative analysis [149].

Peptide	Match score	*m/z*	z	RT	Mass	ppm
AVSGLR	98.5	301.6847	2	6.3995	601.3547	0.1
VNFYAWK	98.2	464.2405	2	10.6465	926.465	1.5
VYSNFLR	97.8	449.743	2	9.6077	897.4708	0.7
TLTADTFR	97.3	462.7435	2	8.6968	923.4713	1.3
SNFLR	96.9	318.6768	2	7.7858	635.3391	0
YLLEAK	96.5	368.7169	2	8.7643	735.4167	3.6
TADTFRK	96.5	419.7245	2	7.5215	837.4344	0
SLTTLLR	95.6	402.2533	2	10.5286	802.4912	1.1
ALLSEAVLR	95.2	486.298	2	11.0779	970.5811	0.4
SEAVLR	92.5	337.6951	2	6.8391	673.3759	-0.3

Table 4.1. Peptides identified from recombinant human erythropoietin (rhEPO) using De Novo Sequencing in PEAKS Studio 12.5. The table lists peptides with a match score higher than 90, including their mass-to-charge ratio (m/z), charge state (z), retention time (RT), mass, and mass error in ppm.

Both the SLTTLLR peptide and its stable isotope-labeled internal standard (IS) were purchased from Thermo Fisher Scientific. The peptides were resuspended in USP-purified H_2O at a concentration of 2.5 mg/mL and stored at -80°C to ensure stability throughout the study.

4.4.2) EPO calibration curve, recovery and accuracy estimation

The signal intensities obtained for rhEPO calibration standards in spiked plasma are reported in Table 4.2. While the absolute signal was relatively low, the optimization of chromatographic separation combined with immunopurification significantly reduced to zero the background noise in the RT of interest. This improvement allowed for a clear and linear response across concentrations, even at 1 ng/mL, where one of the diagnostic ions (m/z 173.1283) was still detectable in the product ion spectra of the parent mass at the expected retention time. These results confirm the method's ability to maintain sensitivity and reproducibility in the low ng/mL range.

Calibration standard	Protein concentration (ng/mL)	Target peak area	IS peak area	Target/IS
CS1	0.37	0	912	0
CS2	0.75	0	878	0
CS3	1	20	924	0,022
CS4	4	95	899	0,106
CS5	10	205	932	0,220
CS6	50	914	995	0,919
CS7	85	1825	982	1,858
CS8	100	2259	971	2,326

Table 4.2. Signal intensities obtained for rhEPO calibration standards in spiked plasma at different concentrations.

Calibration standards CS3–CS8, where a detectable signal for the target peptide was obtained, were used to generate the calibration curve presented in Figure 4.2. The curve exhibited a strong linear correlation within the concentration range where the analyte was detected, demonstrating the robustness and reliability of the method for rhEPO quantification in spiked plasma. The optimized workflow, integrating immunopurification and chromatographic separation, ensured consistent signal response and minimal background interference, further enhancing quantification accuracy.

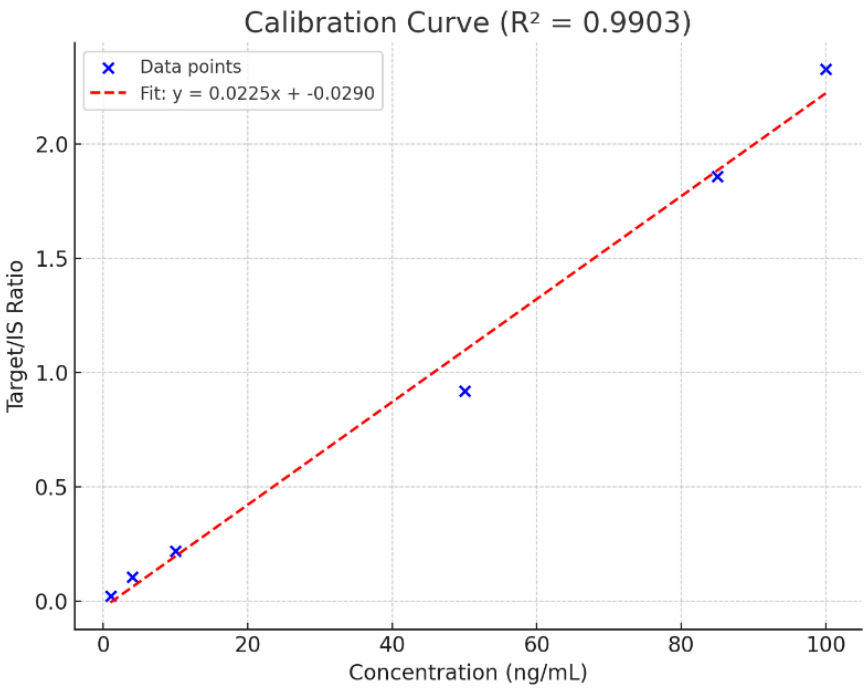

Figure 4.2 Calibration curve for the target peptide quantification. The curve was generated using calibration standards (CS3–CS8) and shows a strong linear correlation ($R^2 = 0.9903$) between the target/internal standard (IS) ratio and the analyte concentration (ng/mL).

Recovery was evaluated by comparing the signal intensities of the target peptide in spiked calibration standards (CS3–CS8) with their corresponding neat solutions. The measured signal intensities for the neat standards were: CS3 – 32, CS4 – 111, CS5 – 233, CS6 – 1525, CS7 – 2927, and CS8 – 3771. Recovery was calculated using the formula (Spiked-Neat)/Neat*100, yielding values of -37.5%, -14.41%, -12.02%, -40.07%, -37.64%, and -40.11% across CS3–CS8. The overall average recovery was determined to be 69.71%, demonstrating the effectiveness of the sample preparation and extraction strategy.

Accuracy was expressed as relative error (RE) using the formula: RE=(Measured-expected)/expected*100. The target/IS ratios for the QC samples were 0.099 (5 ng/mL), 0.458 (25 ng/mL), and 1.663 (75 ng/mL), corresponding to estimated concentrations of 5.72, 21.64, and

76.68 ng/mL, respectively. The calculated RE values were +14.4% (5 ng/mL), -13.4% (25 ng/mL), and +2.2% (75 ng/mL), confirming that the method provides reliable quantification within the acceptable ±15% range for bioanalytical validation.

4.4.3) Samples analysis

Sample analysis resulted in non-detectable signals in all intranasally administered samples dosed biweekly at high (100 µg/rat), medium (46.5 µg/rat), and low (15.5 µg/rat) concentrations. However, in the two IV positive controls (rats administered intravenously at 100 µg/rat), the signal was significantly higher, with calculated concentrations of 760 ng/mL and 712 ng/mL based on the calibration curve equation. These values were approximately 10 times higher than CS8, suggesting either a saturation effect in the immunoaffinity SPE capture or an actual concentration aligning with the expected levels. Given that the study focused on intranasal administration, further dilution of the IV samples was deemed unnecessary, as their primary purpose was to serve as a qualitative positive control rather than a quantitative benchmark.

4.5) Conclusion

The primary objective of this study was to develop an ultra-sensitive method for protein quantification in biological matrices, focusing on improving mass spectrometry-based detection of low-abundance proteins. Erythropoietin (EPO) served as a proof of concept to evaluate the feasibility of integrating immunoprecipitation (IP) extraction into industry workflows for enhanced protein quantification. The method successfully achieved sensitivity in the low ng/mL range, demonstrating the potential of coupling IP with LC-MS/MS to improve protein enrichment and detection in serum samples. Recovery was estimated at approximately 69%, which is considered acceptable for plasma protein analysis, while accuracy remained within the acceptable range for bioanalytical methods.

Despite these advancements, the method did not achieve the necessary sensitivity for detecting EPO following intranasal administration, as all test samples remained below the detection limit. However, the method demonstrated adequate sensitivity and reliability through the accurate quantification of quality control (QC) samples at 5, 25, and 75 ng/mL, with measured concentrations of 5.72, 21.64, and 76.68 ng/mL, corresponding to accuracy values of 114.4%,

86.6%, and 102.2%, respectively. This confirmed the method's suitability for quantification within the validated range. Since the sensitivity was insufficient for intranasal EPO detection, full method validation, including precision (CV%) and further robustness testing, was not pursued. Nevertheless, intravenous positive controls yielded EPO concentrations of approximately 760 ng/mL and 712 ng/mL, confirming that the workflow is effective for higher-concentration samples and reinforcing the need for further refinement in lower concentration ranges.

Alternative analytical are currently being explored to complete the study. An ELISA-based method for EPO quantification was developed in-house and optimized, reaching a sensitivity of 50 pg/mL in its lowest calibration standard. However, even this sensitivity proved insufficient to detect rhEPO in the serum of treated rats, as no signal increase was observed compared to non-spiked controls—suggesting that circulating levels remained below this threshold. To overcome these limitations, further development of orthogonal approaches is currently underway in our laboratories, encompassing both ELISA and mass spectrometry-based workflows, as proposed by Florentinus-Mefailoski et al. [151], to achieve the required sensitivity for reliable EPO detection in this preclinical model.

Chapter five: Conclusion and future work

This dissertation explored the development and application of advanced MS techniques for metabolite profiling and biomolecule quantification across diverse biological contexts. The studies conducted demonstrated the versatility, sensitivity, and efficiency of different MS methodologies, including SSI, MALDI, and LC-MS/MS, in addressing analytical challenges in both plant and clinical research.

The application of SSI-MS to infected maple leaves revealed its potential as a high-throughput and solvent-efficient screening tool for plant-pathogen interactions. The method successfully differentiated healthy and infected leaves through distinct metabolic fingerprints, showcasing its ability to provide rapid and direct analysis without extensive sample preparation. These findings contribute to the broader field of environmental and agricultural diagnostics, demonstrating how ambient ionization MS can aid in fungal identification and plant disease monitoring.

In plant metabolomics, the development of a MALDI-HRMS method enabled the absolute quantification of the phytoalexins camalexin and scopoletin in *Arabidopsis thaliana*. This approach offered novel insights into the plant's biochemical defense mechanisms against environmental stressors. The successful application of this method in wild-type and mutant *Arabidopsis* plants underscores the value of MALDI-MS for metabolite quantification and comparative biochemical analyses in plant sciences.

In clinical and pharmaceutical research, the development of an ultra-sensitive IP-LC-MS/MS method provided a robust strategy for detecting low-abundance proteins in rat serum. This method enhances the precision and sensitivity of biomolecule quantification, allowing for accurate detection at trace levels. Notably, this high sensitivity was achieved without the need for capillary or nano-LC systems, demonstrating the effectiveness of the developed approach while maintaining analytical simplicity and robustness. The ability to achieve reliable quantification with small sample volumes positions this approach as a valuable tool for both preclinical and clinical biomarker studies, addressing the growing demand for highly sensitive bioanalytical techniques.

Collectively, these studies underscore the adaptability of modern MS in solving complex biological problems, from environmental monitoring to clinical diagnostics. The methodologies developed here serve as a foundation for future research, with potential applications in high-throughput screening, precision medicine, and plant metabolic studies. As MS continues to evolve, its

integration with novel ionization techniques and advanced data analysis strategies will further enhance its role in biological research and translational science.

Future work may focus on refining mass spectrometric techniques by integrating machine learning algorithms for advanced spectral analysis, improving ionization efficiency for challenging biological matrices, and developing novel extraction strategies to enhance analyte recovery. Additionally, the implementation of orthogonal analytical methods that combine the strengths of mass spectrometry with complementary techniques could further increase sensitivity, specificity, and robustness. Expanding these approaches to new biomarker discovery and biomolecule quantification represents a promising direction for future research. The findings presented in this dissertation contribute to the growing body of knowledge in analytical mass spectrometry and underscore its pivotal role in advancing modern biomedical science.

Bibliography

1) G. Münzenberg, "Development of mass spectrometers from Thomson and Aston to present," International Journal of Mass Spectrometry, Vols. 349-350, pp. 9-18, 2013.

2) J. J. Thomson, "Cathode Rays (Reprinted from Philosophical Magazine Series 5, vol 44, pg 293-316, 1897)," Philosophical magazine, vol. 90, pp. 25-29, 2010.

3) K. Wien, "100 Years of Ion Beams: Willy Wien's Canal Rays," Brazilian Journal of Physics, vol. 29, no. 3, pp. 401-414, 1999.

4) De Hoffmann, Edmond, and Vincent Stroobant. *Mass spectrometry: principles and applications*. John Wiley & Sons, 2007.

5) Glish, G., Vachet, R. The basics of mass spectrometry in the twenty-first century. *Nat Rev Drug Discov* **2**, 140–150 (2003). https://doi.org/10.1038/nrd1011

6) McLafferty FW. A century of progress in molecular mass spectrometry. Annu Rev Anal Chem (Palo Alto Calif). 2011;4:1-22. doi: 10.1146/annurev-anchem-061010-114018. PMID: 21351881.

7) Züllig, T., & Köfeler, H. C. (2021). High resolution mass spectrometry in lipidomics. *Mass spectrometry reviews*, *40*(3), 162-176.

8) Meissner, Felix, et al. "The emerging role of mass spectrometry-based proteomics in drug discovery." *Nature Reviews Drug Discovery* 21.9 (2022): 637-654.

9) Shuken, Steven R. "An introduction to mass spectrometry-based proteomics." *Journal of Proteome Research* 22.7 (2023): 2151-2171.

10) Perez de Souza, Leonardo, et al. "Mass spectrometry-based untargeted plant metabolomics." *Current protocols in plant biology* 4.4 (2019): e20100.

11) Allen, Darren R., and Brett C. McWhinney. "Quadrupole time-of-flight mass spectrometry: a paradigm shift in toxicology screening applications." *The Clinical Biochemist Reviews* 40.3 (2019): 135.

12) Mogollon, Noroska Gabriela Salazar, et al. "New advances in toxicological forensic analysis using mass spectrometry techniques." *Journal of analytical methods in chemistry* 2018.1 (2018): 4142527.

13) Dong, Xue, et al. "Advances in mass spectrometry-based glycomics." *Electrophoresis* 39.24 (2018): 3063-3081.

14) Donohoo, Kaitlyn B., et al. "Advances in mass spectrometry-based glycomics—An update covering the period 2017–2021." *Electrophoresis* 43.1-2 (2022): 119-142.

15) Lebedev AT. Environmental mass spectrometry. Annu Rev Anal Chem (Palo Alto Calif). 2013;6:163-89. doi: 10.1146/annurev-anchem-062012-092604. Epub 2013 Feb 28. PMID: 23527549.

16) Finehout EJ, Lee KH. An introduction to mass spectrometry applications in biological research. Biochem Mol Biol Educ. 2004 Mar;32(2):93-100. doi: 10.1002/bmb.2004.494032020331. PMID: 21706701.

17) Sun T, Wang X, Cong P, Xu J, Xue C. Mass spectrometry-based lipidomics in food science and nutritional health: A comprehensive review. Compr Rev Food Sci Food Saf. 2020 Sep;19(5):2530-2558. doi: 10.1111/1541-4337.12603. Epub 2020 Aug 13. PMID: 33336980.

18) Wang, Jing, et al. "Portable mass spectrometry system: instrumentation, applications, and path to ‘omics analysis." *Proteomics* 22.23-24 (2022): 2200112.

19) Shen, Qing, et al. "Revolutionizing food science with mass spectrometry imaging: A comprehensive review of applications and challenges." *Comprehensive Reviews in Food Science and Food Safety* 23.4 (2024): e13398.

20) Richardson, Susan D. "Environmental mass spectrometry: emerging contaminants and current issues." *Analytical Chemistry* 84.2 (2012): 747-778.

21) Gross, Jürgen H. *Mass spectrometry: a textbook*. Springer Science & Business Media, 2006.

22) Raposo, Francisco, and Damià Barceló. "Challenges and strategies of matrix effects using chromatography-mass spectrometry: An overview from research versus regulatory viewpoints." *TrAC Trends in Analytical Chemistry* 134 (2021): 116068.

23) Cortese, Manuela, et al. "Compensate for or minimize matrix effects? Strategies for overcoming matrix effects in liquid chromatography-mass spectrometry technique: a tutorial review." *Molecules* 25.13 (2020): 3047.

24) Meissner, Felix, et al. "The emerging role of mass spectrometry-based proteomics in drug discovery." Nature Reviews Drug Discovery 21.9 (2022): 637-654.

25) Goodwin, Richard JA, Zoltan Takats, and Josephine Bunch. "A critical and concise review of mass spectrometry applied to imaging in drug discovery." SLAS DISCOVERY: Advancing the Science of Drug Discovery 25.9 (2020): 963-976.

26) Williams, Jon D., et al. "Ultra-high-throughput mass spectrometry in drug discovery: fundamentals and recent advances." Expert Opinion on Drug Discovery 19.3 (2024): 291-301.

27) Banerjee, S., & Mazumdar, S. (2012). Electrospray ionization mass spectrometry: A technique to access the information beyond the molecular weight of the analyte. *International Journal of Analytical Chemistry*, 2012, 1–40.

28) Konermann, L., Ahadi, E., Rodriguez, A. D., & Vahidi, S. (2013). Unraveling the mechanism of electrospray ionization. *Analytical Chemistry*, 85(1), 2–9.

29) Fenn, J. B., Mann, M., Meng, C. K., Wong, S. F., & Whitehouse, C. M. (1989). Electrospray ionization for mass spectrometry of large biomolecules. Science, 246(4926), 64–71.

30) Kebarle, P., & Verkerk, U. H. (2009). Electrospray: From ions in solution to ions in the gas phase, what we know now. *Mass Spectrometry Reviews*, 28(6), 898–917.

31) Wilm, Matthias. "Principles of electrospray ionization." *Molecular & cellular proteomics* 10.7 (2011).

32) Lei Z, Huhman DV, Sumner LW. Mass spectrometry strategies in metabolomics. J Biol Chem. 2011 Jul 22;286(29):25435-42. doi: 10.1074/jbc.R111.238691. Epub 2011 Jun 1. PMID: 21632543; PMCID: PMC3138266.

33) Indelicato S, Bongiorno D, Ceraulo L. Recent Approaches for Chemical Speciation and Analysis by Electrospray Ionization (ESI) Mass Spectrometry. Front Chem. 2021 Jan 20;8:625945. doi: 10.3389/fchem.2020.625945. PMID: 33553108; PMCID: PMC7855954.

34) Wang, H., Liu, J., Cooks, R. G., & Ouyang, Z. (2010). Paper spray for direct analysis of complex mixtures using mass spectrometry. *Angewandte Chemie International Edition*, 49(5), 877–880.

35) Li, X., Hu, B., Ding, J., & Chen, H. (2009). Leaf spray mass spectrometry for direct analysis of plant metabolites in living plant tissue. *Analytical Chemistry*, 81(14), 5497–5503.

36) Dos Santos, Larissa Batista, et al. "Sandpaper: efficient medium for analysis of polishable solid samples by ambient mass spectrometry." *Journal of the American Society for Mass Spectrometry* 34.8 (2023): 1761-1767.

37) Parasecolo L, Dabija LG, Shouk R, Shouk D, Augusti R, Ifa DR. Application of sandpaper spray ionization mass spectrometry to comprehensively examine maple leaves infected with distinct fungi. J Mass Spectrom. 2024 Feb;59(2):e5000. doi: 10.1002/jms.5000. PMID: 38263874.

38) Rodrillo KAM, Costa DM, Viana SFC, Shahbazi H, Augusti R, Ifa DR. Forensic application of sandpaper spray ionization mass spectrometry (SPS-MS): Direct analysis of solid pharmaceutical formulations and edible cannabis products. J Forensic Sci. 2024 Nov;69(6):2209-2221. doi: 10.1111/1556-4029.15592. Epub 2024 Aug 5. PMID: 39101585.

39) Karas, M., & Krüger, R. (2003). Ion formation in MALDI: The cluster ionization mechanism. *Chemical Reviews*, 103(2), 427–439.

40) Hillenkamp, F., & Peter-Katalinić, J. (2007). *MALDI MS: A practical guide to instrumentation, methods, and applications*. Wiley-VCH.

41) Knochenmuss, Richard. "Ion formation mechanisms in UV-MALDI." *Analyst* 131.9 (2006): 966-986.

42) Dreisewerd, K. (2003). The desorption process in MALDI. *Chemical Reviews*, 103(2), 395–426.

43) Franssen, M. C., & Eeltink, S. (2018). Advanced applications of MALDI-MS for polymer analysis. *Analytical Chemistry*, 90(6), 3417–3427.

44) Shanta, S. R., et al. "A new combination MALDI matrix for small molecule analysis: application to imaging mass spectrometry for drugs and metabolites." *Analyst*, 137.24 (2012): 5757–5762.

45) Calvano, Cosima Damiana, et al. "MALDI matrices for low molecular weight compounds: an endless story?." *Analytical and bioanalytical chemistry* 410 (2018): 4015-4038.

46) Bag, S., et al. "NanoLC MALDI MS/MS based quantitative metabolomics reveals the alteration of membrane biogenesis in oral cancer." *RSC Advances*, 6.67 (2016): 62556–62566.

47) Müller, Wendy H., et al. "Surface-assisted laser desorption/ionization mass spectrometry imaging: A review." *Mass Spectrometry Reviews* 41.3 (2022): 373-420.

48) Dong, Xiaoli, et al. "Graphene as a novel matrix for the analysis of small molecules by MALDI-TOF MS." *Analytical Chemistry* 82.14 (2010): 6208-6214.

49) Lin, Zian, and Zongwei Cai. "Negative ion laser desorption/ionization time-of-flight mass spectrometric analysis of small molecules by using nanostructured substrate as matrices." *Mass spectrometry reviews* 37.5 (2018): 681-696.

50) Horatz, Kilian, et al. "Conjugated polymers as a new class of dual-mode matrices for MALDI mass spectrometry and imaging." *Journal of the American Chemical Society* 140.36 (2018): 11416-11423.

51) Dabija, Laurentiu G., et al. "Assessment of MALDI matrices for the detection and visualization of phosphatidylinositols and phosphoinositides in mouse kidneys through matrix-assisted laser desorption ionization mass spectrometry imaging (MALDI-MSI)." *Analytical and Bioanalytical Chemistry* 416.8 (2024): 1857-1865.

52) Yousefi-Taemeh M, Duli E, Dabija LG, Lemaire M, Ifa DR. Sublimation application of 5-chloro-2-mercaptobenzothiazole matrix for matrix-assisted laser desorption/ionization mass spectrometry imaging of mouse kidney. Rapid Commun Mass Spectrom. 2023 Aug 30;37(16):e9594. doi: 10.1002/rcm.9594. PMID: 37430447.

53) Perry, William J., et al. "Uncovering matrix effects on lipid analyses in MALDI imaging mass spectrometry experiments." *Journal of mass spectrometry* 55.4 (2020):e4491 .

54) Ferreira, Mônica Siqueira, et al. "MALDI-MSI: a fast and reliable method for direct melatonin quantification in biological fluids." *Journal of Analytical Science and Technology* 7 (2016): 1-6.

55) Nakamura, Masahiro, et al. "Quantitative MALDI-MS/MS assay for serum cortisol through charged derivatization." *Journal of Pharmaceutical and Biomedical Analysis* 178 (2020): 112912.

56) Song, Zhijing, et al. "Quantitative MALDI-MS assay of steroid hormones in plasma based on hydroxylamine derivatization." *Analytical Biochemistry* 616 (2021): 114089.

57) Bae, J., Park, M., Lee, J., Song, I., Ju, Y., Lee, C. S., Kwon, J., Moon, B., & Oh, H. B. (2019). Quantitative MALDI-TOF mass spectrometric analysis of biocidal polyhexamethylene guanidine (PHMG) oligomers in consumer products. *International Journal of Mass Spectrometry*, *435*, 298-304. https://doi.org/10.1016/j.ijms.2018.10.001

58) McDonald, Heather, et al. "Quantitative MALDI-MS and Imaging of Fungicide Pyrimethanil in Strawberries with 2-Nitrophloroglucinol as an Effective Matrix." *Journal of the American Society for Mass Spectrometry* 35.6 (2024): 1272-1281.

59) Adaway, J. E., Keevil, B. G., & Owen, L. J. (2014). Liquid chromatography tandem mass spectrometry in the clinical laboratory. *Annals of Clinical Biochemistry*. https://doi.org/10.1177/0004563214557678

60) Wong, A. L., et al. (2018). A Review on Liquid Chromatography-Tandem Mass Spectrometry Methods for Rapid Quantification of Oncology Drugs. *Pharmaceutics*, *10*(4), 221.

61) Adamowicz, P., & Tokarczyk, B. (2016). Simple and rapid screening procedure for 143 new psychoactive substances by liquid chromatography-tandem mass spectrometry. *Drug Testing and Analysis*, *8*(7), 652–667.

62) Sarafian, M. H., et al. (2015). Bile acid profiling and quantification in biofluids using ultra-performance liquid chromatography tandem mass spectrometry. *Analytical Chemistry*, *87*(19), 9662–9670.

63) Zhong, F., et al. (2017). Targeted high performance liquid chromatography tandem mass spectrometry-based metabolomics differentiates metabolic syndrome from obesity. *Experimental Biology and Medicine*, *242*(7), 773–780.

64) Petras, D., et al. (2017). High-resolution liquid chromatography tandem mass spectrometry enables large scale molecular characterization of dissolved organic matter. *Frontiers in Marine Science*, *4*, 405.

65) Perez de Souza, L., et al. (2021). Ultra-high-performance liquid chromatography high-resolution mass spectrometry variants for metabolomics research. *Nature Methods*, *18*(7), 733–746.

66) Wong, A. L., et al. (2018). LC-MS/MS in therapeutic drug monitoring of anticancer drugs. *Pharmaceutics*, *10*(4), 221.

67) Adamowicz, P., et al. (2016). Screening for psychoactive substances with LC-MS/MS. *Drug Testing and Analysis*, *8*(7), 652–667.

68) Hosseini, S., Vázquez-Villegas, P., Rito-Palomares, M., Martinez-Chapa, S.O. (2018). Advantages, Disadvantages and Modifications of Conventional ELISA. In: Enzyme-linked Immunosorbent Assay (ELISA). SpringerBriefs in Applied Sciences and Technology(). Springer, Singapore. https://doi.org/10.1007/978-981-10-6766-2_5

69) Suraj, J., et al. "Development, validation and application of a micro–liquid chromatography–tandem mass spectrometry based method for simultaneous quantification of selected protein biomarkers of endothelial dysfunction in murine plasma." *Journal of Pharmaceutical and Biomedical Analysis* 149 (2018): 465-474.

70) Stachniuk, A., et al. "Liquid chromatography–mass spectrometry bottom-up proteomic methods in animal species analysis of processed meat for food authentication and the detection of adulterations." *Mass Spectrometry Reviews* 40.1 (2021): 3-30.

71) Boulund, F., et al. "Typing and characterization of bacteria using bottom-up tandem mass spectrometry proteomics." *Molecular & Cellular Proteomics* 16.6 (2017): 1052-1063.

72) Prasad, B., et al. "Toward a consensus on applying quantitative liquid chromatography-tandem mass spectrometry proteomics in translational pharmacology research." *Clinical Pharmacology & Therapeutics* 106.4 (2019): 525-527.

73) Wu, Chaochao, et al. "Contributions of immunoaffinity chromatography to deep proteome profiling of human biofluids." *Journal of Chromatography B* 1021 (2016): 57-68.

74) Eivazi, Sadeq, et al. "Production and purification of a polyclonal antibody against purified mouse IgG2b in rabbits towards designing mouse monoclonal isotyping kits." *Advanced Pharmaceutical Bulletin* 5.1 (2015): 109.

75) Liu, Shuangshuang, et al. "Purification of a polyclonal antibody against CD147 for ELISA using antigen-immunoaffinity chromatography." *Molecular Medicine Reports* 15.6 (2017): 4035-4040.

76) Dubois, Mathieu, et al. "Immunopurification and mass spectrometric quantification of the active form of a chimeric therapeutic antibody in human serum." *Analytical Chemistry* 80.5 (2008): 1737-1745.

77) Sun, Li, et al. "Incorporating protein precipitation to resolve hybrid IP-LC-MS assay interference for ultrasensitive quantification of intact therapeutic insulin dimer in human plasma." *Journal of Pharmaceutical and Biomedical Analysis* 212 (2022): 114639.

78) Breitkopf, Susanne B., et al. "Detection of a rare BCR–ABL tyrosine kinase fusion protein in H929 multiple myeloma cells using immunoprecipitation (IP)-tandem mass spectrometry (MS/MS)." *Proceedings of the National Academy of Sciences* 109.40 (2012): 16190-16195.

79) Thermo Electron Corporation. *LTQ Hardware Manual*. Thermo Fisher Scientific, 2004.

80) Thermo Scientific. *Exactive Series Operating Manual.* Thermo Fisher Scientific, 2017.

81) Thermo Scientific. *Orbitrap Exploris Series Operating Manual.* Thermo Fisher Scientific, 2021.

82) Thermo Scientific. *Vanquish UHPLC and HPLC Systems Operating Manual*. Thermo Fisher Scientific, 2022.

83) Calla-Quispe E, Fuentes-Rivera HL, Ramírez P, Martel C, Ibañez AJ. Mass spectrometry: a Rosetta stone to learn how fungi interact and talk. *Life*. 2020;10(6):89. doi:10.3390/life10060089

84) Batista L, dos Santos D, Costa M, Almeida MR, Augusti R. Sandpaper: efficient medium for analysis of polishable solid samples by ambient mass spectrometry. *J Am Soc Mass Spectrom*. 2023;34(8):1761-1767. doi:10.1021/jasms.3c00188

85) Bi W, Gao Y, Shen J, et al. Traditional uses, phytochemistry, and pharmacology of the genus *Acer* (maple): a review. *J Ethnopharmacol*. 2016;189:31-60. doi:10.1016/j.jep.2016.04.021

86) Liu M, Braun U. Powdery mildews on crops and ornamentals in Canada: a summary of the phylogeny and taxonomy from 2000–2019. *Can J Plant Pathol*. 2022;44(2):191-218. doi:10.1080/07060661.2021.1986744

87) Hirose S, Tanda S, Kiss L, Grigaliunaite B, Havrylenko M, Takamatsu S. Molecular phylogeny and evolution of the maple powdery mildew (*Sawadaea*, *Erysiphaceae*) inferred from nuclear rDNA sequences. *Mycol Res*. 2005;109(8):912-922. doi:10.1017/S0953756205003527

88) Held BW, Hoffmeister D, Blanchette RA. Occurrence of European tar spot (*Rhytisma acerinum*) on Norway maple (*Acer platanoides*) causing severe infections in Minnesota. *Plant Disease*. 2018.

89) Weber R, Webster J. Teaching techniques for mycology: 18. *Rhytisma acerinum*, cause of tar-spot disease of sycamore leaves. *Mycologist*. 2002;16(3):120-123. doi:10.1017/S0269915X02002070

90) Van der Kolk JH, Wijnberg ID, Westermann CM, et al. Equine acquired multiple acyl-CoA dehydrogenase deficiency (MADD) in 14 horses associated with ingestion of maple leaves (*Acer pseudoplatanus*) covered with European tar spot (*Rhytisma acerinum*). *Mol Genet Metab*. 2010;101(2-3):289-291. doi:10.1016/j.ymgme.2010.06.019

91) Mao HP, Wang YF, Yang N, Liu Y, Zhang XD. Effects of nutrient solution irrigation quantity and powdery mildew infection on the growth and physiological parameters of greenhouse cucumbers. *Int J Agric Biol Eng*. 2022;15(2):68-74. doi:10.25165/j.ijabe.20221502.6838

92) Zhang X, Wang Y, Zhou Z, Zhang Y, Wang X. Detection method for tomato leaf mildew based on hyperspectral fusion terahertz technology. *Foods*. 2023;12(3):535. doi:10.3390/foods12030535

93) Kunova A, Pizzatti C, Saracchi M, Pasquali M, Cortesi P. Grapevine powdery mildew: fungicides for its management and advances in molecular detection of markers associated with resistance. *Microorganisms*. 2021;9(7):1541. doi:10.3390/microorganisms9071541

94) Qasim M, Akutse KS, Hussain D, et al. Powdery mildew fungus *Oidium lycopersici*-infected tomato plants attract the non-vector greenhouse whitefly, *Trialeurodes vaporariorum*, but seem to impair their development. *Agronomy*. 2022;12(11):2791. doi:10.3390/agronomy12112791

95) Medeiros TCT, Dabija LG, Parasecolo L, Melo IS, Moraes LAB, Ifa DR. Differentiation of the metabolic profile of actinobacteria isolated from the soil of the Caatinga biome by paper spray mass spectrometry. *J Mass Spectrom*. 2023;58(7):e4956. doi:10.1002/jms.4956

96) Chambers MC, Maclean B, Burke R, et al. A cross-platform toolkit for mass spectrometry and proteomics. *Nat Biotechnol*. 2012;30(10):918-920. doi:10.1038/nbt.2377

97) Pluskal T, Castillo S, Villar-Briones A, Orešič M. MZmine 2: modular framework for processing, visualizing, and analyzing mass spectrometry-based molecular profile data. *BMC Bioinformatics*. 2010;11(1):395. doi:10.1186/1471-2105-11-395

98) Pang Z, Chong J, Zhou G, et al. MetaboAnalyst 5.0: narrowing the gap between raw spectra and functional insights. *Nucleic Acids Res*. 2021;49(W1):W388-W396. doi:10.1093/nar/gkab382

99) Liu J, He Wang R, Cooks G, Ouyang Z. Leaf spray: direct chemical analysis of plant material and living plants by mass spectrometry. *Anal Chem*. 2011;83(20):7608-7613. doi:10.1021/ac2020273

100) Ziv C, Zhao Z, Gao YG, Xia Y. Multifunctional roles of plant cuticle during plant–pathogen interactions. *Front Plant Sci*. 2018;9:1088. doi:10.3389/fpls.2018.01088

101) Liu J, Wang H, Manicke NE, Jin-Ming Lin R, Cooks G, Ouyang Z. Development, characterization, and application of paper spray ionization. *Anal Chem*. 2010.

102) Cabral EC, Mirabelli MF, Perez CJ, Ifa DR. Blotting assisted by heating and solvent extraction for DESI-MS imaging. *J Am Soc Mass Spectrom*. 2013;24(6):956-965. doi:10.1007/s13361-013-0616-y

103) Bjarnholt N, Li B, D'Alvise J, Janfelt C. Mass spectrometry imaging of plant metabolites—principles and possibilities. *Nat Prod Rep*. 2014;31(6):818-837. doi:10.1039/c3np70100j

104) Monsalvo I., Lin J., and Kovinich N., "Phytoalexin Gene Regulation in Arabidopsis thaliana—On the Verge of a Paradigm Shift?," Current Plant Biology 39 (2024): 100367.

105) Ahmed S. and Kovinich N., "Regulation of Phytoalexin Biosynthesis for Agriculture and Human Health," Phytochemistry Reviews 20, no. 2 (2021): 483–505.

106) Jahan M. A., Harris B., Lowery M., Infante A. M., Percifield R. J., and Kovinich N., "Glyceollin Transcription Factor GmMYB29A2 Regulates Soybean Resistance to Phytophthora sojae," Plant Physiology 183, no. 2 (2020): 530–546. doi:10.1104/pp.19.01293.

107) Graham T. L., Graham M. Y., Subramanian S., and Yu O., "RNAi Silencing of Genes for Elicitation or Biosynthesis of 5-Deoxyisoflavonoids Suppresses Race-Specific Resistance and Hypersensitive Cell Death in Phytophthora sojae Infected Tissues," Plant Physiology 144, no. 2 (2007): 728–740. doi:10.1104/pp.107.097865.

108) Saga H., Ogawa T., Kai K., et al., "Identification and Characterization of ANAC042, a Transcription Factor Family Gene Involved in the Regulation of Camalexin Biosynthesis in Arabidopsis," Molecular Plant-Microbe Interactions 25, no. 5 (2012): 684–696.

109) Gao X. Y., Li X. Y., Zhang C. Y., and Bai C. Y., "Scopoletin: A Review of Its Pharmacology, Pharmacokinetics, and Toxicity," Frontiers in Pharmacology 15 (2024): 1268464. doi:10.3389/fphar.2024.1268464.

110) Zhou J., Mu Q., Wang X., et al., "Multilayered Synergistic Regulation of Phytoalexin Biosynthesis by Ethylene, Jasmonate, and MAPK Signaling Pathways in Arabidopsis," Plant Cell 34, no. 8 (2022): 3066–3087. doi:10.1093/plcell/koac139.

111) Birkenbihl R. P., Kracher B., Roccaro M., and Somssich I. E., “Induced Genome-Wide Binding of Three Arabidopsis WRKY Transcription Factors during Early MAMP-Triggered Immunity,” Plant Cell 29, no. 1 (2017): 20–38. doi:10.1105/tpc.16.00681.

112) Frerigmann H., Glawischnig E., and Gigolashvili T., “The Role of MYB34, MYB51 and MYB122 in the Regulation of Camalexin Biosynthesis in Arabidopsis thaliana,” Frontiers in Plant Science 6 (2015): 654. doi:10.3389/fpls.2015.00654.

113) Jeandet P., Hébrard C., Deville M. A., et al., “Deciphering the Role of Phytoalexins in Plant-Microorganism Interactions and Human Health,” Molecules 19, no. 11 (2014): 18033–18056. doi:10.3390/molecules191118033.

114) Egbuonu A. C. C. and Eneogwe J. C., “Phytoalexins: Current and Possible Future Applications in Human Health and Diseases Control,” International Journal of Molecular Biology: Open Access 3, no. 3 (2018): 107–112.

115) Zigová M., Michalková R., and Mojžiš J., “Anticancer Potential of Indole Phytoalexins and Their Analogues,” Molecules 29, no. 10 (2024): 2388. doi:10.3390/molecules29102388.

116) Glinski M. and Weckwerth W., “The Role of Mass Spectrometry in Plant Systems Biology,” Mass Spectrometry Reviews 25, no. 2 (2006): 173–214. doi:10.1002/mas.20063.

117) Jorge T. F., Mata A. T., and António C., “Mass Spectrometry as a Quantitative Tool in Plant Metabolomics,” Philosophical Transactions. Series A, Mathematical, Physical, and Engineering Sciences 374, no. 2079 (2016): 20150370. doi:10.1098/rsta.2015.0370.

118) Yousefi-Taemeh M., Lin J., Ifa D. R., Parrott W., and Kovinich N., “Metabolomics Differences of Glycine max QTLs Resistant to Soybean Looper,” Metabolites 11, no. 10 (2021): 710. doi:10.3390/metabo11100710.

119) Patel P., Raval M., Patel N., Patel S., Vyas N., and Patel A., “Quantification of Scopoletin From the Roots of Argyreia speciosa (Linn. F) Sweet Using HPLC Through the Concept of Design of Experiment,” Journal of AOAC International 104, no. 4 (2021): 1167–1180. doi:10.1093/jaoacint/qsab013.

120) Großkinsky D. K., Primisser S. M., Reichenauer T., and Pfeifhofer H., “Camalexin Quantification Using HPLC and the Novel Internal Standard Thiabendazole,” Journal of General Plant Pathology 90 (2024): 173–179. doi:10.1007/s10327-024-01175-3

121) Savatin D. V., Bisceglia N. G., Gravino M., Fabbri C., Pontiggia D., and Mattei B., “Camalexin Quantification in Arabidopsis thaliana Leaves Infected With Botrytis cinerea,” Bio-Protocol 5, no. 2 (2015): e1379. doi:10.21769/BioProtoc.1379.

122) Beets C. and Dubery I., “Quantification of Camalexin, a Phytoalexin From Arabidopsis thaliana: A Comparison of Five Analytical Methods,” Analytical Biochemistry 419, no. 2 (2011): 260–265. doi:10.1016/j.ab.2011.08.031.

123) Bréard D., Barrit T., Sochard D., et al., “Development of a Quantification Method for Routine Analysis of Glucosinolates and Camalexin in Brassicaceous Small-Sized Samples by Simultaneous Extraction Prior to Liquid Chromatography Determination,” Journal of Chromatography. B, Analytical Technologies in the Biomedical and Life Sciences 1205 (2022): 123348. doi:10.1016/j.jchromb.2022.123348.

124) Koprivova A., Schuck S., Jacoby R. P., et al., “Root-Specific Camalexin Biosynthesis Controls the Plant Growth-Promoting Effects of Multiple Bacterial Strains,” Proceedings of the National Academy of Sciences of the United States of America 116, no. 31 (2019): 15735–15744. doi:10.1073/pnas.1818604116.

125) Choi S. I., Kwon H. Y., La I. J., et al., “Development and Validation of an Analytical Method for Deacetylasperulosidic Acid, Asperulosidic Acid, Scopolin, Asperuloside and Scopoletin in Fermented Morinda citrifolia L. (Noni),” Separations 8, no. 6 (2021): 80.

126) Tan D. C., Quek A., Kassim N. K., Ismail I. S., and Lee J. J., “Rapid Quantification and Validation of Biomarker Scopoletin in Paederia foetida by qNMR and UV–Vis for Herbal Preparation,” Molecules 25, no. 21 (2020): 5162.

127) Mert-Türk F., Bennett M. H., Mansfield J. W., and Holub E. B., “Camalexin Accumulation in Arabidopsis thaliana Following Abiotic Elicitation or Inoculation With Virulent or Avirulent Hyaloperonospora parasitica,” Physiological and Molecular Plant Pathology 62, no. 3 (2003): 137–145.

128) Duncan M. W., Roder H., and Hunsucker S. W., “Quantitative Matrix-Assisted Laser Desorption/Ionization Mass Spectrometry,” Briefings in Functional Genomics & Proteomics 7, no. 5 (2008): 355–370. doi:10.1093/bfgp/eln041.

129) Ren J. L., Zhang A. H., Kong L., and Wang X. J., “Advances in Mass Spectrometry-Based Metabolomics for Investigation of Metabolites,” RSC Advances 8, no. 40 (2018): 22335–22350. doi:10.1039/c8ra01574k.

130) Denoux C., Galletti R., Mammarella N., et al., “Activation of Defense Response Pathways by OGs and Flg22 Elicitors in Arabidopsis Seedlings,” Molecular Plant 1, no. 3 (2008): 423–445. doi:10.1093/mp/ssn019.

131) Xu N., Huang Z. H., Watson J. T., and Gage D. A., “Mercaptobenzothiazoles: A new Class of Matrices for Laser Desorption Ionization Mass Spectrometry,” Journal of the American Society for Mass Spectrometry 8, no. 2 (1997): 116–124.

132) Wishart D. S., Tzur D., Knox C., et al., “HMDB: The Human Metabolome Database,” Nucleic Acids Research 35, no. Database issue (2007): D521–D526. doi:10.1093/nar/gkl923.

133) Siwinska J., Kadzinski L., Banasiuk R., et al., “Identification of QTLs Affecting Scopolin and Scopoletin Biosynthesis in Arabidopsis thaliana,” BMC Plant Biology 14 (2014): 280. doi:10.1186/s12870-014-0280-9.

134) Ihnatowicz A., Siwinska J., Perkowska I., et al., “Genes to Specialized Metabolites: Accumulation of Scopoletin, Umbelliferone and Their Glycosides in Natural Populations of Arabidopsis thaliana,” BMC Plant Biology 24 (2024): 806. doi:10.1186/s12870-024-05491-w.

135) Döll S., Kuhlmann M., Rutten T., et al., “Accumulation of the Coumarin Scopolin Under Abiotic Stress Conditions Is Mediated by the Arabidopsis thaliana THO/TREX Complex,” Plant Journ

136) Dupree EJ, Jayathirtha M, Yorkey H, Mihasan M, Petre BA, Darie CC. A Critical Review of Bottom-Up Proteomics: The Good, the Bad, and the Future of this Field. Proteomes. 2020 Jul 6;8(3):14. doi: 10.3390/proteomes8030014. PMID: 32640657; PMCID: PMC7564415.

137) Jelkmann, W. (2007). Erythropoietin: Structure, control of production, and function. *Physiological Reviews, 87*(2), 485–527.

138) Elliott, S., et al. (2008). Erythropoiesis-stimulating agents: Red-cell biology, clinical actions, and risks. *Nephrology Dialysis Transplantation, 23*(7), 2453–2458.

139) Yang, Y., et al. (2016). Hybrid mass spectrometry approaches in glycoprotein analysis and their usage in scoring biosimilarity. *Nature Communications, 7*, 13397.

140) Guan, F., et al. (2007). LC−MS/MS method for confirmation of recombinant human erythropoietin and darbepoetin α in equine plasma. *Analytical Chemistry, 79*(12), 4627–4635.

141) Reichel, C., et al. (2009). Progress in the detection of recombinant erythropoietin in doping control. *Drug Testing and Analysis, 1*(3), 138–142.

142) Domínguez-Vega, E., et al. (2017). Characterization of erythropoietin microheterogeneity by capillary electrophoresis coupled to high-resolution mass spectrometry. *Analytical Chemistry, 89*(3), 1644–1652.

143) Falck, D., et al. (2017). Affinity purification of erythropoietin from cell culture supernatant combined with MALDI-TOF-MS analysis of erythropoietin N-glycosylation. *Scientific Reports, 7*, 5324.

144) van Schaick, G., et al. (2021). Anion exchange chromatography–mass spectrometry for monitoring multiple quality attributes of erythropoietin biopharmaceuticals. *Analytica Chimica Acta, 1143*, 166–172.

145) Yang, Y., et al. (2020). Advances in hybrid MS approaches for glycoproteomics and biosimilarity testing. *Mass Spectrometry Reviews, 39*(5), 401–421.

146) Reichel, C. (2011). Analytical challenges in the detection of erythropoiesis-stimulating agents. *Drug Testing and Analysis, 3*(11–12), 839–845.

147) van den Broek, I., et al. (2015). Glycosylation analysis of erythropoietin: State of the art and future perspectives. *Journal of Pharmaceutical and Biomedical Analysis, 113*, 70–85.

148) Falck, D., et al. (2017). Streamlining the detection of erythropoietin glycoforms: Toward better anti-doping strategies. *Scientific Reports, 7*, 5324.

149) Zhang, J., Xin, L., Shan, B., Chen, W., Xie, M., Yuen, D., Zhang, W., Zhang, Z., Lajoie, G. A., & Ma, B. (2012). PEAKS DB: de novo sequencing assisted database search for sensitive and accurate peptide identification. *Molecular & Cellular Proteomics, 11*(4), M111.010587. https://doi.org/10.1074/mcp.M111.010587

150) The UniProt Consortium. (2021). UniProt: The universal protein knowledgebase in 2021. *Nucleic Acids Research, 49*(D1), D480–D489. https://doi.org/10.1093/nar/gkaa1100al 93 (2018): 431–444. doi:10.1111/tpj.13797.

151) Florentinus-Mefailoski A, Safi F, Marshall JG. Enzyme linked immuno mass spectrometric assay (ELIMSA). Journal of Proteomics. 2014 Jan 16;96:343-52.

Appendices

Appendix A. Supplementary Data for Chapter 2

Leaf spray analysis results

Solvent optimization

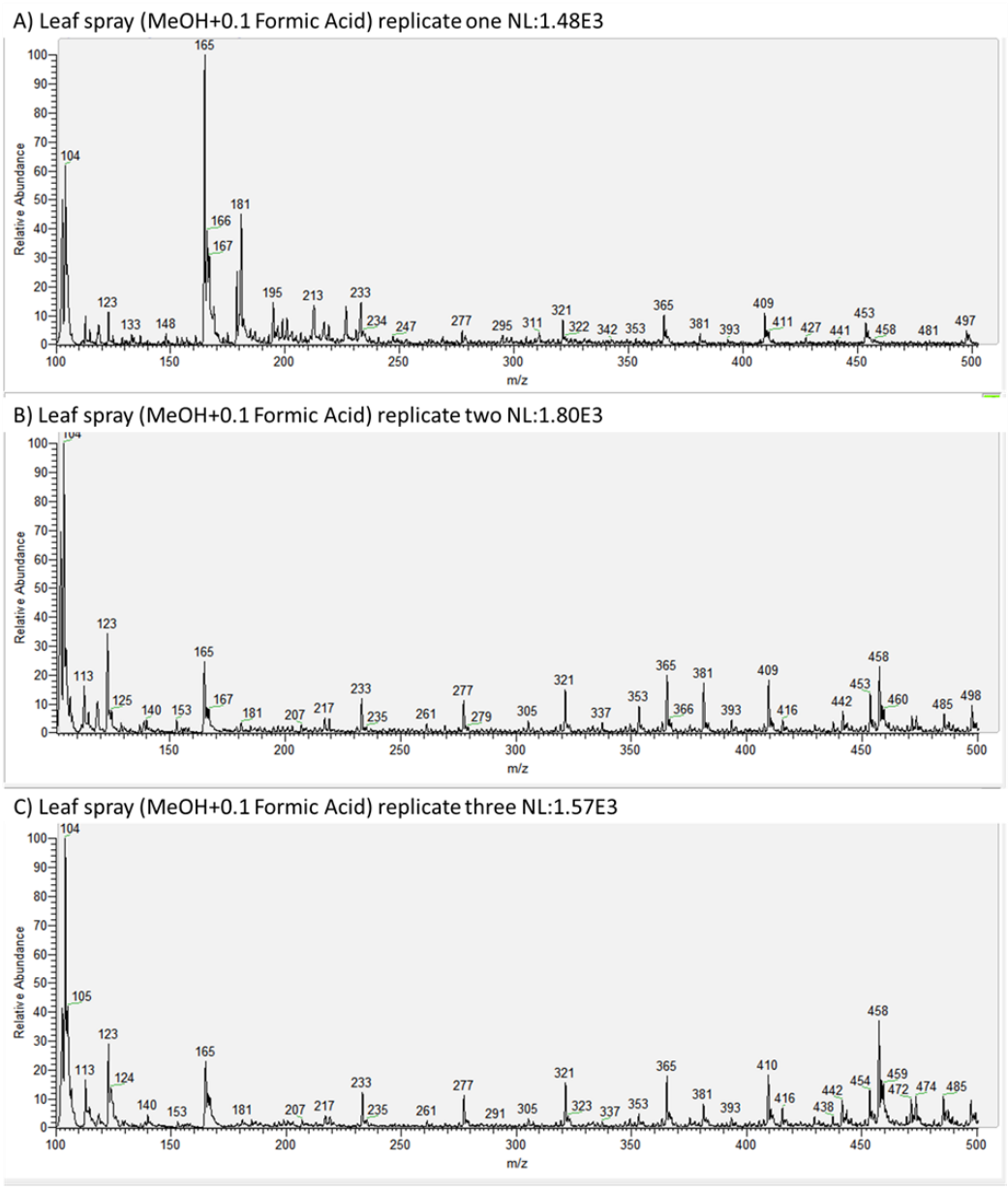

Figure S 2.1 Replicates of leaf spray optimization using Methanol added with 0.1% formic acid. Replicate A) one B) two C) three

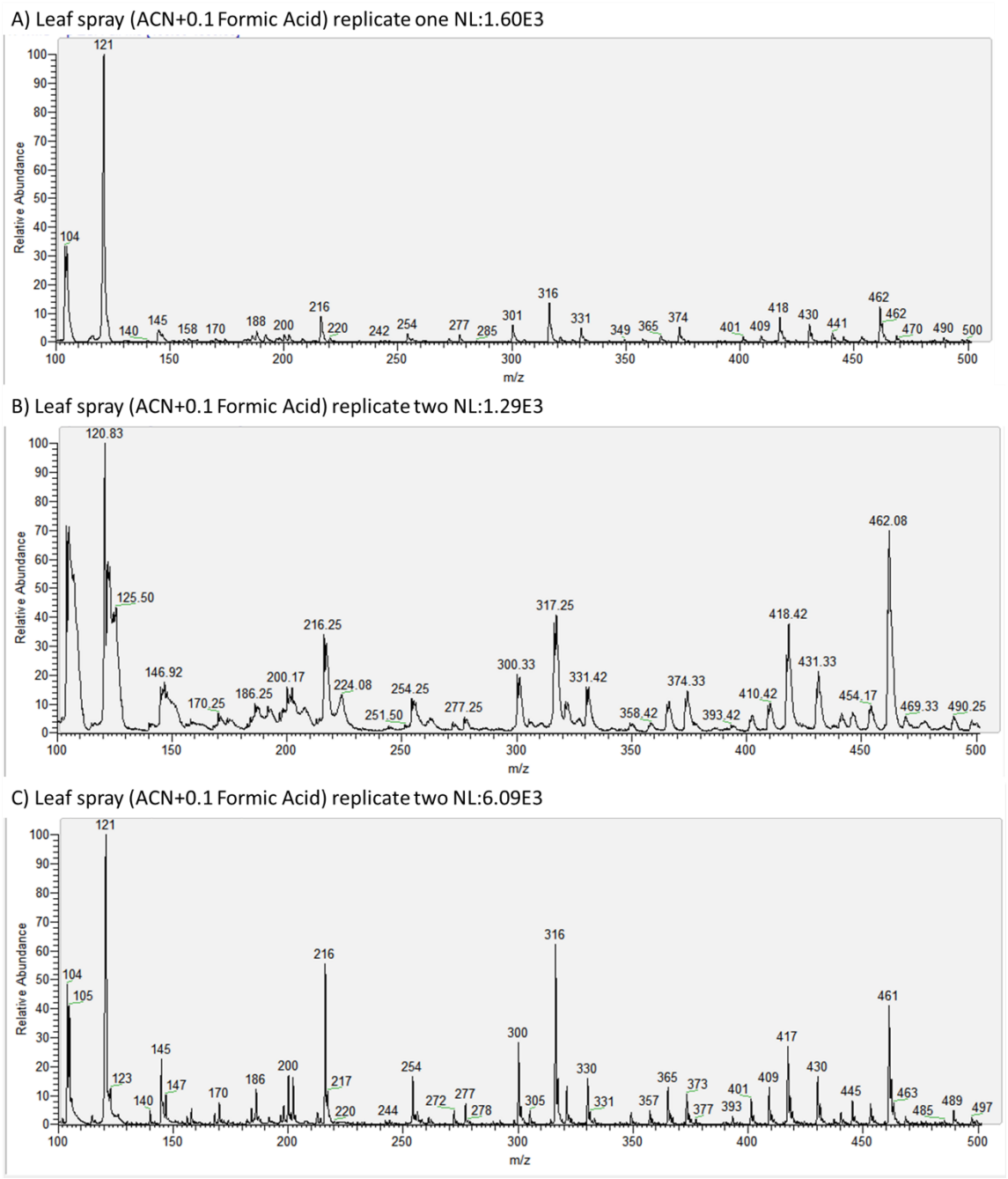

Figure S 2.2 Replicates of leaf spray optimization using Acetonitrile added with 0.1% formic acid. Replicate A) one B) two C) three

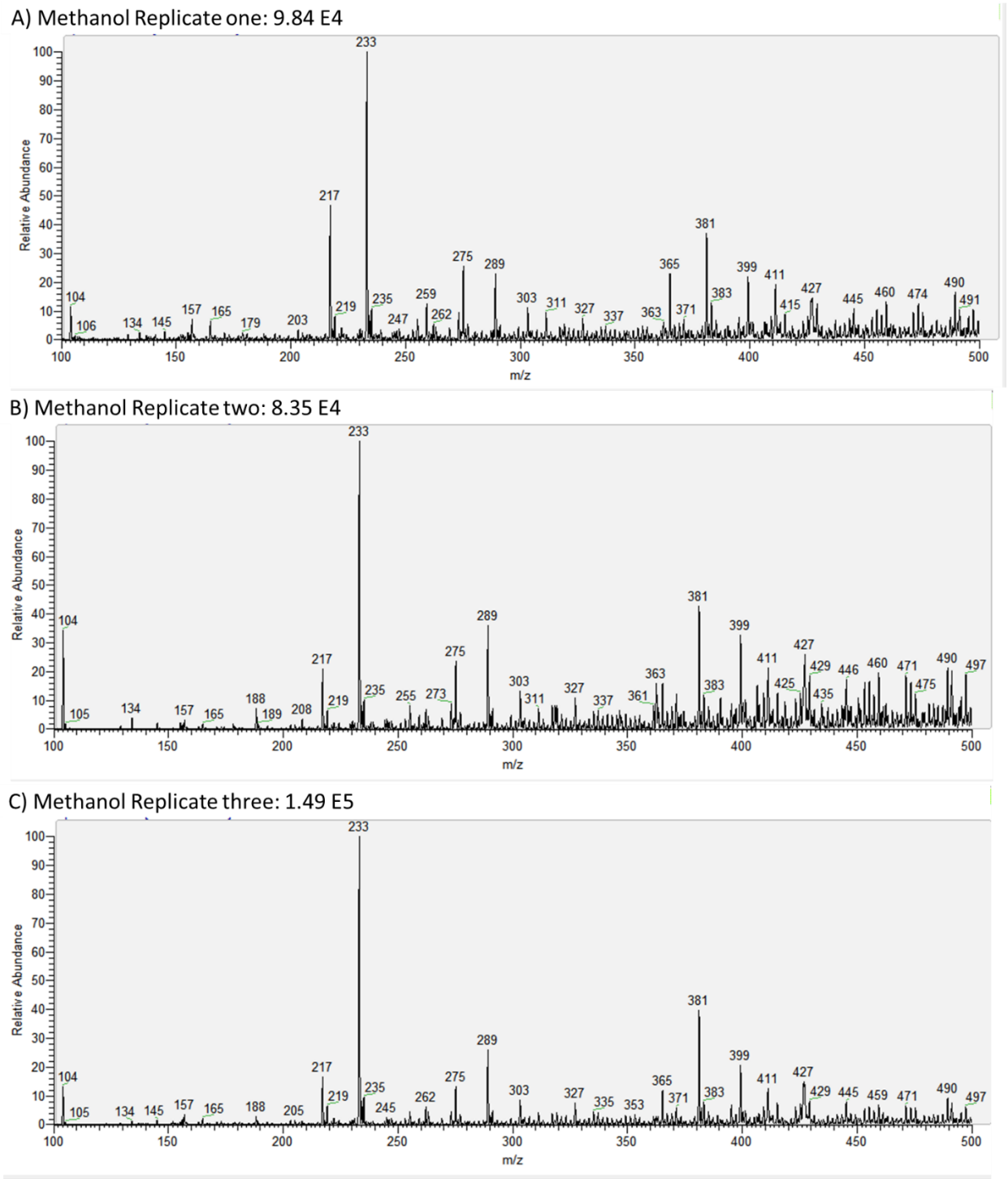

Figure S 2.3 Replicates of SPS-MS using methanol as extraction solvent. Replicate A) one B) two C) three

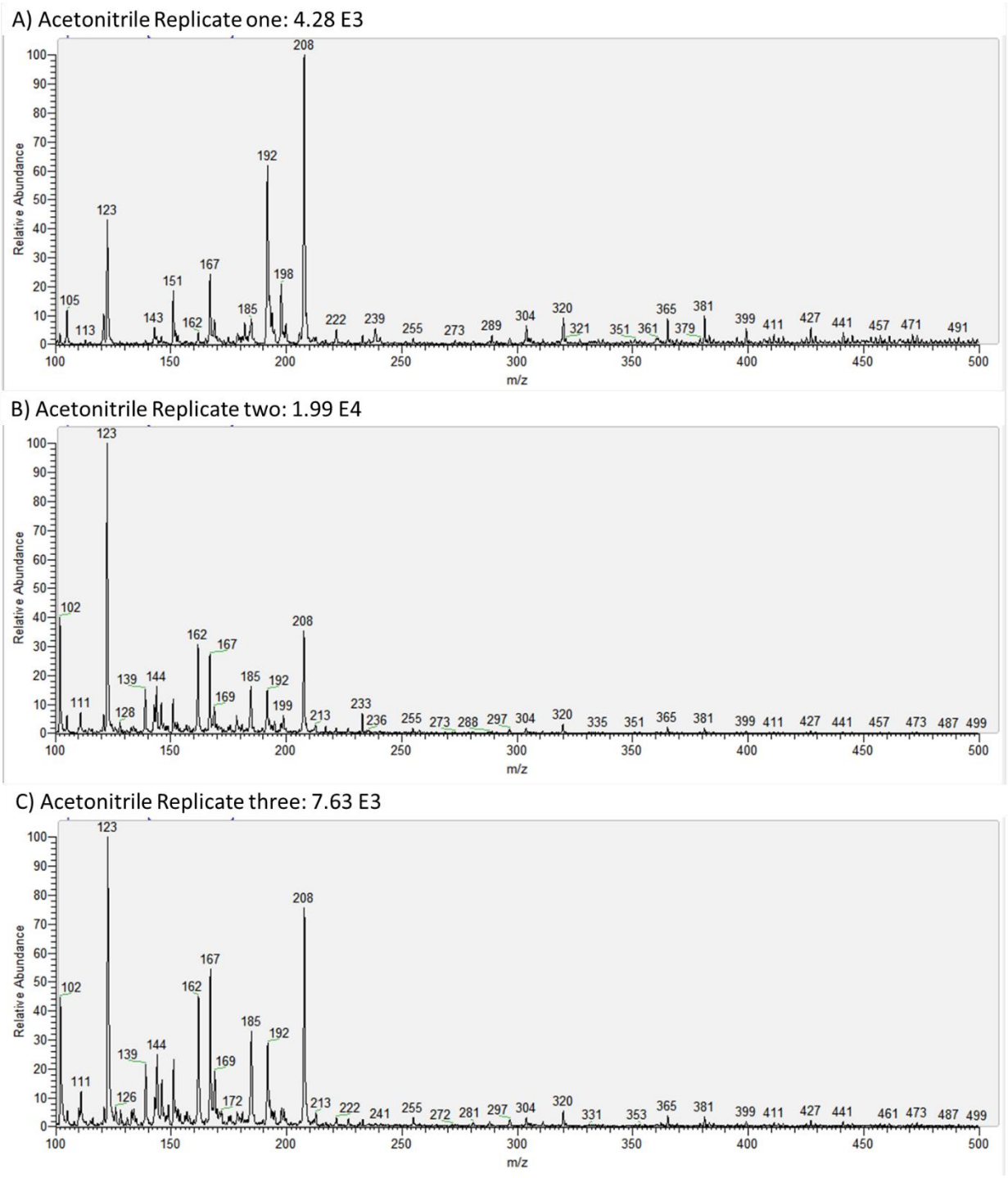

Figure S 2.4 Replicates of SPS-MS using acetonitrile as extraction solvent. Replicate A) one B) two C) three

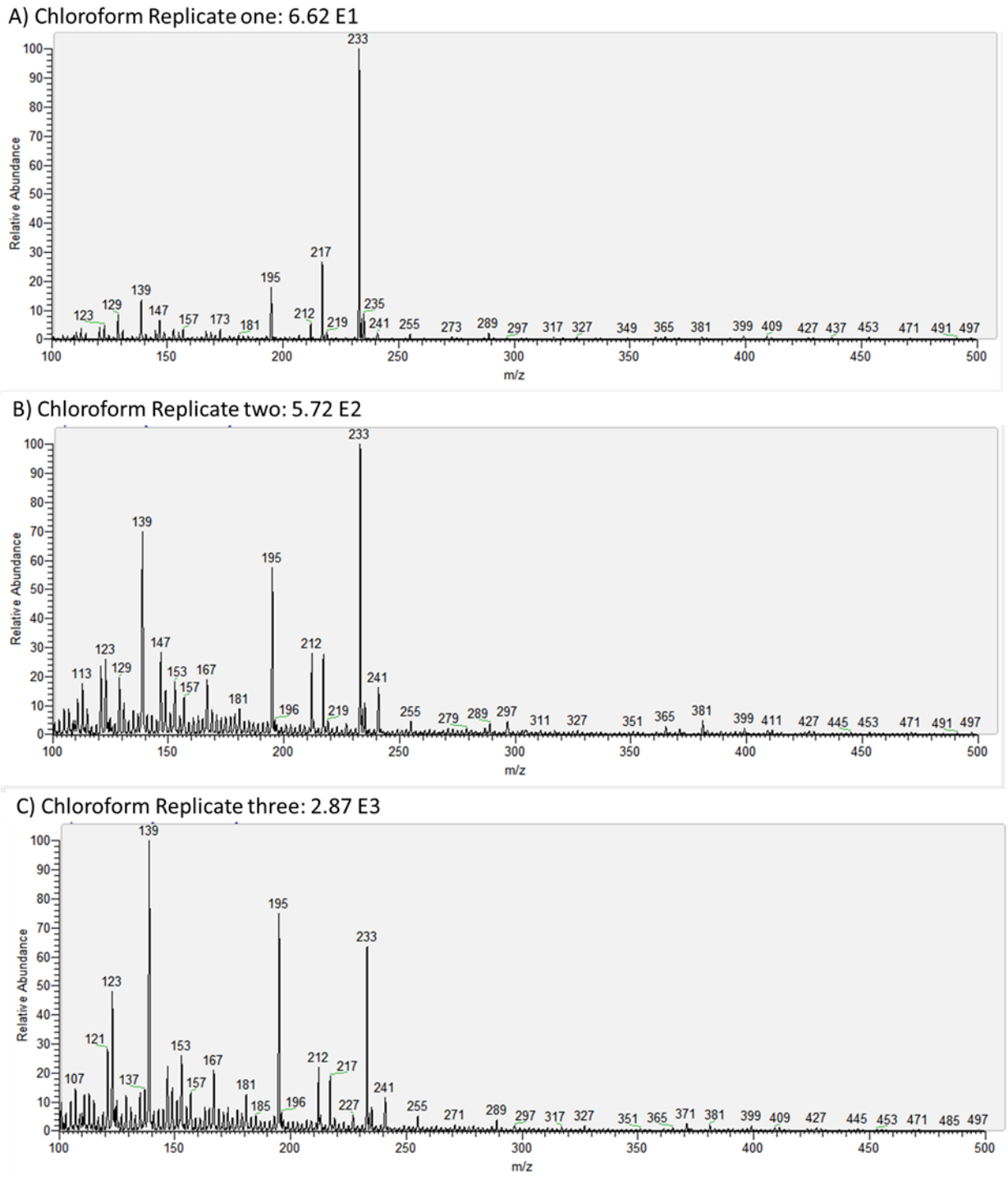

Figure S 2.5 Replicates of SPS-MS using chloroform as extraction solvent. Replicate A) one B) two C) three

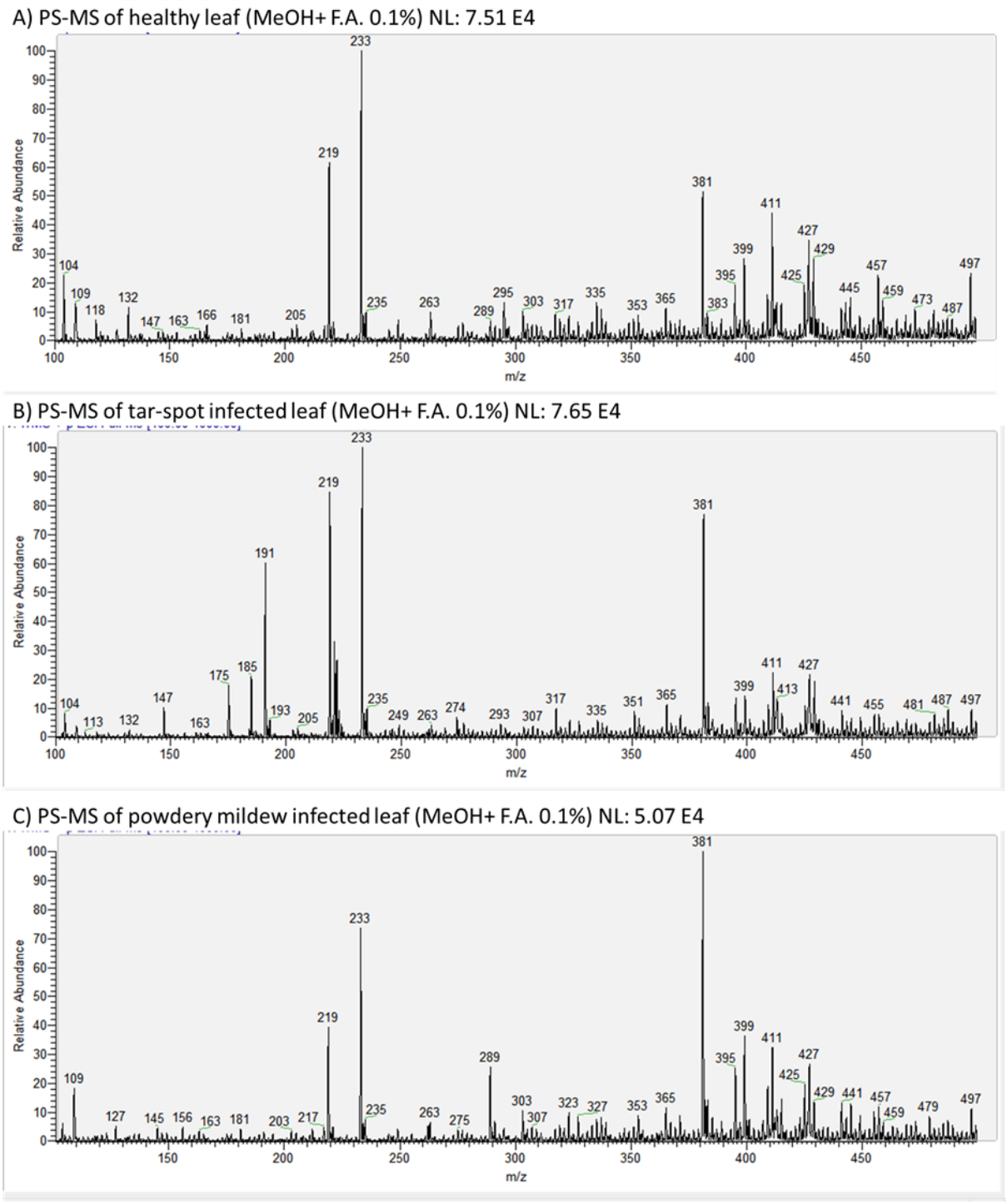

Figure S 2.6 PS-MS analysis of A) healthy leaf, B) Tar-spot infected leaf, and C) Powdery mildew-infected leaf

Negative ionization mode analysis

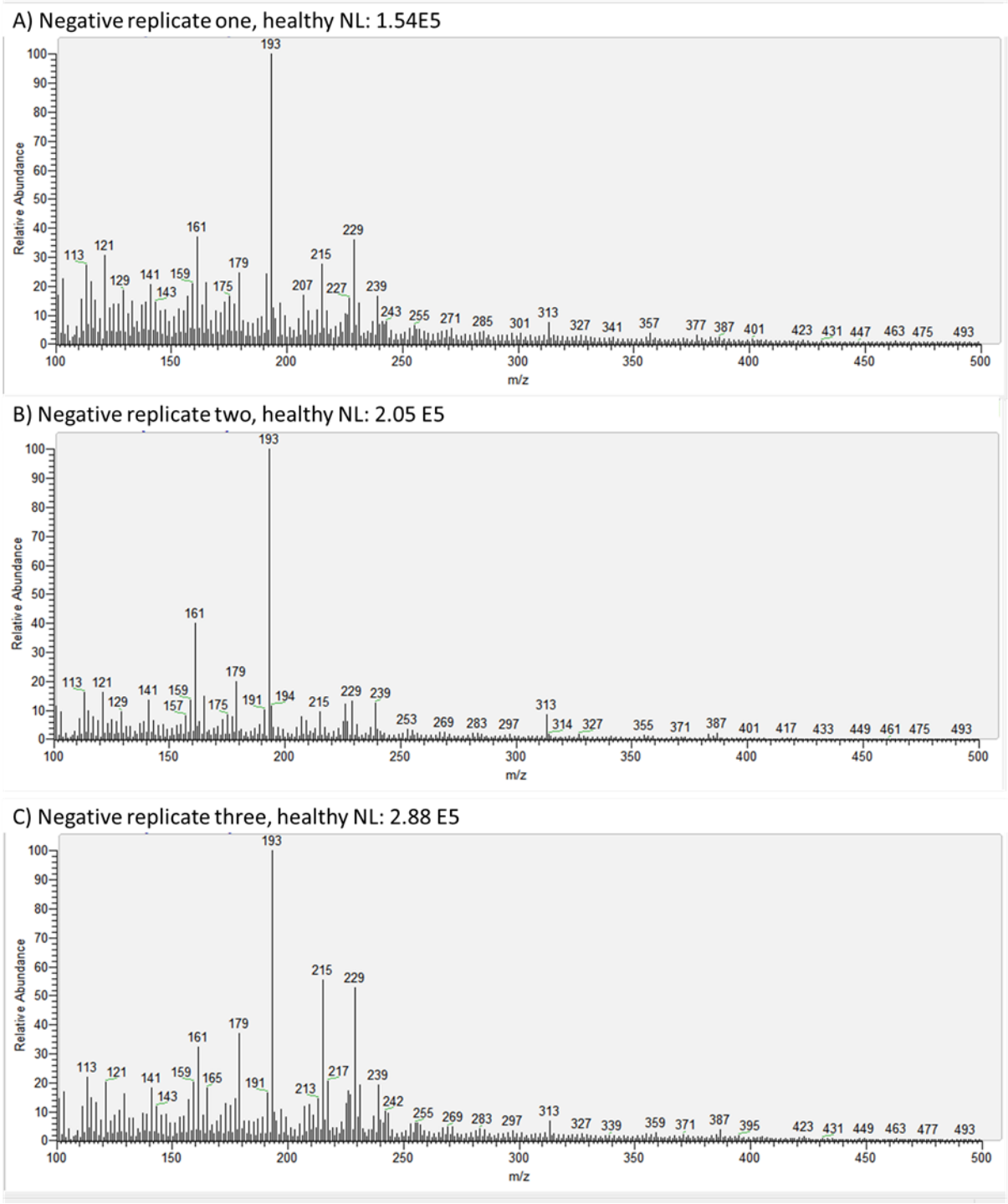

Figure S 2.7. Replicates of healthy leaves using SPS-MS in negative ionization mode. Replicate A) one B) two C) three

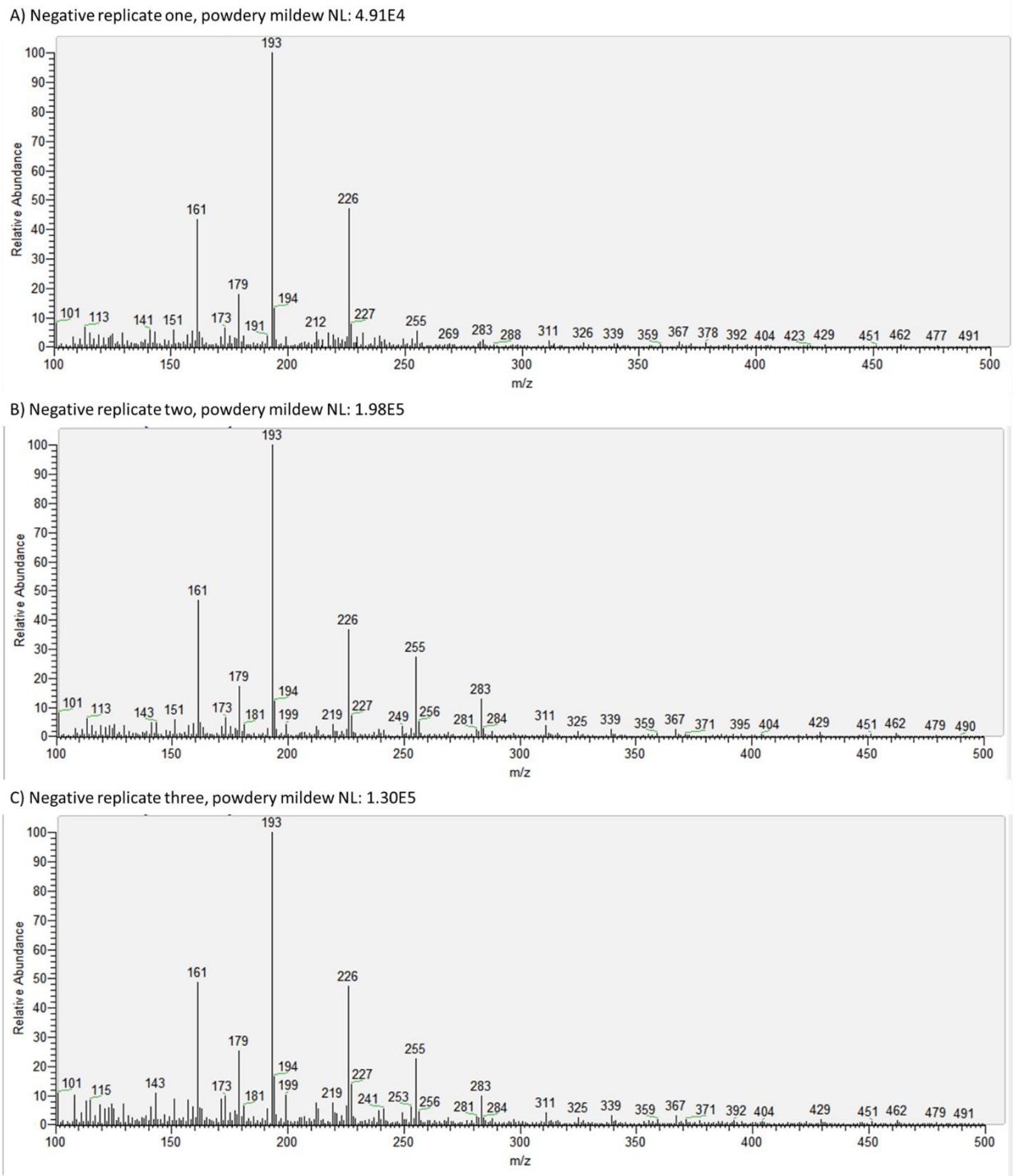

Figure S 2.8 Replicates of leaves infected by powdery mildew using SPS-MS in negative ionization mode. Replicate A) one B) two C) three

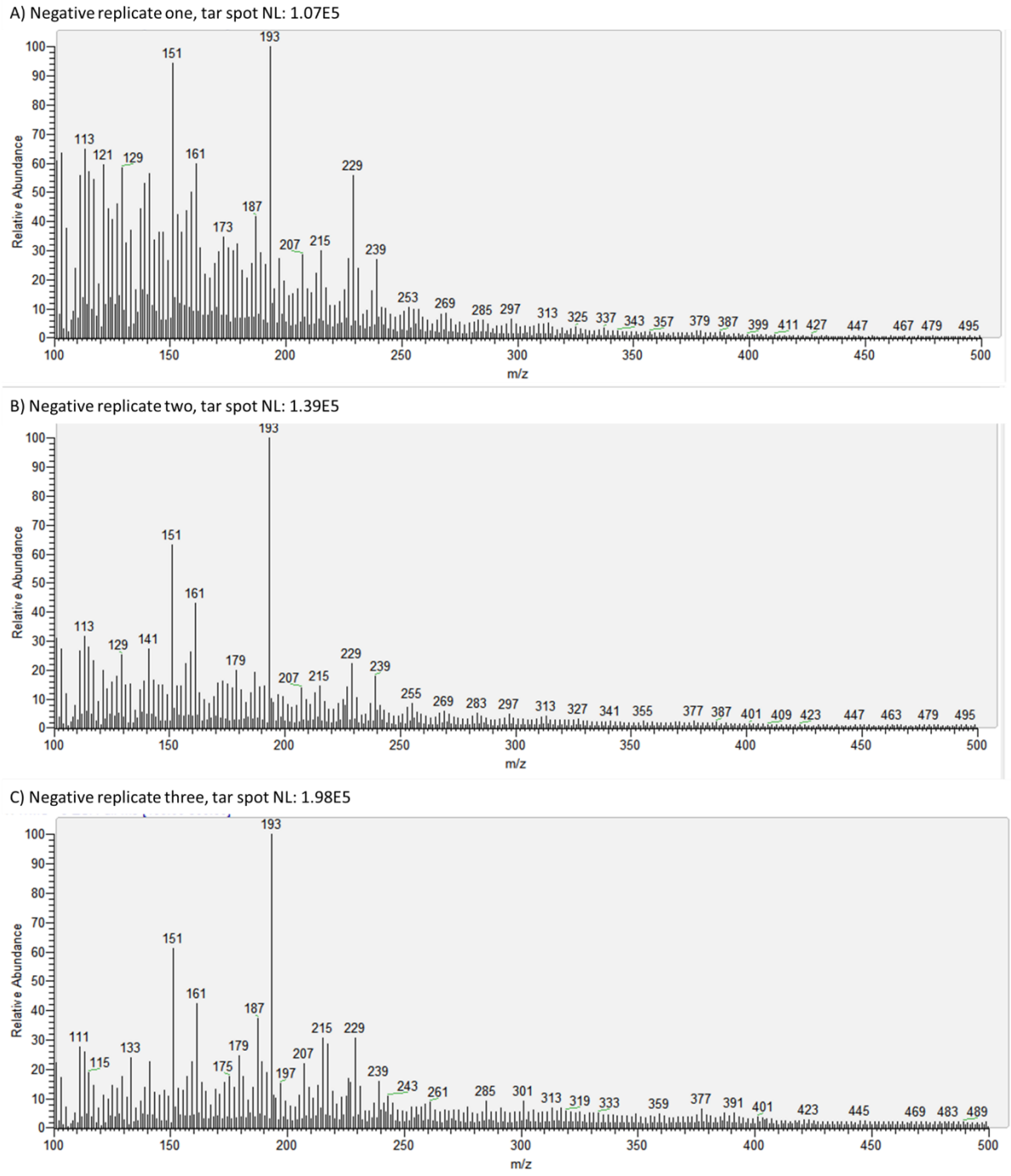

Figure S 2.9 Replicates of leaves infected by tar-spot using SPS-MS in negative ionization mode. Replicate A) one B) two C) three

SPS-MS blank analysis

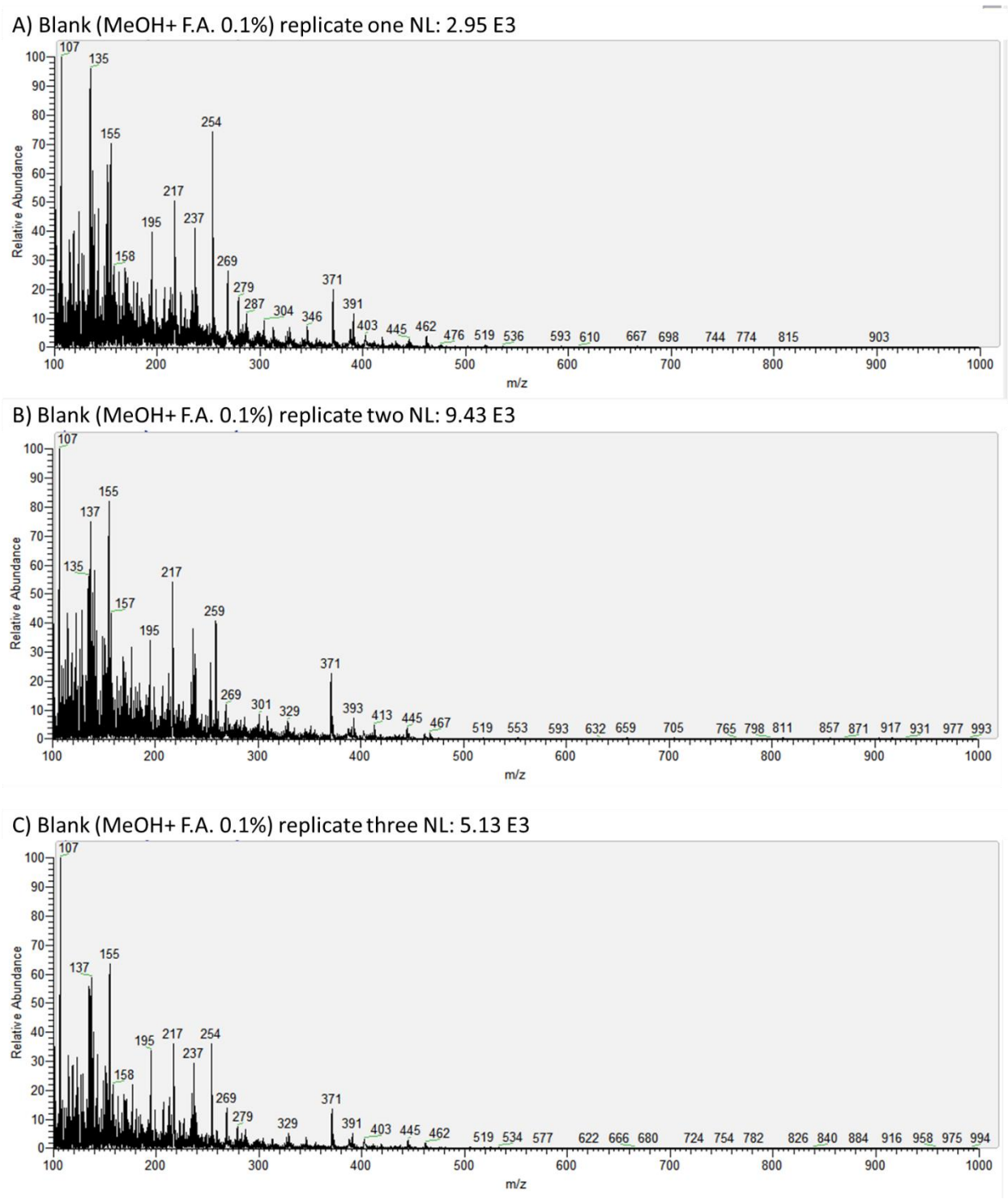

Figure S 2.10 Replicates of blank sandpaper using methanol added with 0.1% formic acid. Replicate A) one B) two C) three

Tandem (MS/MS) mass spectrometry analysis

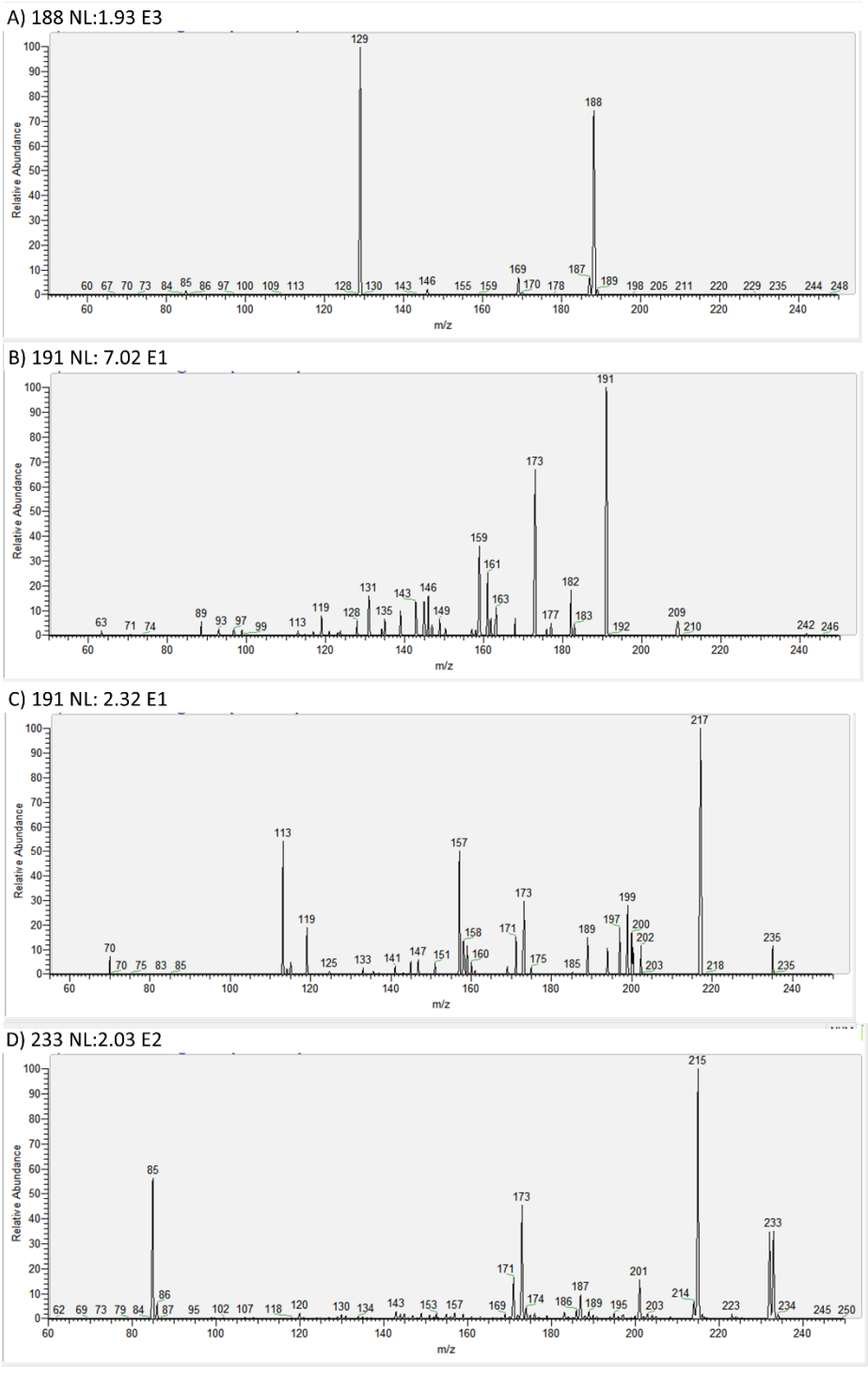

Figure S 2.11 MS/MS spectra of the ions with the highest values on the PCA loading plot: A) *m/z* 188, B) *m/z* 191, C) *m/z* 217, and D) *m/z* 233.

Appendix B. Supplementary Data for Chapter 3

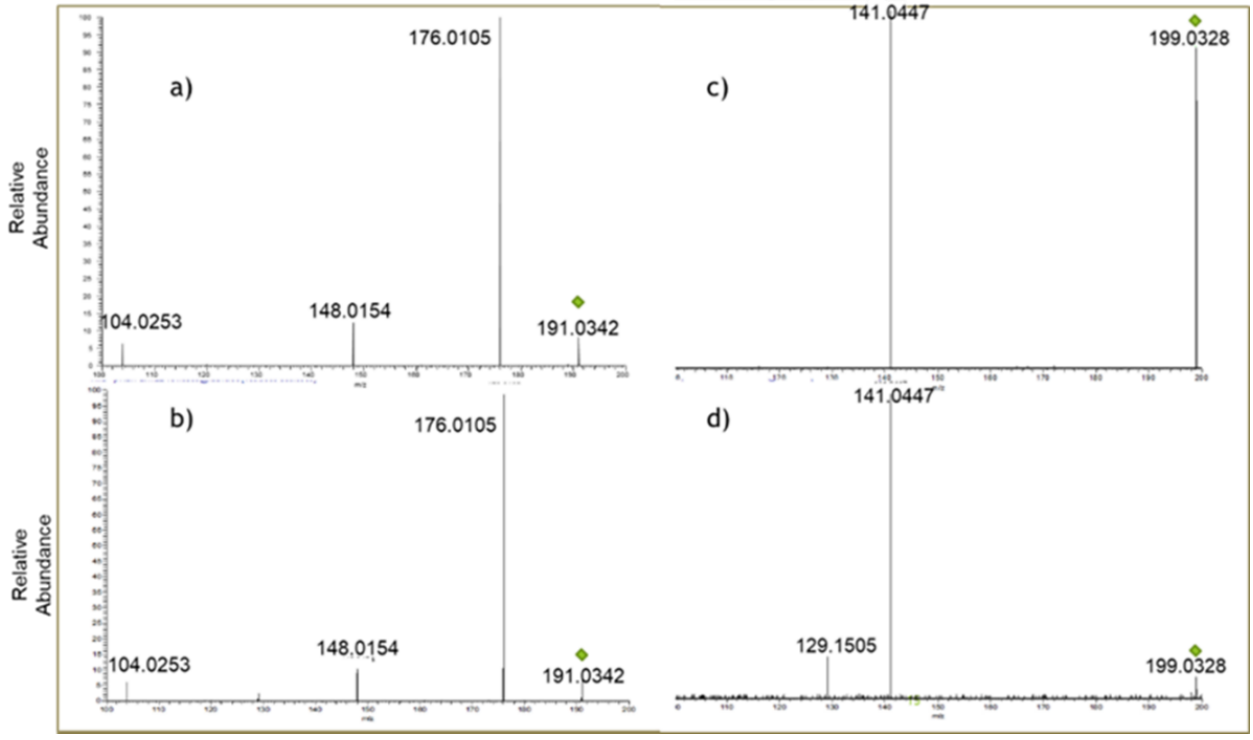

Figure S 3.1: MSMS fragmentation patterns comparison between samples and standard a) Scopoletin in the standard solution, b) Scopoletin in the plant extracts, c) Camalexin in the standard solution, and d) Camalexin in the plant extract. Matching fragmentation patterns confirm compound identities.

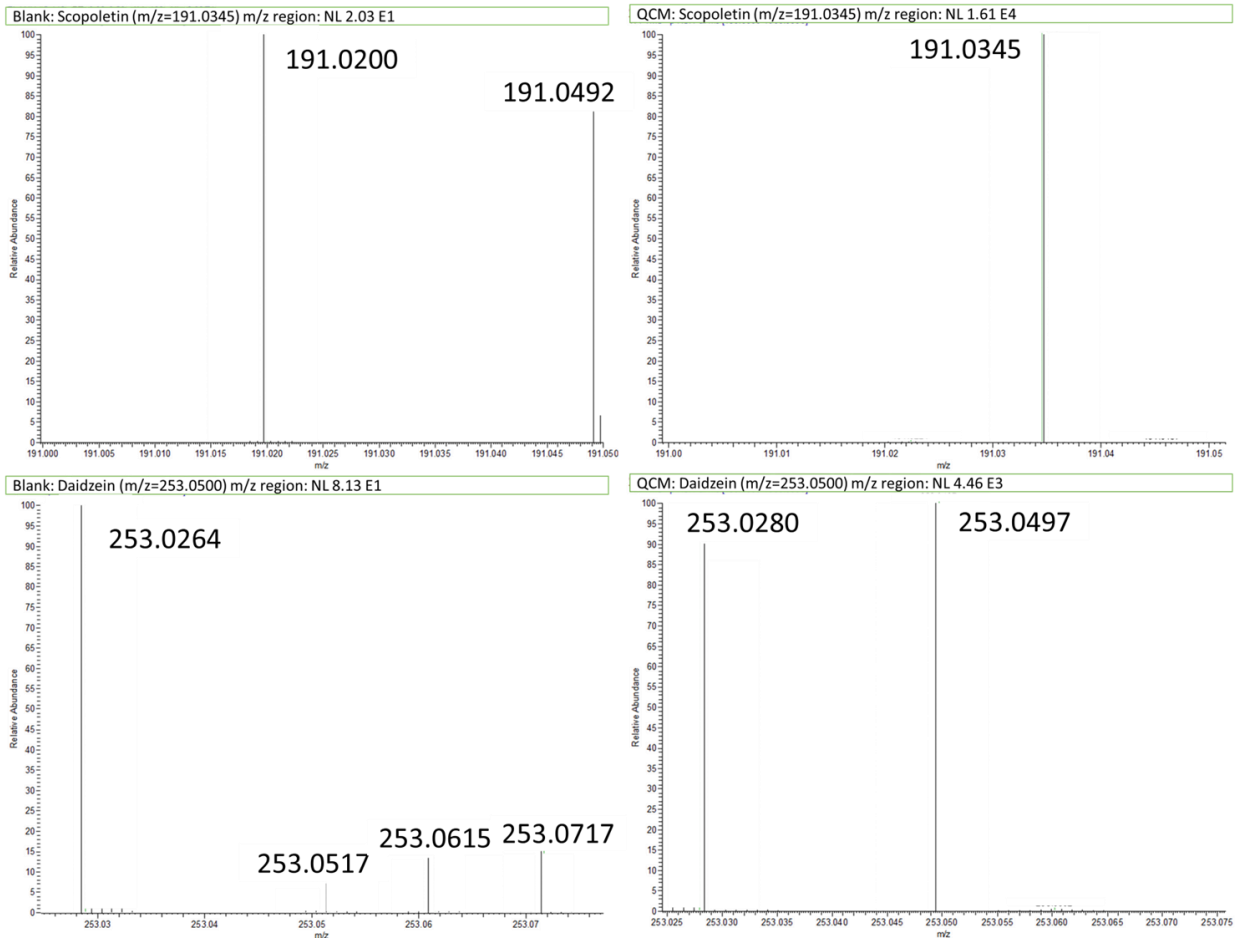

Figure S 3.2 Blank matrix analysis. On the left, the mass spectrum of the blank samples; on the right, the spiked QCM samples. From top to bottom: Scopoletin (*m/z* = 191.0345), Daidzein (*m/z*=253.0500).

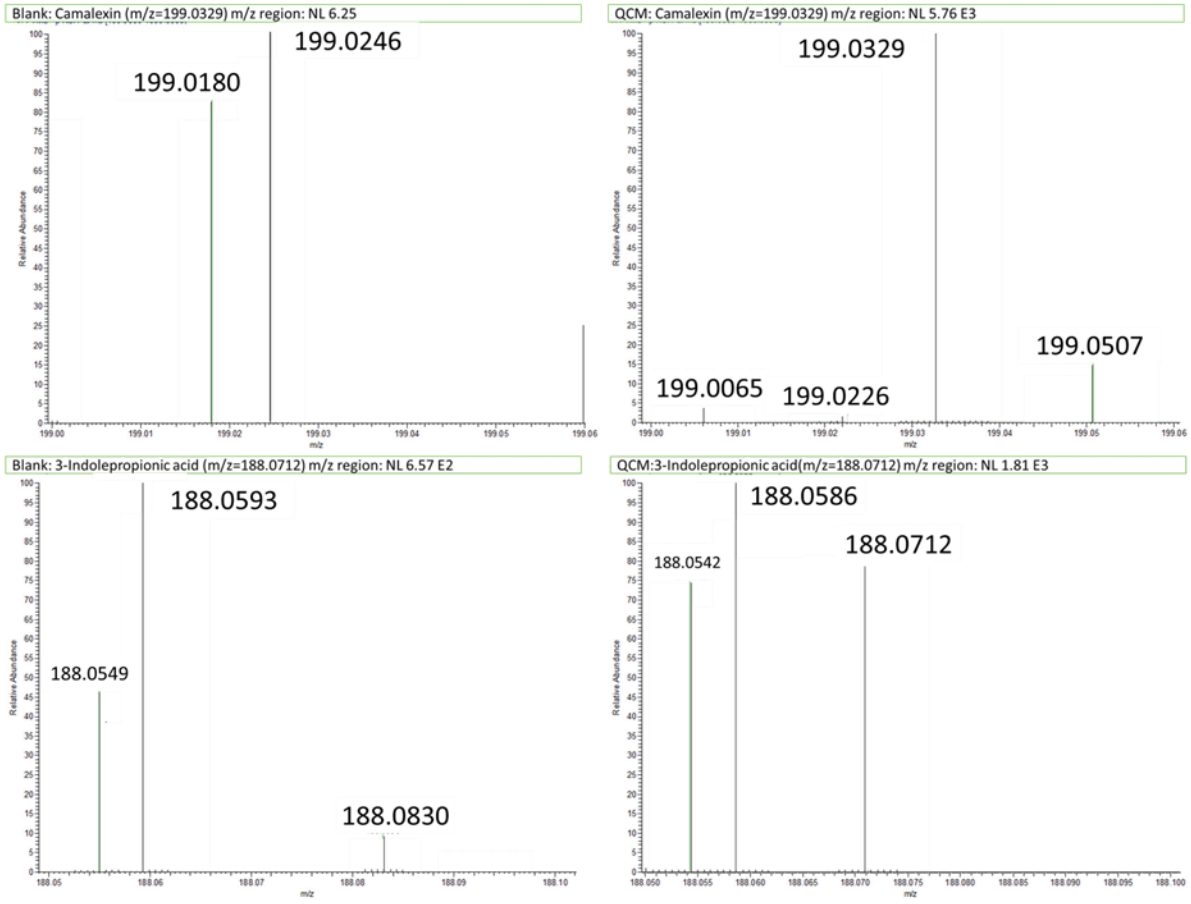

Figure S 3.3 Blank matrix analysis. On the left, the mass spectrum of the blank samples; on the right, the spiked QCM samples. From top to bottom: Camalexin (*m/z* = 199.0329), 3-Indolepropionic acid (*m/z*=188.0712).

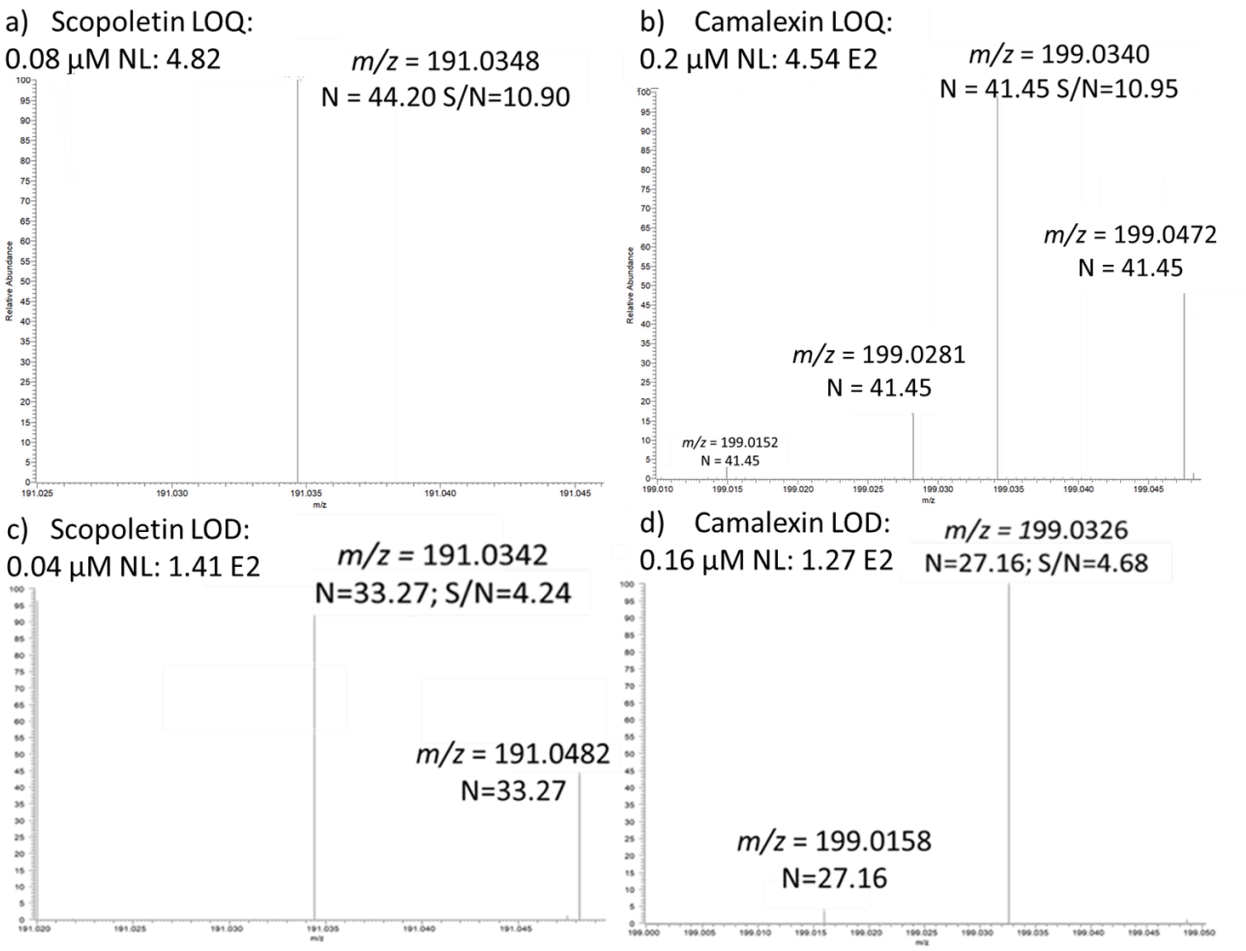

Figure S 3.4: Signal to noise ratio of samples at the established LOD and LOQ a) LOQ for scopoletin at 0.08 µM. b) LOQ for camalexin at 0.2 µM. c) LOD for Scopoletin at 0.04 µM d) LOD for camalexin at 0.16 µM. Noise (N) was estimated using the root-mean-square method over baseline regions. The S/N ratio reflects the relationship between the signal intensity of the peak of interest and the corresponding baseline noise. The S/N was calculated only for the peak of interest.

		Analytical Replicate 1			Analytical Replicate 2			Analytical Replicate 3						
		Target	IS	Ratio	Target	IS	Ratio	Target	IS	Ratio	Average	µM	µg/g	Average per group µM
Camalexin	Sample 1	0	726	0,00	0	248	0,00	0	423	0,00	0,00	0,00	0,00	
Columbia WT	Sample 2	0	833	0,00	0	669	0,00	0	725	0,00	0,00	0,00	0,00	0,00
DMSO	Sample 3	0	771	0,00	0	633	0,00	0	599	0,00	0,00	0,00	0,00	
Camalexin	Sample 1	0	1290	0,00	0	849	0,00	0	1220	0,00	0,00	0,00	0,00	
atwrky33-2	Sample 2	0	781	0,00	0	864	0,00	0	849	0,00	0,00	0,00	0,00	0,00
DMSO	Sample 3	0	373	0,00	0	409	0,00	0	381	0,00	0,00	0,00	0,00	
Camalexin	Sample 1	5010	687	7,29	4530	512	8,85	4020	475	8,46	8,20	2,02	8,08	
Columbia WT	Sample 2	10900	820	13,29	12700	1020	12,45	8160	602	13,55	13,10	3,21	12,82	9,02
flg22	Sample 3	8640	1420	6,08	8850	1370	6,46	9020	1490	6,05	6,20	1,54	6,14	
Camalexin	Sample 1	853	714	1,19	1100	845	1,30	1030	652	1,58	1,36	0,37	1,46	
atwrky33-2	Sample 2	1070	1220	0,88	964	1040	0,93	815	1040	0,78	0,86	0,24	0,98	1,41
flg22	Sample 3	771	512	1,51	1080	577	1,87	758	447	1,70	1,69	0,45	1,78	
Scopoletin	Sample 1	6590	2150	3,07	6030	2200	2,74	7010	2550	2,75	2,85	0,64	2,46	
Columbia WT	Sample 2	7440	2690	2,77	8380	2920	2,87	5570	1940	2,87	2,84	0,64	2,45	2,36
DMSO	Sample 3	9130	3700	2,47	9540	3770	2,53	8810	3340	2,64	2,55	0,57	2,18	
Scopoletin	Sample 1	2200	2510	0,88	1840	2120	0,87	1740	1820	0,96	0,90	0,18	0,69	
atmyb15-1	Sample 2	3020	3180	0,95	2650	1990	1,33	2410	2340	1,03	1,10	0,23	0,87	0,65
DMSO	Sample 3	1960	3300	0,59	1990	3570	0,56	2020	3570	0,57	0,57	0,10	0,39	
Scopoletin	Sample 1	6830	2350	2,91	5510	1690	3,26	6020	1970	3,06	3,07	0,69	2,66	
Columbia WT	Sample 2	9330	2430	3,84	8200	2040	4,02	7180	1920	3,74	3,87	0,88	3,38	2,79
flg22	Sample 3	6140	2190	2,80	6620	2480	2,67	5990	2260	2,65	2,71	0,61	2,33	
Scopoletin	Sample 1	3850	3080	1,25	4240	4070	1,04	4080	4180	0,98	1,09	0,22	0,86	
atmyb15-1	Sample 2	4040	2300	1,76	4290	2230	1,92	3100	1880	1,65	1,78	0,39	1,48	1,20
flg22	Sample 3	3660	2590	1,41	3710	2520	1,47	4570	2650	1,72	1,54	0,33	1,26	

Table S 3.1 Analytical Replicates and Ion Intensity Measurements of Camalexin and Scopoletin in Different Genetic Lines (Columbia WT, atwrky33-2, atmyb15-1) under Treatments with the Elicitor flg22 and DMSO as Control. Table S1 reports ion intensities for target compounds and internal standards (IS) from each analytical replicate across different genetic lines and treatment conditions. Ratios, averages, and calculated concentrations are presented in µM and µg/g, with a final column showing the average concentration per group in µM.